Universidade de Aveiro

Ano 2015/2016

Departamento de Química

Katarzyna
Wozniak

Fabricação de estruturas bio-hibridas contendo ácido fólico para a absorção controlada em células cancerígenas

Fabrication of folic acid-containing biohybrid structures for the controlled uptake in cancer cells

Jury:

President   Prof. Vitor Brás Sequeira Amaral

Prof. Ana Margarida Madeira Viegas de Barros Timmons

Prof. Tito Trindade

Palavras-chave   estrutura bio-híbrida, ácido fólico, interacção biotina-avidina, direccionamento selectivo

Resumo   Neste trabalho foram fabricadas estruturas bio-híbridas (BHS) à base de glicopolímeros dendríticos biotinilados e estreptavidina as quais foram posteriormente funcionalizadas com o ácido fólico com vista ao reconhecimento preferencial por células tumorais. A estratégia de fabricação recorreu, em ambos os casos, a interações não-covalentes. A caracterização das estruturas no que respeita ao seu tamanho hidrodinâmico e potencial zeta, em conjunto com os estudos de citotoxicidade, foram realizados no sentido de avaliar as propriedades físicas, assim como a biocompatibilidade das estruturas. Os resultados obtidos demonstraram que BHS estáveis, com tamanhos definidos, podem ser obtidas através de poliassociação controlada. Além disso, nas condições experimentais consideradas, as BHS apresentam biocompatibilidade e não apresentam toxicidade para as células.

Seguidamente, avaliou-se a influência do ligando do ácido fólico sobre a segmentação de células cancerígenas ricas em receptores de folato por citometria de fluxo. Para tal, foi avaliado o efeito da quantidade de ácido fólico, do comprimento da cadeia de PEG (espaçador) e da concentração de BHS, tal como o impacto das estratégias de purificação.

Adicionalmente foi ainda estudado o mecanismo de absorção celular.

Key words   biohybrid structure, folic acid, biotin-streptavidin interaction, selective targeting

Abstract   In this work, biohybrid structures (BHS) based on streptavidin and pentavalent biotinylated dendritic glycopolymer were fabricated through non-covalent streptavidin-biotin conjugation and further functionalized with the folic acid for the selective targeting to tumor cells. Characterization of the hydrodynamic size and zeta potential of the structures together with the cytotoxicity studies were performed to assess the physical properties and biocompatibility of the structures. It was shown that stable BHS with defined sizes can be obtained due to a controlled polyassociation reaction. Furthermore, BHS are biocompatible and do not cause toxicity to the cells under the given experimental conditions.

Next, the effect of the folic acid ligand on the targeting function towards folate receptor expressing cancer cells was studied in flow cytometry experiments. For this purpose the amount of folic acid, the length of the PEG-chain / spacer, and the type of protein used were evaluated, as well as the impact of purification strategies. Additionally, the cell uptake mechanism was also briefly looked into.

Table of Contents

List of abbreviations

AF4	Asymmetric flow field flow fractionation
BHS	Biohybrid structure
Biotin-PEG	Biotin-PEG-COOH
Con A	Concanavalin A
DB	Degree of branching
DF	Degree of functionalization
DLS	Dynamic Light Scattering
DMEM	Dulbecco's modified eagle medium
DPBS	Dulbecco's phosphate buffered saline
EDL	Electrical double layer
EPR	Enhanced permeability and retention effect
FITC	Fluorescein isothiocyanate
Folate	Biotin-PEG-Folic acid
FR	Folate receptors
HABA	2-(4'-hydroxyazobenzene) benzoic acid
HEK293	Human Embryonic Kidney 293 cells
MFI	Mean fluorescence intensity
NA	Neutravidin

NP	Nanoparticle
PAMAM	Poly(amido amine)
PBS	Phosphate Buffered Saline
PCS	Photon correlation spectroscopy
PEG	Poly(ethylene glycol)
PEI	Hyperbranched poly(ethylene imine)
PPI	Poly(propylene imine)
RFC	Reduced Folate Carrier
QELS	Quasi-elastic light scattering
SA	Streptavidin
SBC-2	Human Cervix Carcinoma cells

List of figures

VI

VII

VIII

List of tables

I.   Theoretical introduction

1.   Dendritic polymers

The high increase of interest in dendrimer's research over the last decade made dendrimer chemistry one of the most rapidly expanding areas of science. Dendrimers are nano-sized, radially symmetric molecules with a well-defined, homogeneous, and monodisperse structure consisting of tree-like arms or branches.[1] The word dendrimer originates from the combination of the Greek words 'dendron' meaning tree or branch, and 'meros' referring to part.[2]
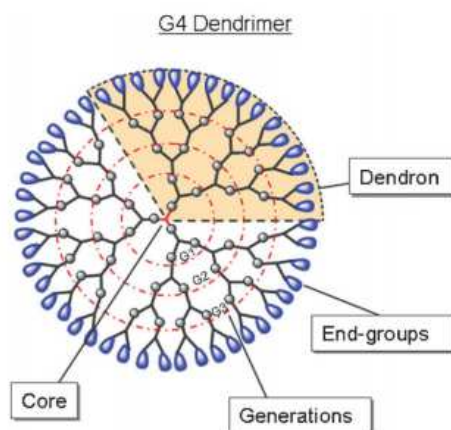
Figure 1: Different structural components of the dendrimer.[3]

These types of molecules were discovered by Fritz Vögtle and his co-workers in 1978 when the first fully controlled synthesis of a dendrimer was conducted.[4] In the 1990s the widespread potential of these hyperbranched structures began to be appreciated and the number of publications in this field of research started to significantly increase.[5] The wide range of potential applications of these new functional materials is a consequence of their unique structure. Dendrimers are complex molecules with a well-defined architecture. They

possess three distinguishing structural components, namely (a) an initiator core, (b) an interior layer consisting of repeating branching units, radially attached to the core (generations), and (c) exterior (terminal groups) attached to the outermost interior generation that can modify the physicochemical or biological properties of dendrimers.[6] A typical dendrimer structure is presented in Figure 1.

Dendrimers can be synthesized via two different synthesis strategies, namely the divergent approach and the convergent approach. The divergent approach is a stepwise layer-by-layer synthesis that starts from the focal core and builds up the molecule towards the periphery. It is based on a pair of basic operations - 'growth of a generation', that consists of coupling of the branching centers, and deprotection or modification of end-functionalities of the periphery to create new reactive surface functionalities. An alternative method of dendrimer synthesis is the convergent approach, in which the reaction begins from the exterior, starting with the molecular structure that ultimately becomes the outermost arm of a dendron. When the growing dendrons are large enough, several are attached to a suitable core to give a complete dendrimer.[7]

The most valuable advantages of dendrimers are the high amount of terminal groups and low viscosity, however their multistep synthesis is complicated to perform. Alternative materials to dendrimers, hyperbranched polymers, have similar properties, but they can be obtained in an easy one-pot synthesis method. They are polymers with a densely branched structure and a large number of end groups. However, hyperbranched polymers differ from dendrimers which have completely branched star-like topologies because they have imperfectly branched or irregular structures. Hyperbranched polymers can be characterized by degree of branching (DB). DB represents the percentage of dendritic and terminal monomers among the total monomers in the polymer and can be calculated according to the following equation:

$$DB = \frac{D + T}{D + L + T}$$

where D, T and L are the fractions of dendritic, terminal and linear units incorporated in a hyperbranched polymer. The common values reported for DB are in the range of 0.4 to 0.8.[8] For perfectly branched dendrimers the DB is equal to 1.

High degree of branching together with other unique properties like globular architecture, well defined molecular weight, and high number of terminal groups make dendritic polymers promising materials for drug delivery.[9] Recent progress has been made in the application of dendrimers as an appropriate host for guest molecules, either in the interior or on the periphery of the dendrimers, as a carrier in transdermal[10] and oral[11] delivery of drugs or as a targeting agent.[12]

Poly(amido amine) (PAMAM) and poly(propylene imine) (PPI) dendrimers are the most widely investigated polymers for the synthesis of dendrimers. Due to differences in the chemical composition, the properties of dendrimers, such as solvent penetration and guest doping, are different from each other in dependence upon a different chemical structure. The interest in physicochemical properties of PPI dendrimers gained attention to use hyperbranched poly(ethylene imine) (PEI),[13] which have a shorter alkyl spacer than PPI. Poly(ethylene imine) is one of the commercially available cationic polyamines which have been widely used as an efficient drug carrier or a gene delivery system.[14] Among the non-viral gene vectors, PEI shows outstanding gene complexation efficiency and great endosome escape activity, however, it can destabilize the cell membrane, which will cause cytotoxicity. Transfection efficiency and toxicity of cationic polymers are highly dependent on molecular weight and structure. Low molecular weight PEI has low cytotoxicity, but its transfection efficiency is very poor. In contrast, high molecular weight PEI shows a high transfection efficiency but it also induces higher cytotoxicity.[15] There have been several approaches to decrease the toxicity of hyperbranched PEI, while maintaining the merits of high transfection efficiency by combining PEI with biodegradable polymer to make an ideal non-viral vector, for example through PEGylation[16] or decorating with an oligosaccharide architecture.[14]

1.1. Glycopolymers

Glycopolymers are natural or synthetic carbohydrate-containing polymers, as well as synthetically modified natural sugar-based polymers. With functions similar to those of natural carbohydrates, synthetic glycopolymers are fabricated with specific pendant saccharide moieties. Sugars are a large group of organic compounds, which are essential components of living organisms, serving for the source of energy and as structural components. Beside their use as key chemical raw materials, they have been recognized as crucial components of a wide variety of complex biological processes. Terminal sugar units of natural glycoconjugates play a decisive role in molecular recognition of multivalent carbohydrate–protein interactions and are involved in a large variety of intercellular processes including, for example, targeting drugs, cell growth regulation, cell differentiation, cell–cell interactions, or cancer cell aggregation.[17, 18]

Most commonly used synthetic polymers for design and synthesis of dendrimers, such as polyamine dendrons and dendrimers have hydrophobic surfaces and poor solubility. Therefore, a chemical modification of the polymer surfaces by carbohydrates is an attractive way to increase the solubility and decrease the cytotoxicity of the polymer. Decoration of dendritic polymers with carbohydrates was developed as an alternative way to PEGylation, which is so far the dominating choice for establishing highly biocompatible delivery systems and therapeutics for in vitro and in vivo applications.[19]

Dendritic glycopolymers can be characterized by the degree of (oligo-)saccharide functionalization (DF) of dendritic polyamine scaffolds (PPI dendrimers and hyperbranched PEI) and the terms "open shell" and "dense shell" have been introduced to describe their molecular characteristics.[20] The "dense shell" architecture is characterized by conversion of the primary amino groups of the dendritic polyamine scaffolds into tertiary amino groups bearing two chemically coupled (oligo-)saccharide units (disubstitution).[14, 21] In the "open shell" architecture primary amino groups are fully or partially converted into secondary amino groups only bearing one chemically attached (oligo-)saccharide unit (monosubstitution).[14]

4
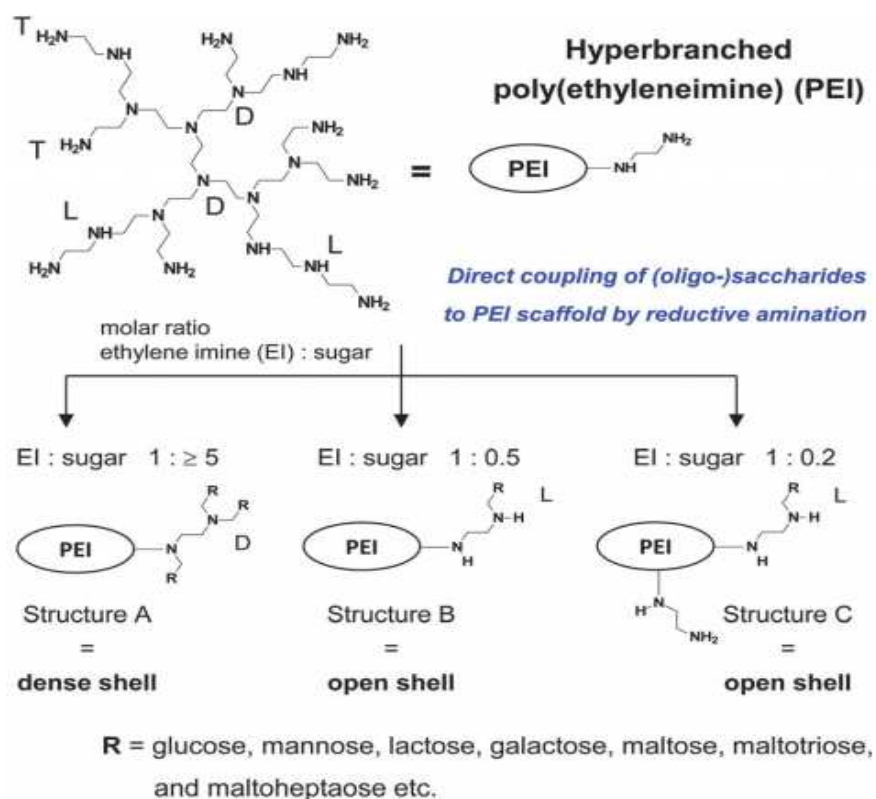
Figure 2: Schematic presentation of PEI dendrimers with different degrees of oligosaccharide functionalization. Branching units: L= linear unit; T= terminal unit and D = dendritic unit.[20]

For the generation of various oligosaccharide substitution degrees, there is an easy one pot approach for the synthesis on the PEI surface. Sugar moieties are covalently bound to the primary and secondary amines of PEI by reductive amination reaction. HPEI offers primary amines (terminal units T) and secondary amines (linear units L) that can be converted to the tertiary amines. Different architectures could be obtained with regards to their structure and the degree of substitution as presented in Figure 2. All the structures can be described using DF, which is characterized by the fact that two (oligo-)saccharide units can be coupled to one T unit and one (oligo-)saccharide can be additionally attached to one L unit [DF is presented as $\frac{n(Mal)}{2\times T + L}$ (%)].

5

(i) Structure A: PEI surface is decorated with a densely organized oligosaccharide shell. It is characterized with preferred D units over the PEI macromolecule with nearly all T units and also most L units converted into D units [the T unit had to react twice with an (oligo-) saccharide]. The synthesis of structure **A** is based on the use of oligosaccharides excess with the corresponding DF in the range between 75 and 95% (Figure 2).

(ii) Structure B: PEI surface has a lower degree of functionalization and a loose shell. It is characterized with preferred L peripheral groups. It has less secondary amines converted to tertiary amines, and could be obtained by utilization of low EI:sugar ratio (1:0.5). DF is in the range between 32 and 48% (Figure 2).

(iii) Structure C: PEI surface is characterized with a mixture of T and L units as peripheral groups. It shows an open sugar shell with free primary amines in comparison to structure A and B. It could be obtained by utilization of EI:sugar ratio (1:0.2). DF of structure C is in the range between 16 and 30% (Figure 2).[14]

Dense and open shell dendritic PEI glycopolymers exhibit pH-dependent cationic surface charges and charge density over a broad pH range (2 to isoelectric point) tailored by the given (oligo-) saccharide architectures. Dense shell architecture has the lowest cationic charge and open shell architecture with remaining primary amines possesses larger cationic charge.[20] PEI is a weak polyelectrolyte and the higher the degree of chemically coupled oligosaccharide units on the PEI surface, the lower the charge density is.[14] Appropriate modifications of cationic surface groups of dendritic polymers with sugar moieties can significantly reduce their toxicity which is dependent on the number and nature of functional surface groups.[22]

2. Used proteins

2.1. Avidin

Avidin is a 67-kDa glycoprotein found in egg white, which has a strong avidity for biotin, a 244-Da water-soluble vitamin H.[23] In recent years, the avidin-biotin complex has gained

great attention as an extremely versatile, general mediator in a wide variety of bioanalytical applications. The reason for interest in the research of this system is the highest known affinity ($K_a \approx 10^{15}$ M^{-1})[24] in nature and consequently high stability of this noncovalent interaction between a ligand and a protein which has been widely used as an universal tool, particularly for diagnostic purposes.[23]
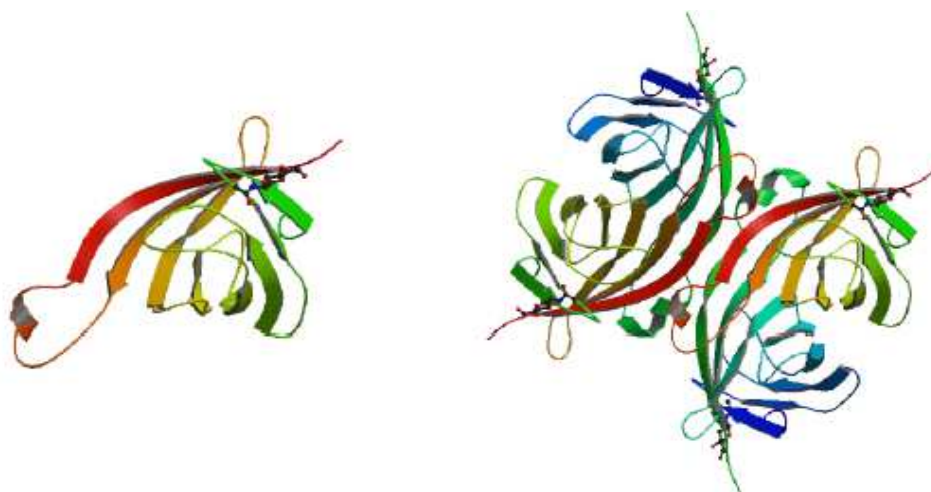
Figure 3: Structure of avidin. Monomer unit (left) and natural tetramer (right).[24]

Avidin is a tetrameric protein, composed of four subunits of identical amino acid composition and sequence, each possessing one biotin binding site. Structure of avidin is presented in Figure 3. A binding site which exhibits such a strong affinity to biotin is also expected to interact with other molecules with smaller strength or specificity. Avidin is able to bind to a variety of different dyes and peptides which have no structural similarity to biotin. One such compound for avidin is a dye, 2-(4'-hydroxyazobenzene) benzoic acid (HABA), which provides an additional system for studying low-affinity protein–ligand interactions. HABA has become very important in avidin-biotin technology since it can be readily used to determine the amount and biotin binding activity of avidin in solution.[25]

7
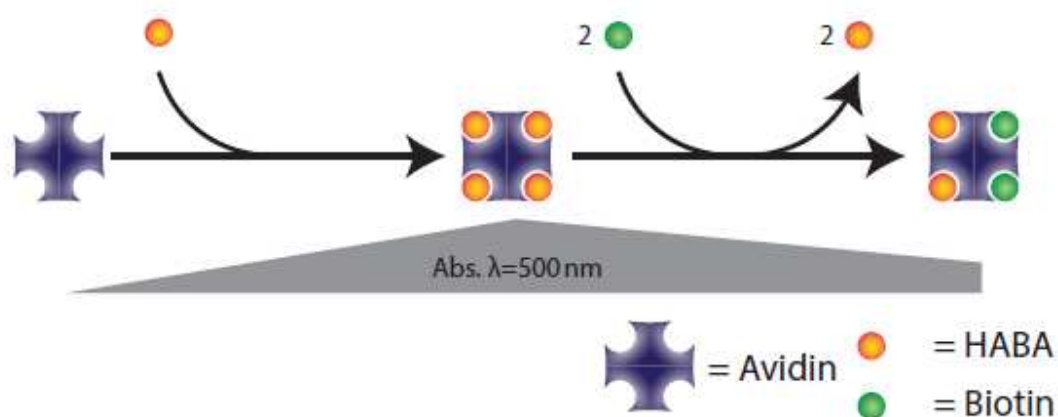
Figure 4: Scheme presenting the ability of HABA to determine biotin binding activity of avidin in solution.[26]

The use of HABA enables a quick estimation of the mole-to-mole ratio of biotin to protein. Quantification of the amount of incorporated biotin is based on the change in absorbance related to the amount of biotin in the sample. A solution containing the biotinylated protein is added to a mixture of HABA and avidin and because of its higher affinity to avidin, biotin displaces the HABA from its interaction with avidin. Figure 4 presents the use of HABA for the estimation of biotin to protein ratio.

2.1.1. Streptavidin

Streptavidin is a 53-kDa protein isolated from the bacterium *Streptomyces avidinii*. It is similar to avidin with respect to its binding affinity toward biotin ($K_a \approx 10^{15}$ M^{-1}).[23] Streptavidin also has a high thermostability (T_m of 112°C for biotin-streptavidin) and is resistant against extreme pH, denaturing agents, and enzymatic degradation, which are important traits for the use under a wide range of experimental conditions.[27] The structure of streptavidin, similarly to avidin, consists of four identical subunits, where each subunit has a single biotin-binding site. The protein structure is shown in Figure 5.

Despite the similarities between avidin and streptavidin in their affinity to biotin and protein subunit conformation, they show different behavior in biochemical properties. Avidin is highly glycosylated containing terminal *N*-acetylglucosamine and mannose residues and approximately 10% of its mass belongs to carbohydrates,[28] whereas streptavidin contains no carbohydrate residues. Additionally, avidin contains twice as many basic amino acids, lysine and arginine as streptavidin, which makes it positively charged with an isoelectric point of approximately 10, whereas the isoelectric point of streptavidin is in the range of 5-8.[23] Moderation in overall charge of streptavidin substantially reduces the amount of nonspecific binding due to the ionic interaction with other molecules. Due to these factors, the use of streptavidin – biotin system leads to better signal-to-noise ratios in different assays than employing an avidin-biotin system.
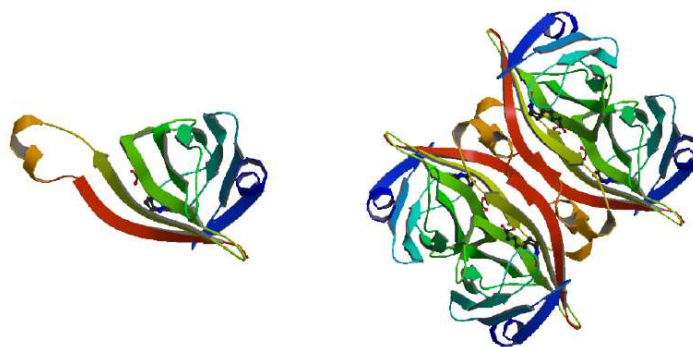
Figure 5: Structure of Streptavidin. Monomer unit (left), Tetramer unit with biotin molecules.[29]

2.1.2. Neutravidin

Due to its glycosylation and high pI the utility of avidin is somewhat limited by nonspecific interactions. Neutravidin is a 60-kDa deglycosylated form of avidin, which possesses enhanced biotin binding specificity. The neutravidin protein does not contain carbohydrates, thus lowering the nonspecific binding, relative to avidin, without significantly affecting the affinity to biotin.[30] Table 1 presents the comparison between different biotin-binding proteins.

9

Table 1. Properties of different biotin-binding proteins.[31]

Protein	Avidin	Strepavidin	Neutravidin
Molecular Weight	67 kDa	53 kDa	60 kDa
Biotin-binding Sites	4	4	4
Isoelectric Point	10	5-8	6.3
Specificity to biotin binding	Low	High	Highest

3. Molecular recognition of folic acid by folate receptors

Nowadays, nanomaterials are being tested and used for the improvement and development of new technologies in cancer detection, prevention, and treatment. Due to their size and possibility for surface functionalization, nanoparticles can be designed to be used as passive or active targeting systems with superior tumor specificity compared to the currently used drug methods.

Passive targeting takes advantage of the permeability of tumor tissue. Cancer cells grow rapidly, what requires rapid vascularization leading to a leaky and defective architecture. Such vascular architecture with defects is more permeable to bigger particles than it is in normal tissues, and with the lack of lymphatic drainage in the tumor bed the result is the accumulation of the drug within cancer cells. This effect is called the enhanced permeability and retention effect (EPR) and is illustrated in Figure 6(a). The EPR effect also affects the ability of a cell to uptake vital nutrients and oxygen. If a suitable polymer carrier is coupled with a chemotherapeutic agent via a degradable linker, then such carriers have the potential of increasing the concentration of the chemotherapeutic agent within the tumor tissue. As a result, the concentrations of polymer-drug conjugates in tumor tissue can reach levels 10 to 100 times higher than the ones resulting from the administration of the free drug. [32]

Folate targeted drug delivery has emerged as an alternative therapy for the treatment of many cancers and inflammatory diseases. Because of its small molecular size and high binding affinity to cell surface folate receptors (FR), folate conjugates gained attention due to the ability to deliver a variety of molecular complexes to pathologic cells without causing harm to normal tissues.[33] FR are overexpressed on epithelial cancers of the ovary, mammary gland, colon, kidney, lung, prostate, thymus and brain.[34, 35]
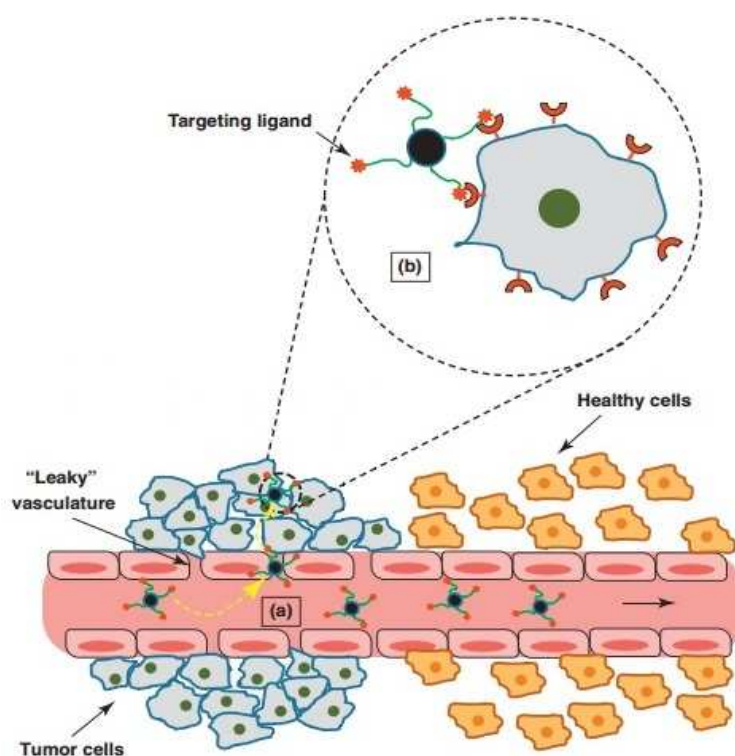
Figure 6: Concept of tumor-targeting nanoparticles. (a) EPR effect. Leaky vasculature in tumor cells compared to healthy cells, owing to fenestrations and gaps between endothelial cells that result from abnormal angiogenesis. Nanoparticles in circulation can passively extravagate through these gaps and enter the tumor interstitium. (b) Molecular targeting. Nanoparticles with folate ligands targeted toward folate receptors overexpressed on the surface of tumor cells can be used to actively enhance accumulation of the drug at the tumor site and can also help to internalize nanoparticles into cells via endocytosis. [36]

Folates (vitamin B9) are important one-carbon donors involved in the amino acid metabolism, the synthesis of purines and thymidine — essential components of nucleic acids and formation of the primary methylating agent, *S*-adenosylmethionine, involved in synthesis of DNA, proteins and lipids.[37] Cell survival and proliferation are dependent on the cell's ability to acquire the vitamin and its deficiency is therefore associated with many diseases, including fetal neural tube defects, cardiovascular disease and cancers.[38]

Folates are hydrophilic anionic molecules that do not cross the cellular membrane alone. They can enter the cell through two different routes. One way is by the reduced folate carrier (RFC), a bidirectional anion-exchange mechanism, which has low affinity to folate. The ubiquitously expressed RFC is the major transporter of folates in mammalian cells and tissues, which transports folate cofactors from the blood into cells of peripheral tissues. The other possibility to enter the cell is by using the FR pathway, which has a high affinity to folate. Such an active targeting system using FR and folate conjugates is presented in Figure 6(b). The FR is overexpressed on many rapidly dividing cancer cells and not significantly expressed on most normal tissues.[39] Once folate conjugates are bound to a cell surface FR, they are transported into the cell through a process called receptor-mediated endocytosis by engulfing them within a vesicle called the endosome.[40] After membrane invagination and internalization to form an endosome, a proton pump lowers the pH inside the endosome. Since the binding of folic acid to its receptor is pH dependent, by decreasing the pH it can be anticipated that some of the folate conjugates will escape the endosome resulting in drug deposition in the cytoplasm and membrane bound FR mostly recycle back to the cell surface, allowing for delivery of additional folate-linked drugs into the cell. [33]
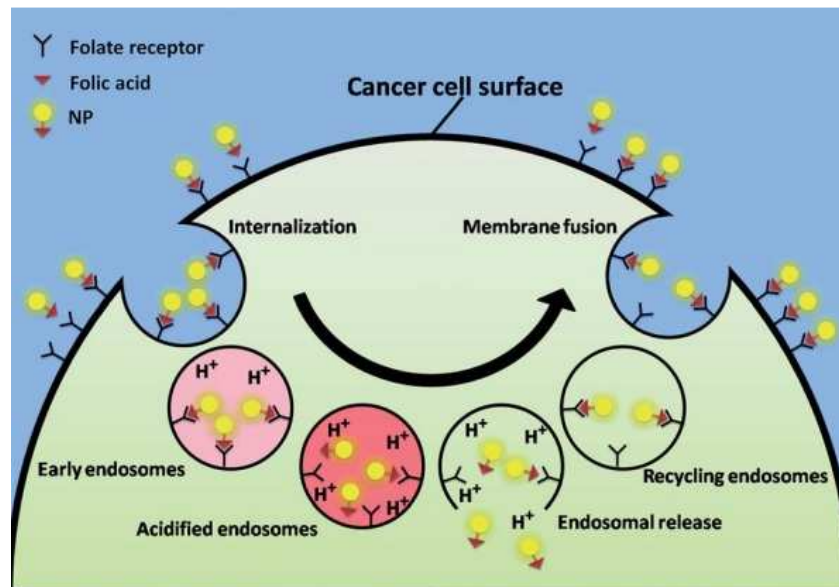
Figure 7: Folate-mediated delivery of therapeutic agents to cancer cells expressing folate receptors. Two types of strategies can be envisioned: a fraction of the drug carrying nanoparticle (NP) functionalized with folic acid will traffic into the cancer cells by receptor-mediated endocytosis (left side of diagram), while the rest will remain on the cell surfaces (right side of diagram).[41]

4. Biohybrid structures

Hybrid has been used as a fashionable term in scientific publications during the past years to describe a functional unit consisting of two different elements, possessing a mixed character of the initial materials. Biohybrid relates to the material containing or being composed of both biological and non-biological components. The biological part of the biohybrid could consist of cells or bioactive molecules, while the structural part is of non-biological origin. Biohybrid materials are currently used as implants or transplants in regenerative medicine or in vitro applications such as assays, biosensors or bioreactors.[42, 43]

13

4.1.   Conjugation chemistry in biohybrid materials

The choice of conjugation strategy is initially dictated by a combination of factors including the chemical composition of material, size, shape, surface chemistry (the nature of the surface ligands and their available functional groups), the type of biological molecule, its size and chemical composition, and the utility desired in the final application. The two most widely used conjugation methods between the components in biohybrid structures are covalent binding (including covalent coupling of biological component to the nanoparticle surface or surface ligand) or noncovalent interactions (including electrostatic attraction, adsorption, encapsulation and specific secondary interactions).[44]

4.1.1.   Covalent binding

The covalent bond is the most common form of the linkage between the atoms in organic chemistry and biochemistry. The reaction between two functional groups leads to the formation of a covalent bond via sharing electrons between the atoms. Covalent interactions are generally categorized as random (modification at multiple sites) or site-specific (modification at a single site). Many different types of covalent modifications can be performed with the use of reactive functional groups present or introduced (like carboxylic acids, aldehydes, ketones, amines, thiols, etc.) on the macromolecules (peptide, proteins, carbohydrate, nucleic acids etc.). Covalent chemistry also commonly involves the use of activation agents that function as a molecular bridge between the macromolecule and the biological entity.

4.1.2.   Non covalent interactions

The simplest non covalent bioconjugation approach is electrostatic interaction, in which the attraction between oppositely charged species causes the electrostatic immobilization of small molecules or biomolecules. This concept is rather intuitive, nevertheless, its implementation shows several complications at the nanoscale since electrostatic effects are amplified, and

other factors such as ionic strength, the concentration of reagents, and the type and magnitude of charge are significant in obtaining the desired conjugates. Other noncovalent chemistries use encapsulation, hydrophobic–hydrophobic or host–guest interactions etc. Specific secondary interactions between functional groups bound to the surface of a particle are another class of noncovalent interactions. This group is represented by e.g. biotin-avidin interaction, β-cyclodextrin-adamantane, concanavalin A – sugars, which will be described in detail below.

4.1.2.1. β-Cyclodextrin-adamantane host–guest interactions

Supramolecular host-guest chemistry describes the formation of molecular complexes composed of small molecules (guests) noncovalently bound to larger molecules (hosts) in a unique structural relationship.
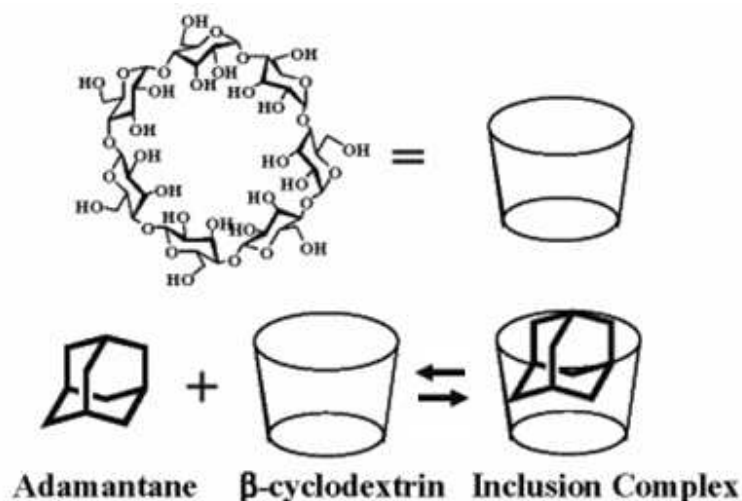
Figure 8: Schematic of adamantane and β-cyclodextrin inclusion complex formation.[45]

Cyclodextrins are naturally occurring water-soluble cyclic oligosaccharides formed by monomers of D-glucopyranose bound together by means of α-1,4-glucosidic linkages and closed in a ring to form a hollow structure of a truncated cone. The three dimensional structure forces the hydroxyl groups on the outer edges, whereas the internal cavity is highly hydrophobic and has the ability to form inclusion complexes with a variety of organic and

15

inorganic substrates. The ability of cyclodextrins to include hydrophobic molecules in order to increase their solubility in water has led to a variety of applications in the field of pharmaceutics.[46] Among many hydrophobic or amphiphilic molecules studied as guests of β-cyclodextrin internal cavity, special attention has been paid to adamantyl moiety because it perfectly fits into the β-cyclodextrin cavity. Adamantane is theoretically formed by four cyclohexanes, achieving a strain free and highly symmetrical stable structure. It has a spherical group which perfectly matches the cavity of β-cyclodextrin, forming an inclusion complex with high values of the association equilibrium constant, typically in the range of 10^4–10^5 M^{-1}.[47] A scheme of adamantane and β-cyclodextrin inclusion complexes formation is shown in Figure 8. Due to their high stability, complexes of β-cyclodextrin with adamantane found numerous important applications in supramolecular chemistry by combining linear or branched polymers bearing cyclodextrin structures and linear polymers bearing adamantyl groups to build polymeric systems[48] and in biomedical applications, such as hydrogels[49] or surface-mediated gene delivery systems.[45]

4.1.2.2. Concanavalin A – sugars

Lectins are proteins representing a class of carbohydrate binding agents, which are primarily extracted from plants and show binding specificity to certain sugar moieties. Concanavalin A (Con A) is a saccharide-binding lectin originally extracted from the jack bean, which shows reversible strong affinity for sugars, glycoproteins, and glycolipids, containing internal and non-reducing terminal α-D-mannosyl and α-D-glucosyl groups. Con A is a tetramer consisting of four identical subunits that bind with moderate affinity (K_d≈120-500 μM) to α-anomers of D-mannose and D-glucose. To depict its binding activity, the protein requires metal ions. In the native state of Con A, one molecule binds two metal atoms: Ca^{2+} and Mn^{2+}. The binding sites for the sugar are located adjacent to the metal atoms. In the active state of Con A, four subunits are combined together to form a functional aggregate with four binding sites. When sugar expressing units are present on the cell surface, Con A binds with high avidity due to the multivalent interactions.[50] Such specific interactions with particular

16

sugars made the Con A capable to use as part of a specific cell recognition process or stimuli responsive material for the delivery of insulin.[51]

4.1.2.3. Biotin – avidin chemistry

The avidin–biotin complex represents one of the strongest known noncovalent interactions with an association constant (K_a) of 10^{15} M^{-1}. Avidin, as described previously in chapter 2.1, is a glycoprotein which comprises a tetrameric subunit structure, with each subunit capable of binding one biotin molecule. Biotin is a water-soluble organic compound, also known as vitamin B7 or vitamin H. It acts as an essential coenzyme for several carboxylase enzymes, which control the metabolism of fatty acids, amino acids, and glucose and are also thought to be involved in transcriptional gene expression and stability.[52]

There is a variety of biotin derivatives that make biotinylation of nanoparticles and biological molecules rather easy. There are also a great number of commercially available products containing biotin which are intended to "biotinylate" their target cognate group on biologicals, particularly proteins and antibodies, along with the nanoparticle. There are two principle methods of bioconjugation using biotin–avidin chemistry, which are illustrated in Figure 9. The first method involves an avidin-functionalized nanoparticle being mixed with a biotinylated biomolecule. Using this method, avidin will probably obscure one or more available biotin binding sites during initial modification of the particle. The final nanoparticle functionalized with the avidin will probably display many different orientations and an average range of available binding sites. In the second method, which is often used in conjunction with polymer-based nanoparticles, the monomer unit is biotinylated prior to its incorporation into the particle. In such an approach, typically the biomolecule is also biotinylated, and the two are cross-linked via an avidin intermediary. It is also possible to add a PEG, or another extended linker, inserted adjacent to the biotin group to facilitate binding within avidin's relatively deep binding pocket.[53]
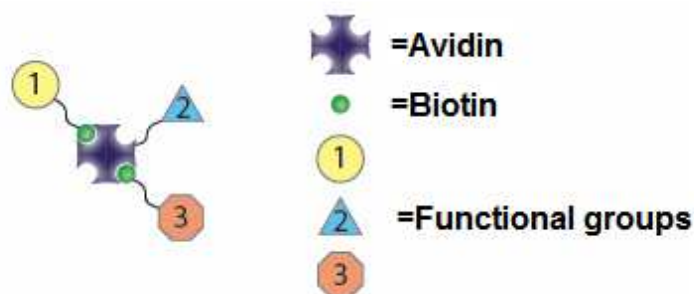
Figure 9: Possible methods of bioconjugation using biotin-avidin chemistry. 1 and 3 – modification through biotinylation of functional groups. 2 – direct modification of avidin.[26]

Avidin-biotin technology has been used in many applications, such as delivery of diagnostic agents,[23] in molecular biorecognition,[54] or cell imaging.[55] The use of the high-affinity nature of avidin is also a versatile approach to target nanoparticles into the tumor tissue. Recently, this technology has been frequently applied for drug targeting.[56, 57] The three-step method using avidin–biotin technology that is used in human imaging and cancer therapy is based on the following steps: (i) administration of biotinylated targeting ligands, (ii) administration of avidin and (iii) administration of biotinylated drug or drug-loaded carrier.[58]

Such avidin – biotin systems were used by Ennen et al. in order to synthesize biohybrid structures consisting of biotinylated glycodendrimers and proteins for future biomedical applications.[53] Poly(propylene imine) dendrimers of the 4th generation modified with an oligosaccharide shell and possessing biotin ligands with varied spacer lengths and different biotinylation degrees were investigated in the frame of interaction with avidin. It was shown that the coupling of the biotinylated glycodendrimers to avidin as a central and bridging building block leads to nanometer-sized biohybrid structures with potential functionalities. Fabrication of such biohybrid structures is tailored by inter- and intramolecular association and dissociation steps until final sizes of the supramolecular structures are achieved. It was determined that by using different molar interaction ratios between mono-, bi- and tetravalent biotinylated glycodendrimers and avidin, different nanometer-sized biohybrid structures can be fabricated. It was shown that size dimension of the biohybrid structures can be controlled

mainly by the degree of biotinylation and the defined ligand–receptor stoichiometries. Furthermore, the longer biotin-PEG$_{12}$-COOH ligand was proved to be the more effective in the bioconjugation strategy than the shorter 6-(N-biotinylamino)caproic acid ligand for establishing the biohybrid structures with avidin as a central unit. In another study it was investigated to what extent the size and flexibility of the dendritic scaffold, the degree of biotinylation of the biotinylated glycopolymer, the ligand–receptor stoichiometry of avidin to biotinylated glycopolymer, and the length and/or chemical structure of the biotin ligand impact the properties of the formed biohybrid structures composed of avidin and biotinylated glycopolymer.[59] Such nanostructures were investigated with regard to their potential biomedical applications as a multifunctional platform with short- and long-term stability properties. This research showed the opportunity to design more complex nanostructures based on sequential polyassociation reactions with at least two different biotinylated molecules and/or the use of at least two different conjugation strategies (e.g. avidin–biotin and adamantane-β-cyclodextrin) for future biomedical and biotechnological applications in the field of fabrication of larger and uniformly nanometer-sized biohybrid structures with specific biological functions.

The challenge for such kinds of systems is a complete conversion of both glycopolymer and avidin. The future task would be to establish a glycopolymer with higher biotinylization degree. The optimal number of biotin ligands should be between 5 and 8 in order to achieve the full conversion of both glycopolymer-biotin system and avidin. The other open question concerns if such materials can be additionally functionalized through further non-covalent interactions. It was proved that avidin still possesses free binding pockets in the formed biohybrid structures that could be possibly used for the other functionalization through the biotin-PEG chain. The other possibility for the future is establishing avidin-biotin-PEG-glycopolymer precomplex for further functionalization of free biotin ligands of the glycopolymers through another biotin acceptor.

5. Methods

5.1. Dynamic light scattering

Light scattering occurs on polarizable solid and liquid particles (or molecules) illuminated with a light beam because of the differences in the dielectric properties of the material and the surrounding media. Colloidal sized particles in a liquid undergo random ("Brownian") motion owing to multiple collisions with the thermally driven molecules of the liquid and causing short-term fluctuations in the measured intensity of the scattered light that carry the information about the diffusion coefficient of the particles.[60] According to the Stokes-Einstein theory of Brownian motion, movement of the particle is dependent on the suspending fluid viscosity, temperature, electrical charge, electrical mobility and the size of the particle, as seen in the following equations:

$$D = \frac{k_B T}{6\pi\eta r}$$

$$D = \frac{\mu_q k_B T}{q}$$

where D is diffusion constant, q is electrical charge, μ_q is electrical mobility of the charged particle, k_B is Boltzmann's constant, T is absolute temperature, η is viscosity, and r is the radius of the spherical particle.[61] Using Stokes-Einstein theory, determination of the particle motion in a fluid of known temperature and viscosity can lead to the determination of particle size. The rate of the movement is inversely proportional to the particle size in solution (the smaller the particles are, the faster their motion or diffusion), and is analyzed by measurement of light intensity fluctuations scattered over the time from the particles when they are illuminated with a laser beam. Various terms have been proposed for this phenomenon: photon correlation spectroscopy (PCS), dynamic light scattering (DLS), quasi-elastic light scattering (QELS) and others. DLS measures the Brownian motion of the particles and relates this movement to an equivalent hydrodynamic size. Through application of the autocorrelation

function and subsequent calculation of the exponential decay, average particle size can be obtained from the time-dependent fluctuations in light intensity.

5.2. Zeta potential

Zeta potential measurement is a measure of the electrical charge developed when a solid surface is brought into contact with an aqueous solution. Zeta potential is the electrical potential at the shear plane of the electric double layer. It depends on the properties of liquid as well as on the properties of the surface.

In the solution free ions tend to rearrange themselves in such a way that a thin region of non-zero net charge density exists near the interface. The development of a net charge at the particle surface affects the distribution of ions in the surrounding interfacial region, resulting in an increased concentration of counter ions close to the surface and an electrical double layer (EDL) formation around each particle. The EDL consists of two parts, an inner region called the Stern layer, in which the ions are strongly bound and an outer region called diffuse layer, in which they are mobile. As presented in Figure 10, the stern layer has an approximate one ion radius thickness. Counterions experience strong electrostatic forces there and are essentially immobilized against the surface. Ions located in the diffuse layer experience a weaker electrostatic attraction. Due to the competing electrostatic and thermal forces, concentration of ions in the diffuse layer is the highest at the surface and decreases gradually with distance until it reaches equilibrium with the bulk concentration. The thickness of the diffuse layer is often characterized by the Debye length λ_D and it can vary from several nanometers to micrometers depending on the concentration and properties of the solution.

The boundary between the stern and diffuse layer is called shear plane and zeta potential is the electrostatic potential at the boundary dividing those regions. Depending on the solid surface and the solution, zeta potentials values are within a range of -100 mV to $+100$ mV for most solid– liquid interfaces in aqueous solutions.[62]
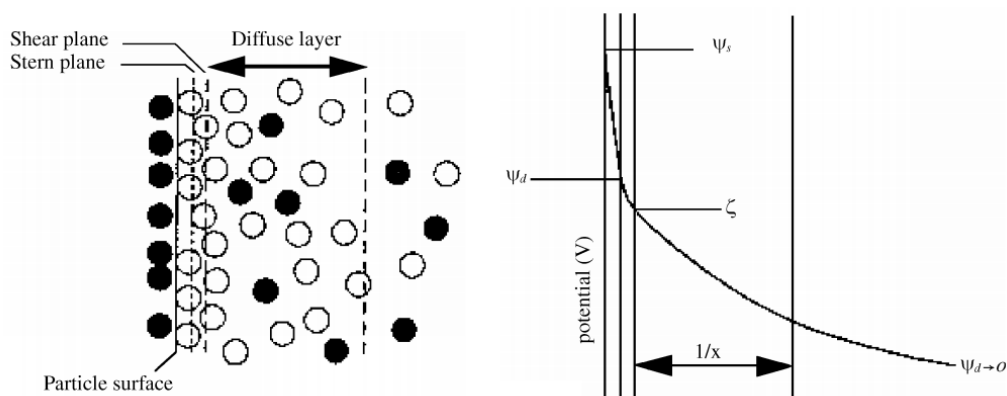
Figure 10: Schematic representation of the electric double layer.[62]

5.3. Alamar Blue Assay

The Alamar Blue test is an assay which has been widely used in studies on cell viability and cytotoxicity in a range of biological and environmental applications. It can be used to assess different types of human and animal cell lines, as well as various bacteria, yeast and fungus species. The Alamar Blue reagent is a water-soluble dye that is used for quantifying in vitro viability of cells. It is very stable, permeable through cell membranes and nontoxic to the cells which allows for continuous monitoring of cultures. The active ingredient of Alamar Blue is resazurin, also known as diazo-resorcinol, azoresorcin, resazoin or resazurine. It is a blue non-fluorescent dye which changes to highly fluorescent pink-colored resorufin upon reduction of the oxidized form. The change of the structure is presented in Figure 11. Resazurin can be reduced by NADPH, FADH, FMNH, NADH, as well as the cytochromes and other enzymes (such as the diaphorases, dihydrolipoamine dehydrogenase, NAD(P)H:quinone oxidoreductase and flavin reductase) located in the cytoplasm and mitochondria. This change from oxidized to reduced state allows for quantitative (colorimetric and/or fluorometric readings) or qualitative measurement (visible change in color indicating presence or absence of viable cells). Spectrophotometric absorbance is measured at two wavelengths (570 and 600 nm or 540 and 630 nm) and fluorescence signals are measured at an excitation wavelength at 530–560 nm and an emission wavelength at 590 nm.[63]

22
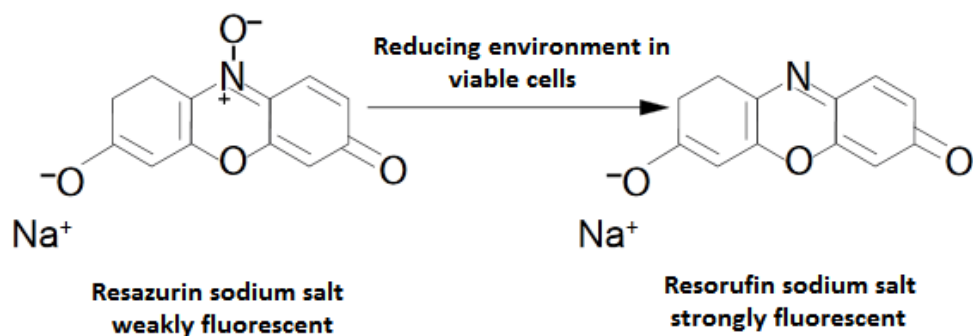
Figure 11: Alamar Blue assay principle. Reduction of resazurin converts the essentially nonfluorescent dye to the highly pink fluorescent resorufin

5.4. Flow cytometry

Flow cytometry is an analytical technique which provides rapid analysis of multiple characteristics of single cells. It measures the optical and fluorescence characteristics of single cells (or any other particle, including nuclei, microorganisms, chromosome preparations, bone marrow, urine, and solid tissues). The information obtained is both qualitative and quantitative and it includes physical properties such as size (represented by forward angle light scatter), internal complexity (represented by right-angle scatter), DNA or RNA content, and a wide range of membrane-bound and intracellular proteins. Typically fluorescent dyes are bound or intercalated with different cellular components such as DNA or RNA, or antibodies conjugated to fluorescent dyes that can bind specific proteins to cell membranes or inside the cells.[64] Inside a flow cytometer, labeled cells pass through a light source, causing the excitation of the fluorescent molecules to a higher energy state. Upon returning to their initial states, light is emitted in all directions and collected via optics that direct the light to a series of filters and dichroic mirrors that isolate particular wavelength bands. Using multiple fluorochromes with similar excitation wavelengths and different emission wavelengths it is possible to measure several cell properties simultaneously. The resulting information is usually displayed in histogram or two dimensional dot-plot graphs.
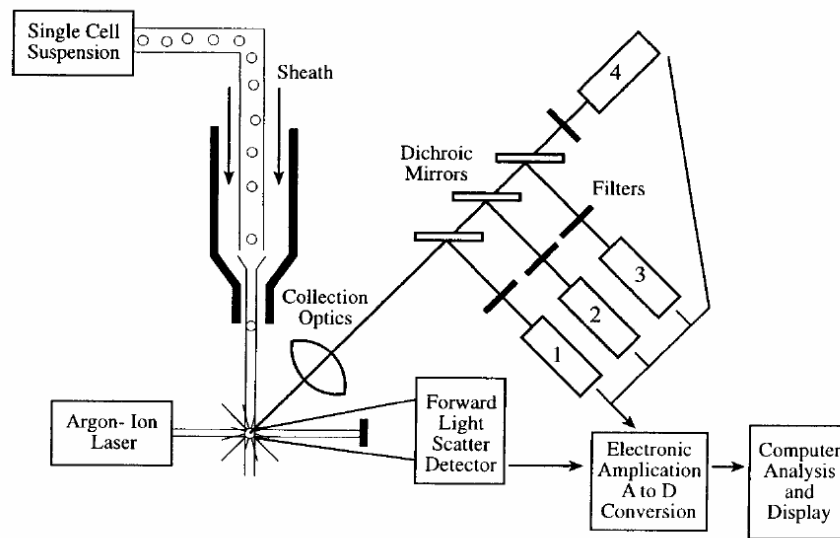
Figure 12: Principle of a flow cytometer. A single cell suspension is hydrodynamically focused with fluid stream to intersect a light source. Signals are collected by a forward angle light scatter detector, a sidescatter detector (1), and multiple fluorescence emission detectors (2–4). The signals are amplified and converted to digital signal and displayed on the computer.[64]

Flow cytometer consists of three main systems: fluidics, optics and electronics. Fluidic system permits the hydrodynamic focusing, which means that it is drawing the suspension of cells into a stream created by a surrounding sheath of isotonic fluid that creates laminar flow, allowing the cells to pass one by one across the laser beam for individual analysis. In the optics system, a beam of monochromatic light intersects the cells and it is the starting point of fluorescence emissions and light scattering (forward scatter and side scatter) which is measured at different angles. Nowadays, diode lasers or lasers are used for the excitation light sources. Optical lenses are also used to control illumination point geometry with very good light focalization. Side scatter and fluorescent lights are filtered by dichroic mirrors and emission filters into an emission optical system which directs lights at different wavelengths towards appropriate detectors. In the electronics system, the light signals are detected by photomultiplier tubes and digitized for computer analysis. Flow cytometers can be also

24

equipped with cell sorters, which has the possibility of isolating subpopulations of cells of interest with high recovery and high degree of purity from heterogeneous cell mixtures based on light scattering and fluorescent characteristics.[65] Figure 12 presents the schematic diagram of the fluidic and optical components of a flow cytometer.

II. Aim of the thesis

The activity of pharmaceuticals against certain diseases is mostly not based on their ability to accumulate selectively in the pathological organ, tissue or cell. Usually, the pharmaceutical agents are rather evenly distributed within large areas of the body, independently from the route of administration. In order to reach the site of action, the drug has to cross many biological barriers, such as other organs, cells and intracellular compartments, where it can be inactivated or express undesirable influence on organs and tissues that are not involved in the pathological processes. As a result, the drug has to be administered in large quantities to achieve a required therapeutic concentration in a certain body compartment, the great part of which is wasted in normal tissues and can cause many negative side effects.[66]

Drug targeting can bring a solution to all these problems. It is the ability of the drug to accumulate in the target organ or tissue selectively and quantitatively, independent of the site and methods of its administration.[67] In the ideal case, the local concentration of the drug at the disease site should be high, while its concentration in the other non-target organs and tissues should be below certain minimal level to prevent any negative side-reactions.

The aim of this thesis is the fabrication and characterization of the novel, tailor-made nanocarrier with the defined size and structure for the selective targeting to the tumor tissues. The biohybrid structures (BHS) based on streptavidin and pentavalent biotinylated dendritic glycopolymer will be fabricated through non-covalent streptavidin-biotin conjugation and further functionalized with the folic acid for the specific targeting to tumor cells. The system is schematically presented in Figure 13. It will be investigated if it is possible to further functionalize such BHS through additional streptavidin-biotin interaction and if such system could be applied in biomedical applications as targeting carrier. It will be determined if there are accessible functional units at the surface of BHS that could be used for further functionalizations.

The cytotoxicity of the BHS will be investigated to assess the biocompatibility of the system. The comparison between the molecular uptake in normal and cancer cells will be made in order to prove the ability of the system for the selective targeting to the tumor cells. The influence of the type of protein, amount of folic acid and the length of the PEG-chain / spacer will be evaluated, just as the impact of purification strategies to show the influence of the folic acid ligand as targeting function towards folate receptor expressing cancer cells. Cell uptake mechanism will be also investigated. Furthermore, the physical properties of the BHS will be analyzed by dynamic light scattering and zeta potential measurements. Additionally, the long term stability properties of the structures together with the stability towards excess biotin ligands will be determined.
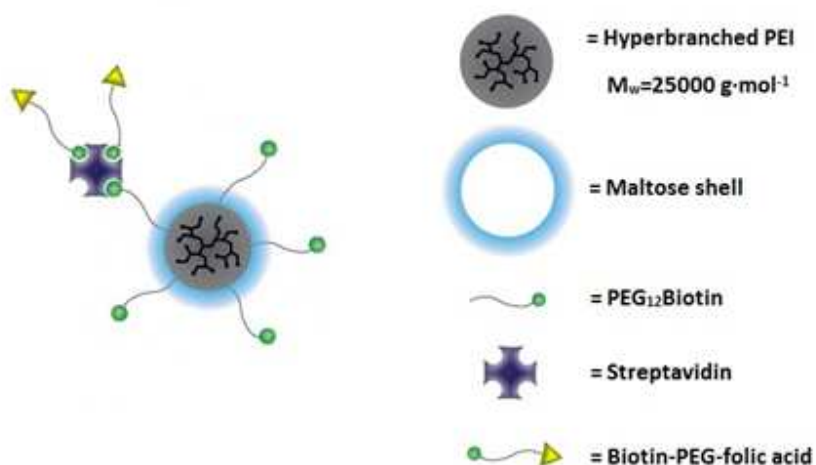
Figure 13: Schematic presentation of the biohybrid structure consisted of biotinylated glycopolymer and streptavidin and modified with folic acid fabricated in the frame of the thesis.

III. Results and discussion

1. Introduction to biohybrid structures

Biohybrid structures (BHS) fabricated in the frame of this thesis consists of dendritic glycopolymers which are conjugated through biotin – streptavidin interaction and further functionalized with chains terminated with the folic acid.
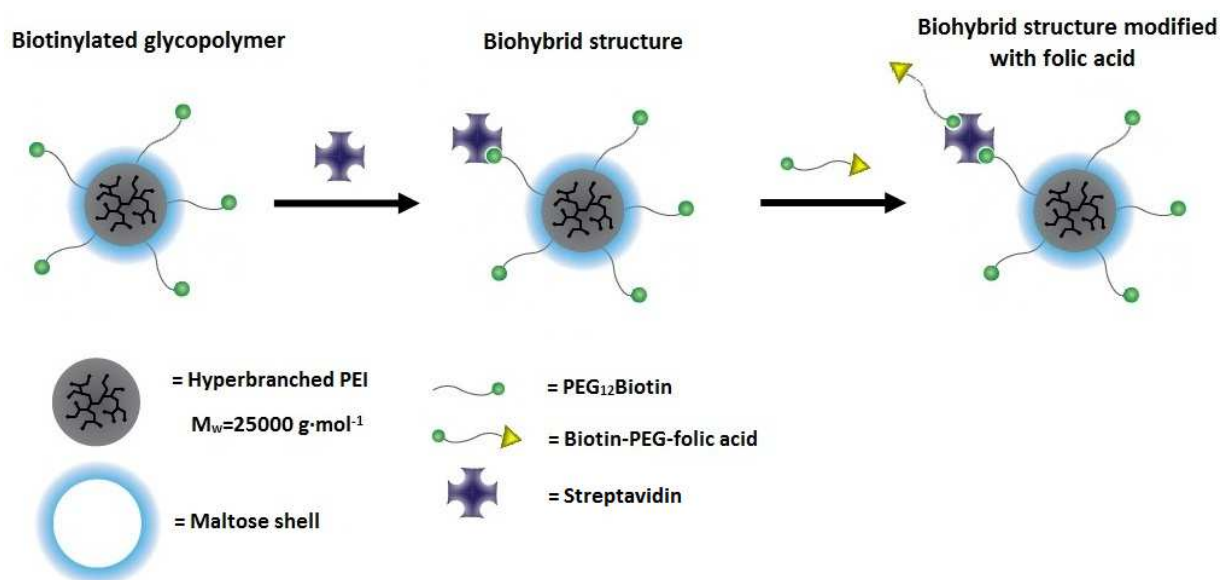
Figure 14: Synthesis scheme of the biohybrid structures modified with the folic acid.

The central unit of the system is hyperbranched poly(ethylene imine) (PEI) with the average molecular weight of 25000 g·mol^{-1}, which was functionalized through the poly(ethylene glycol)$_{12}$-biotin (PEG$_{12}$-biotin) ligand. The fabricated structure possesses five PEG$_{12}$-biotin ligands. Biotinylization of the polymer enabled further formation of BHS by conjugation through one of the strongest known non-covalent interaction of biotin with streptavidin (SA). In order to decrease the cytotoxicity of PEI and decrease the surface charge of the structure,

the polymer was glycosylated using maltose and the glycopolymer with the dense-shell architecture was obtained. The modification of PEI with maltose and PEG_{12}-biotin was performed by Johannes Fingernagel, member of the working group of Dr Appelhans. Total molecular weight of dendritic glycopolymer calculated by elemental analysis was 74 300 $g \cdot mol^{-1}$.

Table 2. Overview of the components and biohybrid structures

Systematic description	Abbreviation
PEI_{25k}-$(PEG_{12}Biotin)_5$-Maltose	PEI-biotin
Streptavidin	SA
PEI_{25k}-$(PEG_{12}Biotin)_5$-Maltose + Streptavidin	BHS
Biotin-PEG-Folic acid	Folate
Biotin-PEG-COOH	Biotin-PEG
PEI_{25k}-$(PEG_{12}Biotin)_5$-Maltose + Streptavidin + Biotin-PEG-Folic $acid_{2k}$	BHS-Folate2k
PEI_{25k}-$(PEG_{12}Biotin)_5$-Maltose + Streptavidin + Biotin-PEG-Folic $acid_{5k}$	BHS-Folate5k
PEI_{25k}-$(PEG_{12}Biotin)_5$-Maltose + Streptavidin + Biotin-PEG-$COOH_{2k}$	BHS-Biotin-PEG2k
PEI_{25k}-$(PEG_{12}Biotin)_5$-Maltose + Streptavidin + Biotin-PEG-$COOH_{5k}$	BHS-Biotin-PEG5k

BHS composed of modified PEI-biotin and SA were further functionalized with the biotin-PEG-folic acid (folate) chain in order to increase the specific targeting to the cancer cells or with the biotin-PEG-COOH (biotin-PEG) chain as a reference. Two different chain lengths

were used: 2000 g·mol^{-1} and 5000 g·mol^{-1} and structures with different ratios of PEI-biotin/SA/Folate were tested. The scheme of the BHS formation and modification with the folic acid is presented in Figure 14 and all the fabricated BHS are listed in Table 2 together with the introduced abbreviations that will be further used in the thesis.

2.   Characterization of the BHS size by DLS

2.1.   Formation of the BHS

In order to prove the formation of BHS, the measurements of size were performed with the use of DLS technique. In Figure 15, the sizes of hydrodynamic diameters of PEI-biotin, SA and the BHS in the molar ratio of SA/PEI-biotin 1/1 are presented.
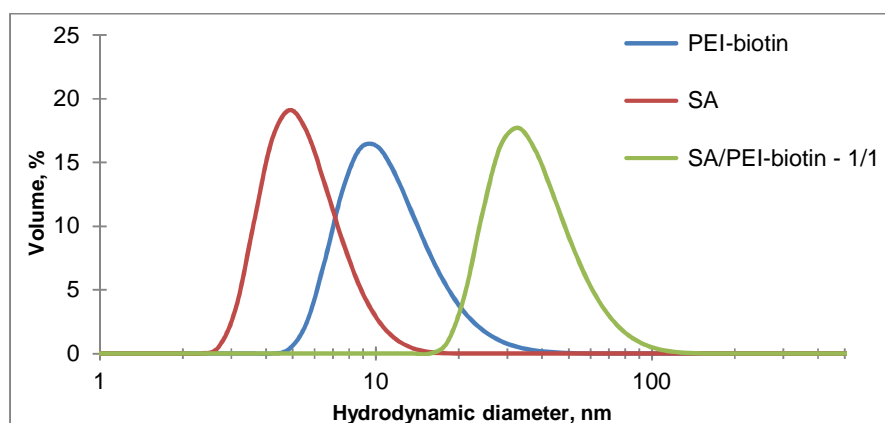
Figure 15: Size of the single components and the biohybrid structures

Solution containing only PEI-biotin was measured having the particles with the diameter of around 10-12 nm. Particles of the protein have the average diameter of 5-6 nm. Measurement of the BHS consisting of these 2 components clearly showed the shift in the size up to 38 nm what proves the formation of the structures via biotin – streptavidin interaction through the polyassociation reaction.

2.2. Comparison between BHS fabricated with different ratios of SA/PEI-biotin

The next step was the comparison of the size of the structures fabricated with different molar ratios of SA/PEI-biotin. Structures with the molar ratios 1/0.5, 1/1 and 1/2 were prepared and the results of DLS measurement are presented in Figure 16.
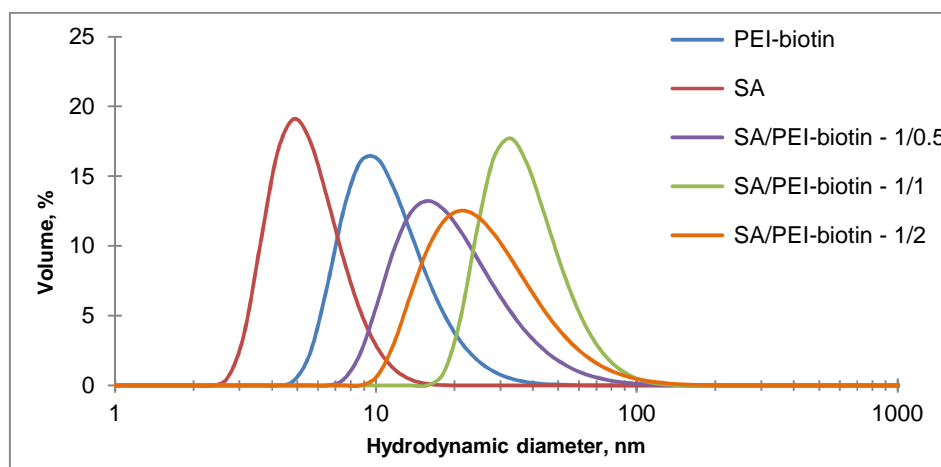
Figure 16: Comparison of the BHS size fabricated from different ratios of SA/PEI-biotin

Using streptavidin–biotin conjugation as the deciding non-covalent interaction step, different nanometer-sized biohybrid structures can be established and size can be controlled by using different molar ratios between SA and PEI-biotin. Structures formed from the mixture of SA and PEI-biotin in the ratio 1/1 have the highest average diameter compared with the structures formed from the ratio 1/0.5 or 1/2. Table 3 presents the comparison between molar ratio and ligand stoichiometry of different BHS. In the previous study of Dr Appelhans group, it was established that SA has in average 3.6 free binding pockets per molecule and PEI is modified with 5 PEG$_{12}$-biotin ligands. In Table 3 it can be seen that depending on the stoichiometry of the components, structures with the excess of free binding pockets or the excess of biotin will be obtained.

Table 3. Comparison between molar ratio and ligand stoichiometry of BHS with different SA/PEI-biotin ratio. Mass concentration is given for the structures with the molar mass of SA 2.5 g·mol^{-1} and the corresponding PEI-biotin concentration.

Molar ratio of SA/PEI-biotin	Average hydrodynamic diameter, nm	Number of binding units		Ligand stoichiometry		Mass concentration, mg·ml^{-1}
		SA	PEI-biotin	SA	PEI-biotin	
1/0.5	22	3.6	2.5	1	0.69	0.31
1/1	38	3.6	5	1	1.39	0.40
1/2	29	3.6	7.5	1	2.08	0.59

In order to fabricate the structures with the optimal sizes, the ratio of the number of free binding pockets to biotin molecules should be close to one. As it can be seen in the example of 1/0.5 molar ratio, ligand stoichiometry below 1/1 dramatically decreased the size of the structure up to 22 nm. When the SA/PEI-biotin molar ratio is increased up to 1/2, the number of biotin molecules is doubled compared with the free binding pockets of the protein. Furthermore, decrease in the molar ratio from 1/1 to 1/0.5 caused a small decrease in the mass concentration of the structures. Doubling the amount of PEI-biotin, the mass concentration raised almost 50% compared with the structures of the ratio 1/1. The most optimal results were obtained for the SA/PEI-biotin ratio 1/1 and only this ratio will be used for the further modifications of the structures.

2.3. Size of non-modified and modified BHS

In the next step, the BHS were modified with folate and the difference between the size of non-modified and modified BHS was tested. Folate ligands were added in the ratio PEI-biotin/SA/Folate 1/1/6. In Figure 17 the influence of modification on the BHS size is presented on the example of BHS modified with Folate5k. After addition of folate there is no

measurable size change or a change is very minimal (around 1 nm). The folate molecules are comparatively small and there is no clear size change after the modification of BHS.
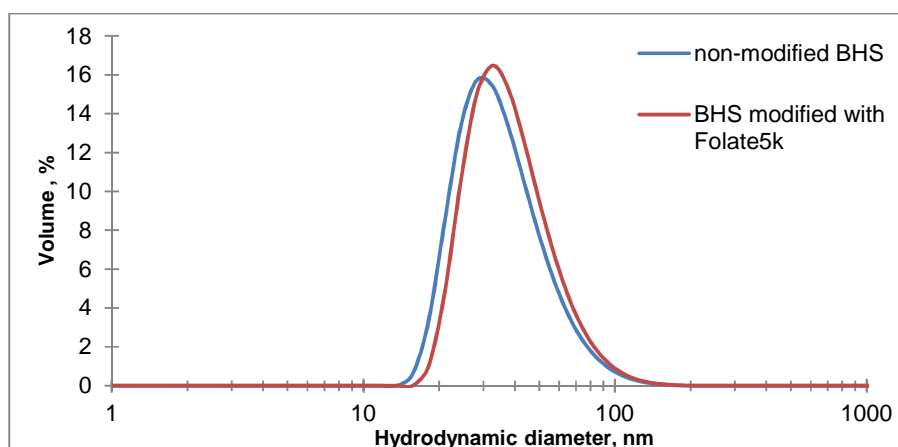
Figure 17: Comparison of the size of non-modified and modified with folate BHS

Important question here is how many folate ligands are able to bind to SA and how many free binding pockets of the protein are accessible on the surface of the structure for further modifications. In order to investigate it, the theoretical calculation how many available binding pockets are accessible on the surface and how many are inside the structure will be presented here. AF4 measurements obtained by Dr. Appelhans working group showed that BHS fabricated from SA/PEI-biotin molar ratio 1/1 have the hydrodynamic diameter of 49 nm and the molar mass of 1 146 000 g·mol^{-1}. Total number of SA molecules in the fabricated BHS is given by:

$$n\,SA = \frac{M_{BHS}}{(M_{PEI-biotin} + M_{SA})} = \frac{1146000\,\text{g}\cdot\text{mol}^{-1}}{(74300\,\text{g}\cdot\text{mol}^{-1} + 55000\,\text{g}\cdot\text{mol}^{-1})} = 8.86$$

Each SA molecule possesses in average 3.6 binding sites which means that the total number of SA binding pockets in BHS is equal to:

$$n\,binding\,pockets = 8.86 * 3.6 = 31.9$$

In the previous study of Dr Appelhans's group it was estimated that 50% of the avidin's binding pockets are available and for SA I will assume similar behavior:

$$n\ free\ binding\ pockets = 50\% * 31.9 = 15.95$$

In the next step the surface area of the BHS where the SA pockets are available to bind to other biotinylated molecules has to be estimated. In this calculation it will be assumed that the other molecules are able to bind to SA pockets which are available up to 5 nm depth from the surface. Total volume of the structure is equal to (R is diameter of the sphere):

$$V_{total} = \frac{4}{3}\pi \left(\frac{R}{2}\right)^3 = \frac{4}{3}\pi \left(\frac{49\ nm}{2}\right)^3 = 61601\ nm^3$$

The inner volume of the structure is given by:

$$V_{inner} = \frac{4}{3}\pi R^3 = \frac{4}{3}\pi \left(\frac{49\ nm - 2 * 5\ nm}{2}\right)^3 = 31059\ nm^3$$

The volume of the surface shell with the depth of 5 nm is equal:

$$V_{shell} = V_{total} - V_{inner} = 30542\ nm^3$$

The ratio of the surface shell volume to the total volume is:

$$\frac{V_{shell}}{V_{total}} = \frac{30542\ nm^3}{61601\ nm^3} = 0.496$$

The number of available binding pockets in the surface shell can be calculated by:

$$\frac{V_{shell}}{V_{total}} * n\ free\ binding\ pockets = 0.496 * 15.95 = 7.9$$

This estimation showed that on the surface shell of the BHS there are in average 7.9 free binding pockets that could be possibly used for further functionalization with folate or other kinds of biotinylated molecules.

2.4. Stability of non-modified and modified BHS

2.4.1. Long term stability of the structures

Important question in the study of such BHS with regard to potential future biomedical applications are the long term stability properties. The measurement of the size of BHS with different SA/PEI-biotin ratio, namely 1/0.5, 1/1 and 1/2 was performed during the period of one month. The samples were stored at 7 °C. In Figure 18, the measurement of the hydrodynamic size of the BHS consisted of SA/PEI-biotin 1/1 over the time is presented. For the other two SA/PEI-biotin ratios the results looked identical and are presented in appendix on the page 84. The size of the structures remained the same over the period of 27 days, which means that after the formation process BHS are stable and the non-covalent interaction between the SA and biotin remains after the long time. Furthermore, there was no additional and uncontrolled aggregation process over the time.
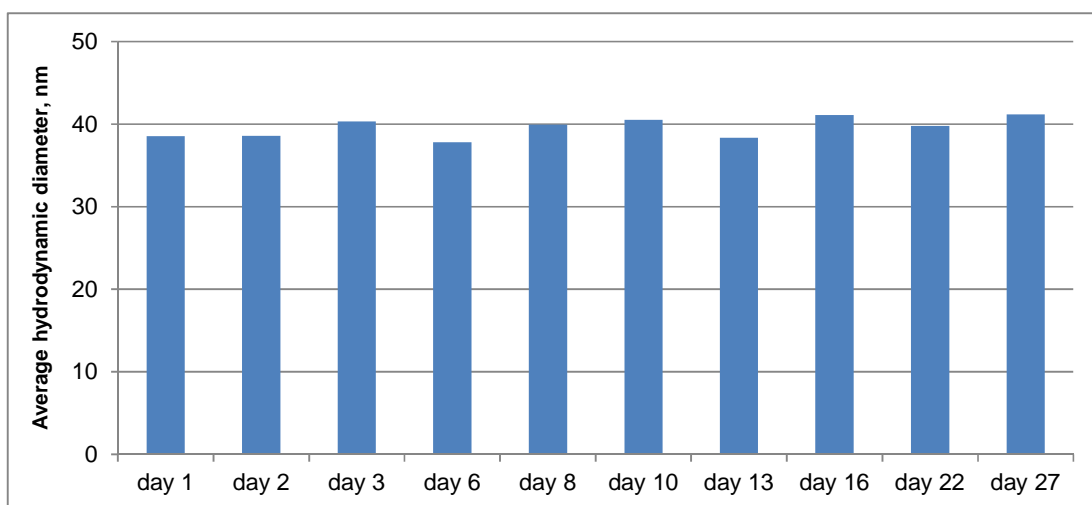
Figure 18: Long term stability study of the non-modified BHS consisted of SA/PEI-biotin 1/1.

In the next step, the long term stability properties of the BHS modified with folate were tested. The measurement was performed for the structures with Folate2k and Folate5k. The impact of

purification was additionally investigated. For all the structures the results looked identical and the example is shown in Figure 19. The graphs for the rest of the structures are shown in appendix on the pages 85 and 86. After addition of folate, there is a very small shift in the size which is stable over the period of one month. It means that additional biotin-streptavidin conjugation added to the system did not cause disaggregation of BHS and the initial biotin-streptavidin binding was not broken.
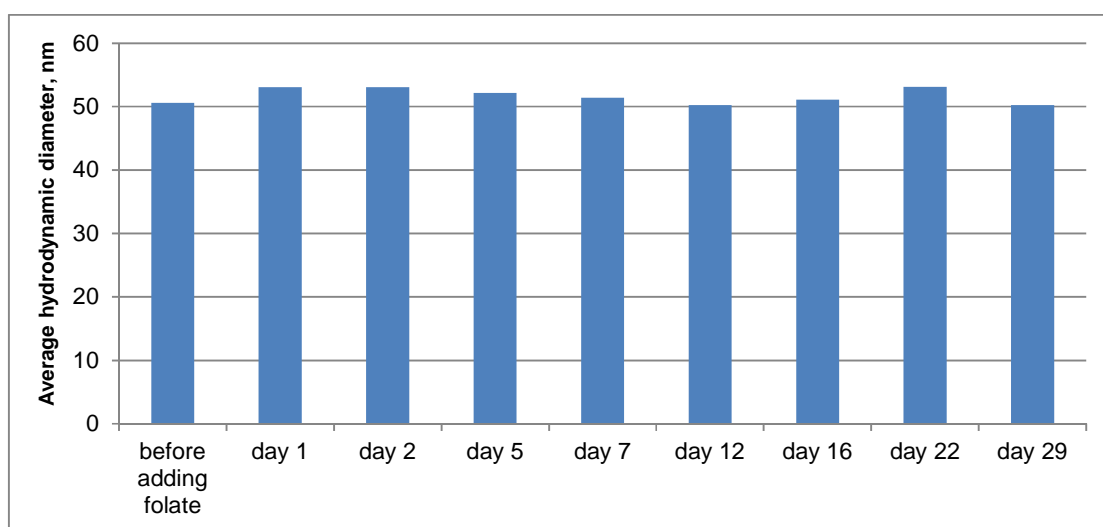
Figure 19: Long term stability study of the purified BHS modified with Folate5k.

2.4.2. Stability against the excess of biotin

In the next step, the stability of the BHS against free biotin molecules was tested. The aim of this investigation was to check if addition of free biotin to the system after the fabrication of BHS will cause disassembling of the structures. In the first step BHS with the PEI-biotin/SA ratio of 1/1 were produced and after 24 hours free biotin molecules were added to the system in the desired molar ratios. Figure 20 presents the DLS results of the BHS with different amounts of biotin.
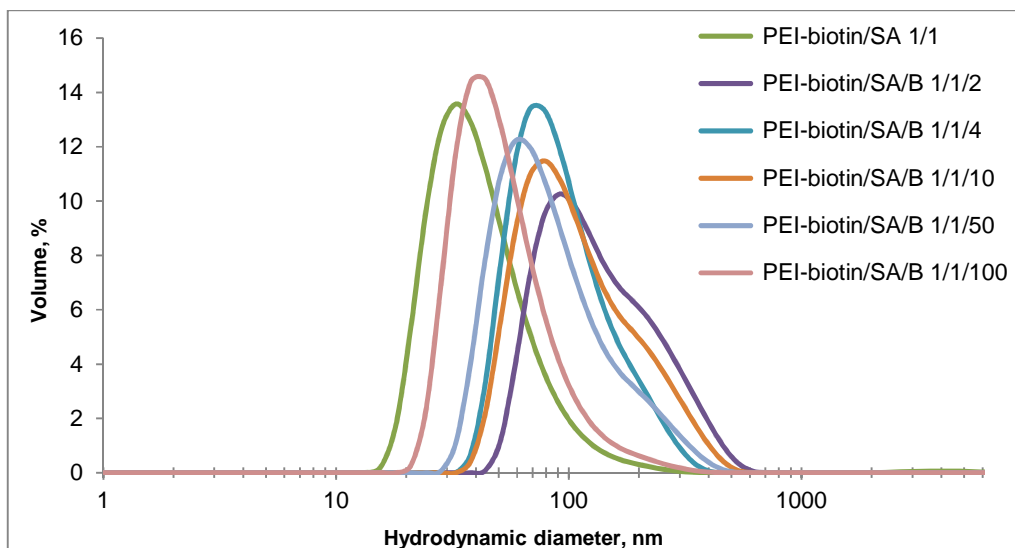
Figure 20: Size of the structures with additional biotin molecules. B = Biotin

After addition of free biotin molecules to the BHS, there is an increase in the sizes of BHS. It means that the rearrangement of BHS takes place. Very small biotin molecules can go deep inside the structures and do not face sterical problems to fit inside the binding pockets. There is no decrease in the size of the structures which means that no degradation of the structures takes place.
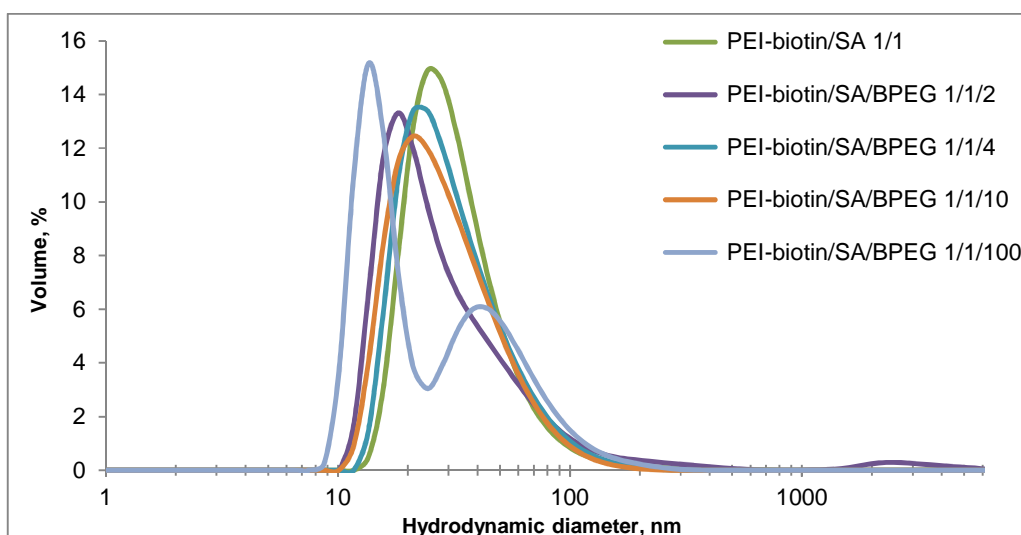
Figure 21: Size of the structures with additional biotin-PEG molecules. BPEG = Biotin-PEG.

In the next step, the stability of BHS against biotin-PEG$_{12}$-COOH (biotin-PEG$_{12}$) molecules was tested. Similarly as for the experiments with free biotin, BHS with the PEI-biotin/SA ratio of 1/1 were produced and after 24 hours free biotin-PEG$_{12}$ molecules were added to the system in the desired molar ratios. Figure 21 presents the DLS results obtained for those structures. In the case of adding free biotin-PEG$_{12}$, there is a small decrease in the size of the structures compared with the non-modified BHS. The use of PEG spacer caused the rearrangement to the smaller particles, but no degradation to the initial components. It can be suggested that compared with free biotin, biotin-PEG$_{12}$ is a bigger molecule which does not penetrate inside the structure. The chain may backfold to the BHS, compress its size and increase the density. Biotin-PEG$_{12}$ can also cause different shielding behavior of BHS. It can have an influence on the Stern-layer of the structure by allowing less water to go through the BHS what cause the decrease in the measured size value (which is directly correlated to the diffusion coefficient).

3. Characterization of BHS by zeta potential

Surface characteristics of the nanocarriers can significantly influence their interaction with the cell membrane and hence their internalization pathways. A cell membrane is anionic because of the anionic head group of phospholipids and the presence of carbohydrates such as sialic acid.[68] Cationic carriers advantageously bind to anionic functional groups on a cell surface and translocate across the plasma membrane inside the cell.[69] Neutral and negatively charged nanoparticles are expected to be less efficiently adsorbed and taken up by negatively charged cell membrane.[69] In order to check the surface charge of the BHS, zeta potential measurements were performed. Similar results were obtained for the BHS modified with Folate2k and Folate5k. Samples result for BHS modified with Folate2k is presented in Figure 22. The dependency obtained for BHS modified with Folate5k is presented in appendix, on the page 86. Isoelectric point of the structure is at the pH=8.78 and at neutral pH the zeta potential is positive. It suggests that fabricated BHS are slightly cationic and the internalization by the cell should be favorable.
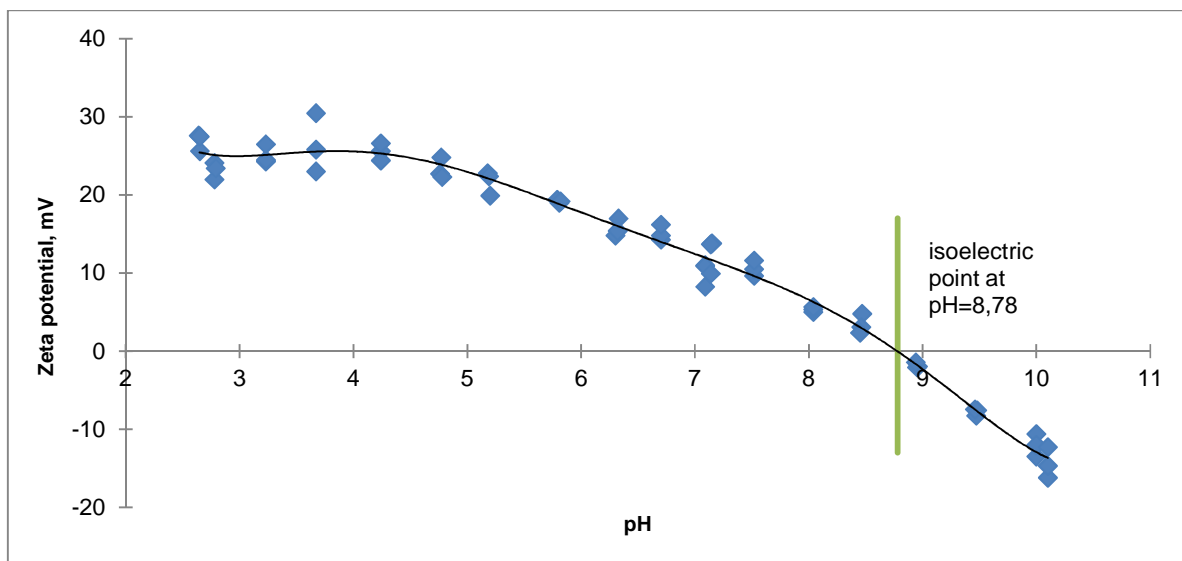
Figure 22: Zeta potential measurement of BHS modified with Folate2k.

4. Cell viability

Prior to evaluating the selectivity of BHS for targeting to cells, the biocompatibility of the structures was proved using the AlamarBlue proliferation assay. In this study, two different cell lines were used, the Human Cervix Carcinoma cells (SBC-2, derivative of HELA), expressing folate receptor (FR +ve) and the Human Embryonic Kidney 293 cells (HEK293) which do not overexpress folate receptor (FR -ve). PEI-biotin, non-modified BHS and BHS modified with folate or biotin-PEG were individually evaluated by treating SBC-2 and HEK293 cells with different concentrations of the corresponding samples for 24 h. The cells were incubated with the mass uptake of 1 μg, 10 μg, 50 μg, 100 μg, 150 μg or 250 μg of the desired system.
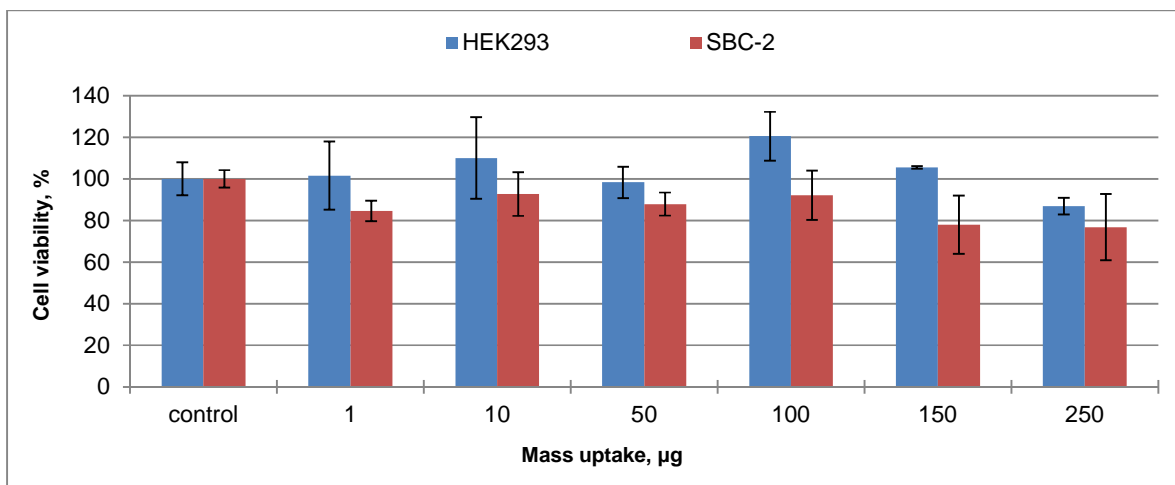
Figure 23: Viabilities of HEK293 and SBC-2 cells treated for 24 h with different concentrations of PEI-biotin.
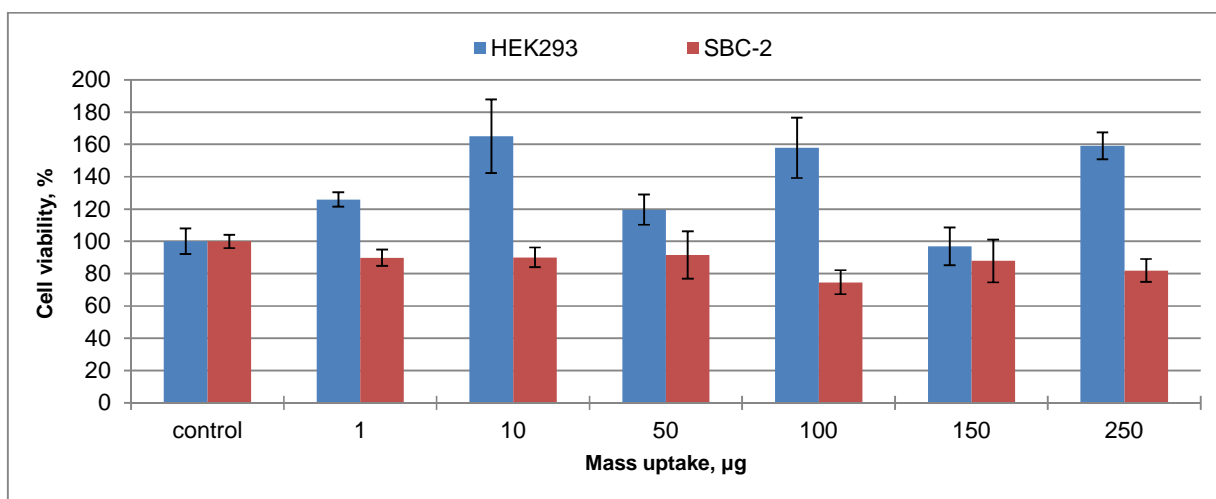
Figure 24: Viabilities of HEK293 and SBC-2 cells treated for 24 h with different concentrations of BHS.

As shown in Figure 23, PEI-biotin had any adverse effect on the proliferation of HEK293 cells. SBC-2 cells demonstrated low cell death level after treating with PEI-biotin, with the drop in viability up to 77 % after incubation with the highest concentrations of PEI-biotin. In Figure 24 cell viabilities after treatment with BHS are presented. Viabilities of HEK293 cells are over 100% for most of the concentrations which suggests that BHS are biocompatible and cause the

cell proliferation. The viabilities of SBC-2 cells, similarly as for PEI-biotin, were reduced up to 80% after incubation with the highest concentrations of BHS. For both systems viabilities of HEK293 cells were higher compared with SBC-2 cells. Comparison of the viabilities after incubation with PEI-biotin and BHS showed that addition of SA to the system significantly increased the viability and proliferation of HEK293 cells.

Figure 25: Viabilities of HEK293 and SBC-2 cells treated for 24 h with different concentrations of BHS modified with Folate2k after the purification

Figure 26: Viabilities of HEK293 and SBC-2 cells treated for 24 h with different concentrations of BHS modified with Folate2k without the purification.

Figure 25 and Figure 26 present the cell viabilities after incubation with BHS modified with Folate2k, with and without the purification, respectively. In both cases viabilities of HEK293 cells were over 100%, usually between 120 % and 140 %, which suggests that modified BHS are also biocompatible and support the cell proliferation. Comparing with the non-modified BHS, addition of Folate2k did not cause any cytotoxic effects to the cells, however the cell proliferation was slightly decreased. After incubation with SBC-2 cells, for both purified and non-purified systems, the cell viabilities were in the range 90 – 115% which means that modified BHS had also any adverse effects on this cell line. Purification of the system increased the viability of SBC-2 cells what is especially seen for the high concentrations. Viabilities of HEK293 cells were similar for non-purified and purified structures.
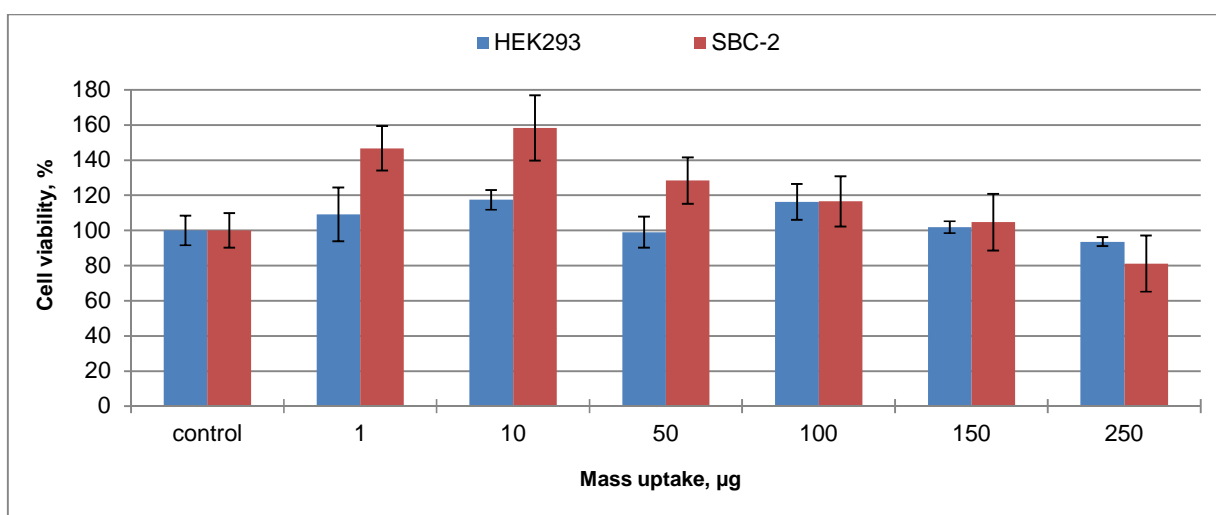
Figure 27: Viabilities of HEK293 and SBC-2 cells treated for 24 h with different concentrations of BHS modified with Folate5k after the purification.
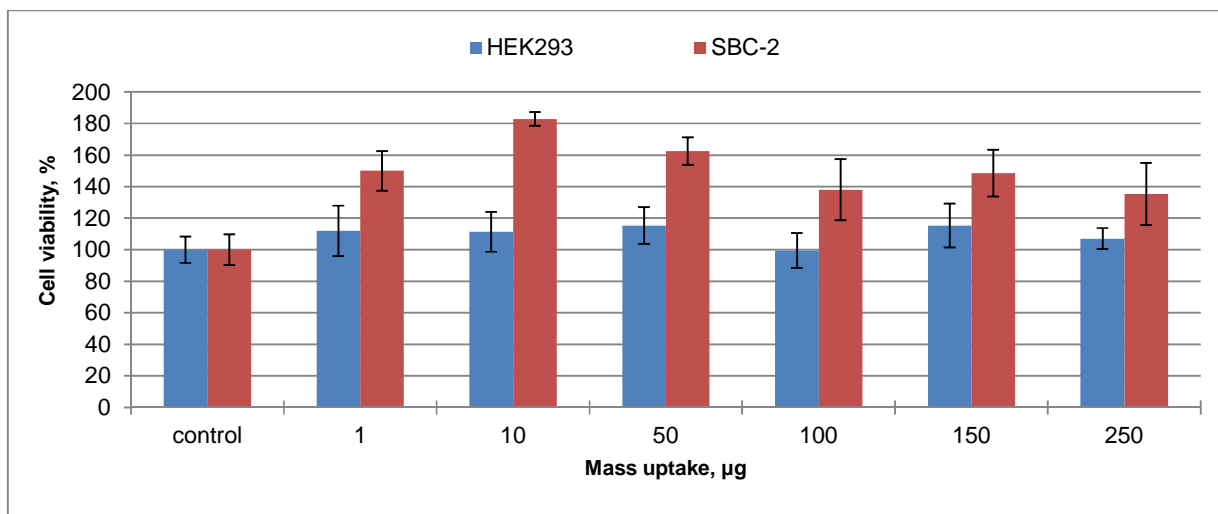
Figure 28: Viabilities of HEK293 and SBC-2 cells treated for 24 h with different concentrations of BHS modified with Folate5k without the purification.

As shown in Figure 27 and Figure 28, for the BHS modified with Folate 5k, irrespectively if purified or not, the viabilities of SBC-2 cells were higher than of HEK293. For the purified samples there is a strong dependency on the mass uptake, for small mass uptakes the viabilities are very high (up to 160%), however for the highly concentrated samples they drop up to 80%. The viabilities of SBC-2 cells after incubation with non-purified BHS modified with Folate5k are also very high, up to 180%. The possible reason for such high viabilities are the stealth properties of SBC-2 cells. The long biotin-PEG spacer interacts with the membrane which causes better cell viability. For both, purified and non-purified samples, the viabilities of HEK293 cells were in the range of 100-120%.

Figure 29 and Figure 30 present the results of cytotoxicity test of non-purified BHS modified with Biotin-PEG2k and Biotin-PEG5k, respectively. In both cases there are no significant differences between the HEK293 and SBC-2 cells and there is no dependency with mass. Most of the viability results are in the range of 100 - 120%.
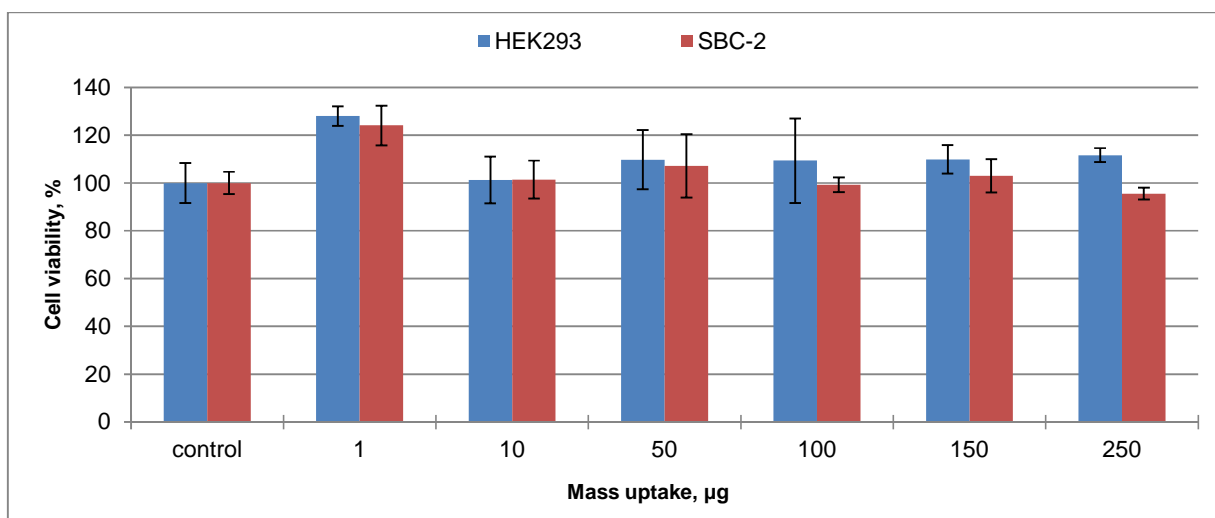
Figure 29: Viabilities of HEK293 and SBC-2 cells treated for 24 h with different concentrations of BHS modified with Biotin-PEG2k.

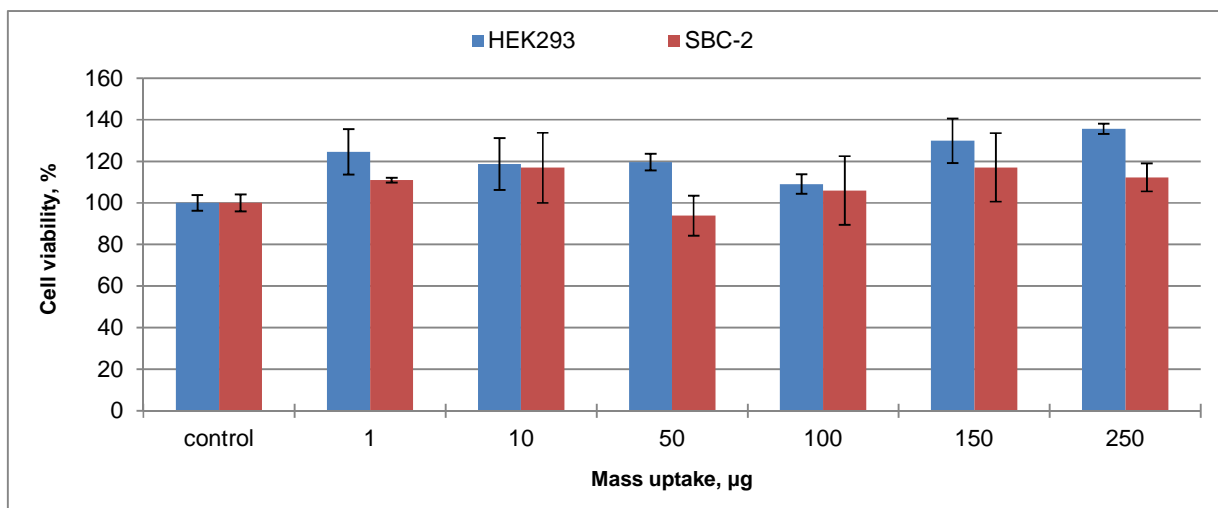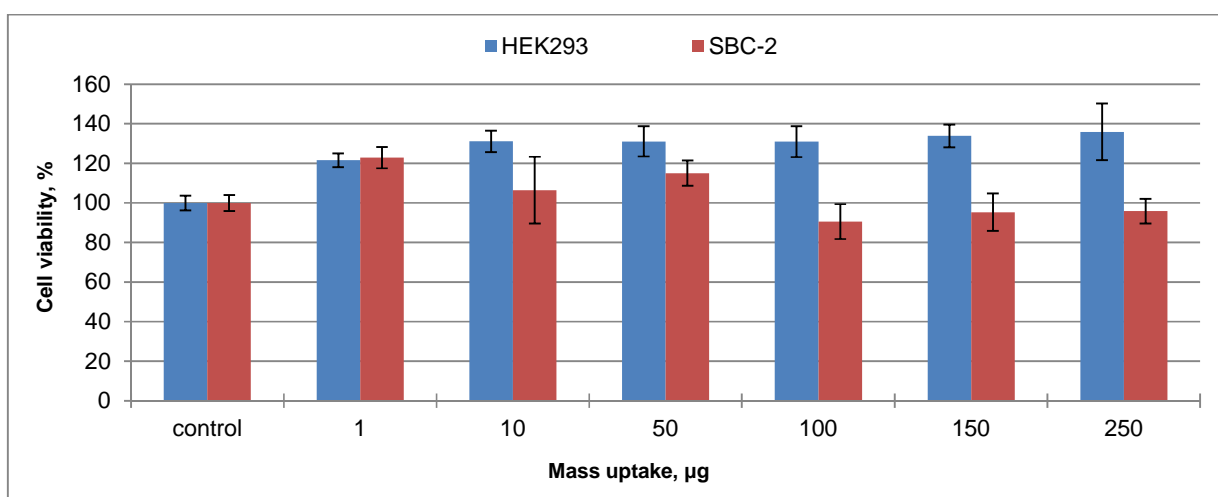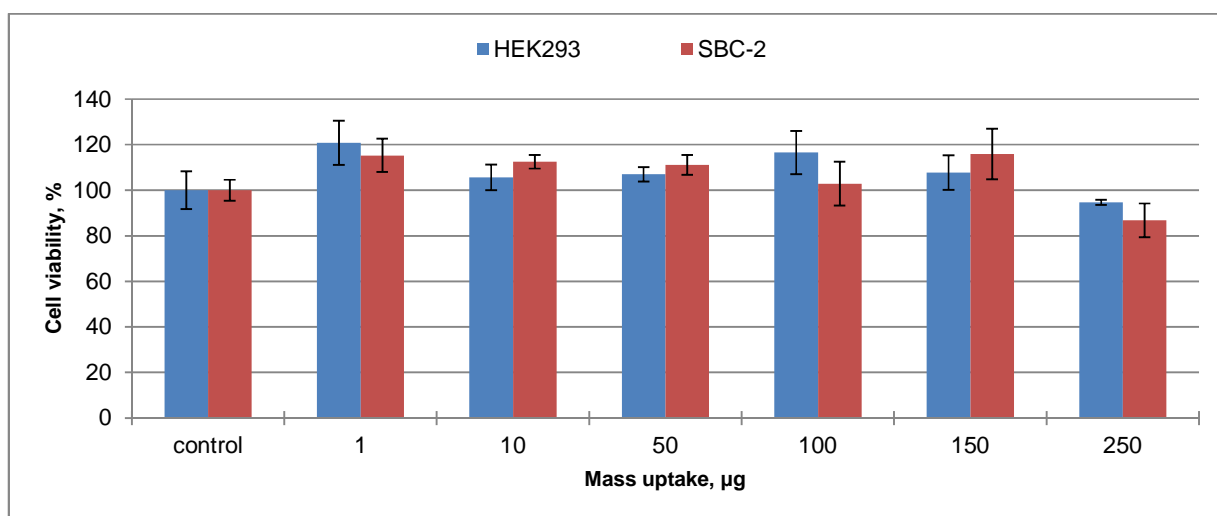**Figure 30:** Viabilities of HEK293 and SBC-2 cells treated for 24 h with different concentrations of BHS modified with Biotin-PEG5k.

In appendix, on the page 87 Figure 58 and Figure 59 present the comparison of the viability tests for all the structures of HEK293 and SBC-2 cells, respectively. In general, the results showed that none of the systems is toxic under given experimental conditions. Typical viability values are around 100% or higher (rarely below 100%). It means that all the

structures are biocompatible and do not cause the cell death. The highest viabilities of HEK293 cells were reached after incubation with non-modified BHS and BHS modified with Folate2k. The highest viabilities of SBC-2 cells were achieved for BHS modified with Folate5k. Modification of BHS with folate or Biotin-PEG slightly decreased the viability of HEK293 cells and increased the viability of SBC-2 cells. Higher viabilities were reached for the BHS modified with Folate2k compared to BHS modified with Folate5k for the HEK293 cells and for SBC-2 cells it was the opposite. Modification of BHS with folate or Biotin-PEG showed that the presence of folic acid can slightly influence the cytotoxicity. For the structures modified with 2k chains, viabilities of HEK293 were higher for the BHS modified with the folate compared with Biotin-PEG. There was no significant trend observed in SBC-2 cells. Viabilities of SBC-2 cells were higher after incubation with BHS modified with Folate5k compared with the BHS modified with Biotin-PEG5k and no significant differences were observed for HEK293 cells. Purification step did not influence the viabilities of HEK293 cells. For the SBC-2 cells, the viabilities were much higher for the non-purified BHS modified with Folate5k than for purified. Due to the stealth properties of SBC-2 cells, long biotin-PEG spacer can interact with the membrane what causes better cell viability. Free folate molecules present in the solution additionally amplify this phenomenon.

5.   Flow cytometry

In order to demonstrate the ability for selective targeting to the cancer cells, the non-modified and modified BHS have been quantitatively evaluated using flow cytometry analysis. Both cell lines, SBC-2 cells (FR +ve) and HEK293 cells (FR -ve), were treated only with 200 μg mL^{-1} of FITC-labeled BHS or single components for different incubation times.

5.1. Non-modified biohybrid structures based on PEI-biotin/SA and PEI-biotin/NA

Neutravidin (NA) is a derivative of avidin which is non-glycosylated and eliminates the non-specific binding compared with avidin. At first, BHS based on PEI-biotin and SA or NA were tested. The single components of the structures were examined as well. As shown in Figure 31, the mean fluorescence intensity (MFI) of both cell lines for SA and NA was very low, similarly to the control where cells were incubated only with the cell culture medium. The molecular uptake after incubation with PEI-biotin was much higher than with proteins and it was higher in HEK293 cells than in SBC-2. After incubation with BHS based on PEI-biotin/SA, the uptake was few times higher compared with PEI-biotin and the MFI was always two times higher for SBC-2 cells than for HEK293 cells.
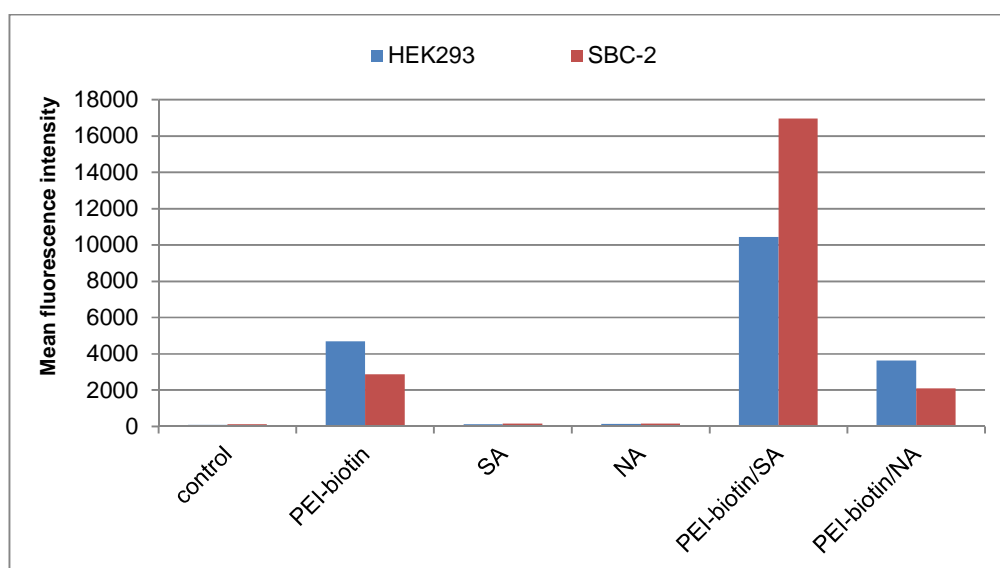
Figure 31: Cellular uptake after incubation with non-modified BHS and single components for 4h.

It shows the synergetic effect of BHS formation. The MFI measured for single components was very low, however, when they were conjugated it was few times higher. It proves that combining the properties of synthetic and biological components we create the biohybrid

material with extraordinary and synergetic functions that significantly increases the molecular uptake or causes the interaction with the cell membrane. At this step of investigation it is not established if the BHS are taken up inside the cell or if they bind to the cellular membrane what could also cause high fluorescence intensity values. The MFI values of BHS based on PEI-biotin and NA were much lower compared with the structures built from PEI-biotin/SA. The value is in the range of MFI for PEI-biotin, which showed that there is no synergetic effect when BHS is fabricated from NA. For the further modification with folate, only the BHS based on PEI-biotin/SA were chosen.
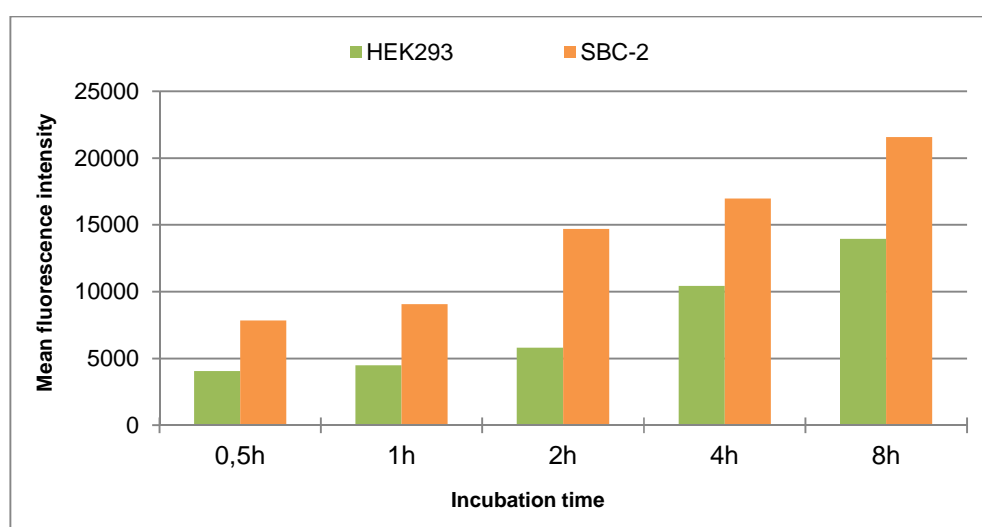
Figure 32: Cellular uptake BHS based on PEI-biotin/SA after different incubation times

In Figure 32 the time dependency of molecular uptake after incubation with BHS based on PEI-biotin/SA is presented. The molecular uptake for both cell lines is increasing with time and the MFI was up to two times higher for SBC-2 cells compared with HEK293 for all the time points. In Figure 33 and Figure 34 the time comparison for all the components is presented for HEK293 and SBC-2 cells, respectively.

47
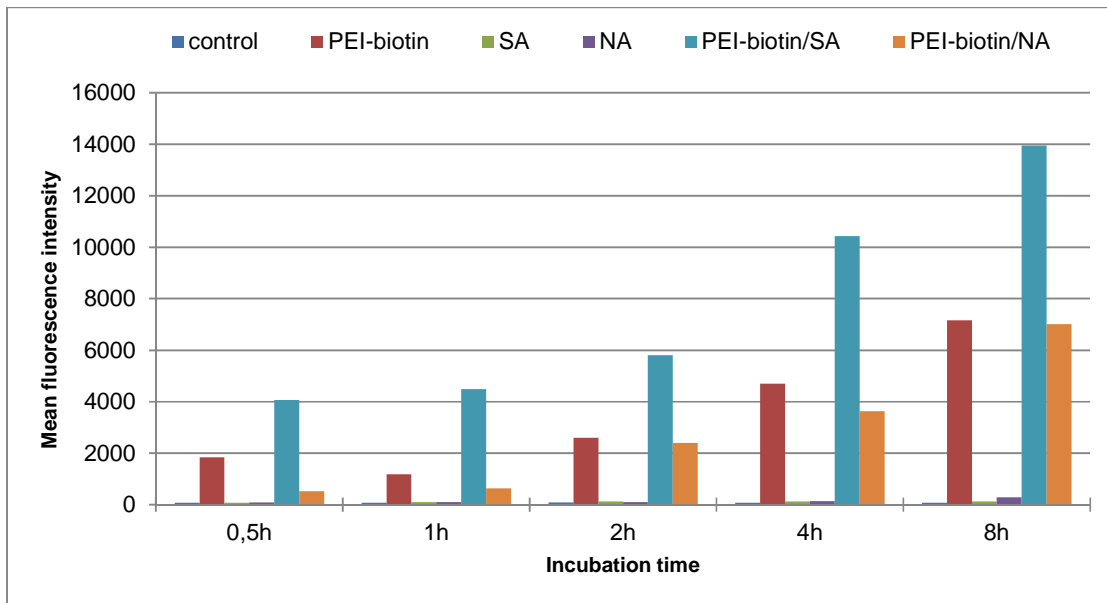
Figure 33: Cellular uptake of HEK293 cells after different incubation times.
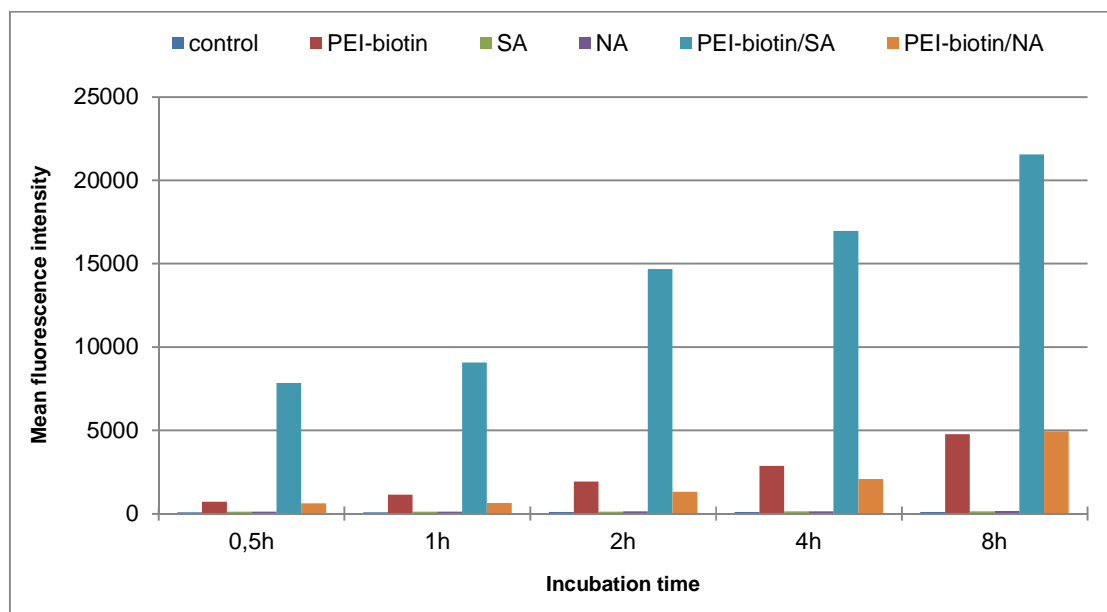
Figure 34: Cellular uptake of SBC-2 cells after different incubation times.

The uptake of HEK293 cells was always the highest for BHS based on PEI-biotin/SA. The MFI results for PEI-biotin and PEI-biotin/NA were similar, always around two times smaller

than for PEI-biotin/SA. For SBC-2 cells, the molecular uptake after incubation with PEI-biotin/SA was also the highest. The MFI results for PEI-biotin and PEI-biotin/NA are again very similar, however few times lower than PEI-biotin/SA. By comparing Figure 33 and Figure 34 it can be seen that the differences between the results for PEI-biotin/SA and the rest of the systems is much bigger for SBC-2 cells. Up to two-times higher MFI value in cancer cells compared with the normal cells shows that BHS could be promising candidates as carriers for selective targeting to tumor cells. Nevertheless, here it is necessary to consider that biologically active molecules present in the extracellular medium either bind to membrane receptors or the lipid matrix of the membrane, or cross the membrane to act inside the cell. Crucial is to know the affinity and binding mechanism of a molecule to the membrane, and whether it interacts only with the outer membrane leaflet or whether and how it can translocate to the inner leaflet. It is not straightforward to predict whether the nanocarrier translocates passively across the membrane and additional experiments on membrane translocation are needed to state if the high MFI values obtained for BHS means internalization inside the cell or binding to the cell membrane.

5.2. BHS modified with short folate moieties

In the next step, the modification of BHS with folate was performed. At first, modification was done by adding the short folate spacers with the molar mass of 2000 Da. The experiments were prepared with the use of purified and non-purified BHS. Purification step included the dialysis of the sample against PBS in order to remove the unbound folate groups from the solution. Different amounts of folic acid were used. Structures were prepared with different molar ratios of PEI-biotin/SA/Folate, namely 1/1/10, 1/1/8, 1/1/6, 1/1/2 and 1/1/1. Furthermore, the cellular uptake after incubation with only Folate2k and the conjugation of SA/Folate2k was tested. SA/Folate2k conjugation was prepared without the purification. As shown in the chapter 2.3, in the surface shell BHS possess approximately 7.9 free binding pockets of SA that could be used for further modifications with biotinylated molecules. It means that using the highest molar ratios of PEI-biotin/SA/Folate, the binding pockets of SA should be fully saturated with folate molecules. Modifying BHS with small amount of folates,

only part of the free pockets should be occupied. Figure 35 shows the results of molecular uptake after incubation with different BHS modified with short folate moieties.
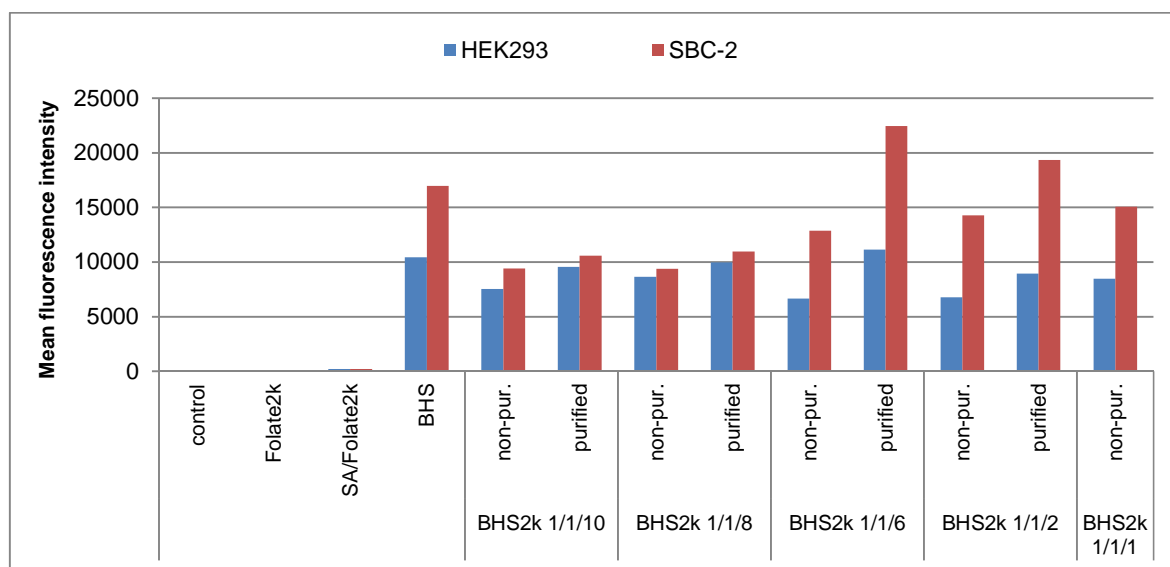
Figure 35: Cellular uptake after incubation with BHS modified with Folate2k or single components for 4 h. BHS2k = PEI-biotin/SA/Folate2k, non-pur. = non-purified

The MFI of Folate2k and SA/Folate2k are very low, in the range of the value obtained for the control that was incubated only with the cell culture medium. Even though Folate2k and SA/Folate2k contained the high number of free folate moieties, there was no uptake by the folate receptors expressing cancer cells. The MFI values of BHS modified with folate was much higher what proves that combining the properties of single components the material with extraordinary and synergetic functions can be fabricated.

The molecular uptake for most of the modified BHS was much higher in SBC-2 cells than in HEK293 cells. Comparing the results for the BHS modified with different amounts of folate, the highest MFI values were obtained for the PEI-biotin/SA/Folate2k of 1/1/6 and 1/1/2, in both cases for the purified samples and the molecular uptake was higher compared with the non-modified BHS. Such enhancement in the cellular uptake was presumably due to the successful recognition of folic acid present in the system by the folate receptors overexpressed on the SBC-2 cells. Figure 36 presents the different cell internalization pathways depending on

the kind of cell for the structures with the above mentioned molar ratios of PEI-biotin/SA/Folate2k. In HEK293 cells which do not overexpress folate receptors, positively charged BHS interact with the negatively charged cell membrane. The high MFI values obtained for this cell line suggests that BHS bind to the cell membrane through the electrostatic interaction or are taken up inside the cell through the endocytosis process. In SBC-2 cells which overexpress folate receptors, BHS can bind to the cell membrane or be taken up through the endocytosis process similarly as in HEK293 cells. The higher MFI values obtained in SBC-2 cells are due to the possibility of cellular uptake via the recognition of folic acid by folate receptors present on the cell membrane. Once folate conjugates are bound to a cell surface folate receptors, they are transported into the cell through a process called receptor-mediated endocytosis by engulfing inside the endosome. In SBC-2 cells, internalization inside the cell is a competition between charge-driven and folate-mediated uptake.
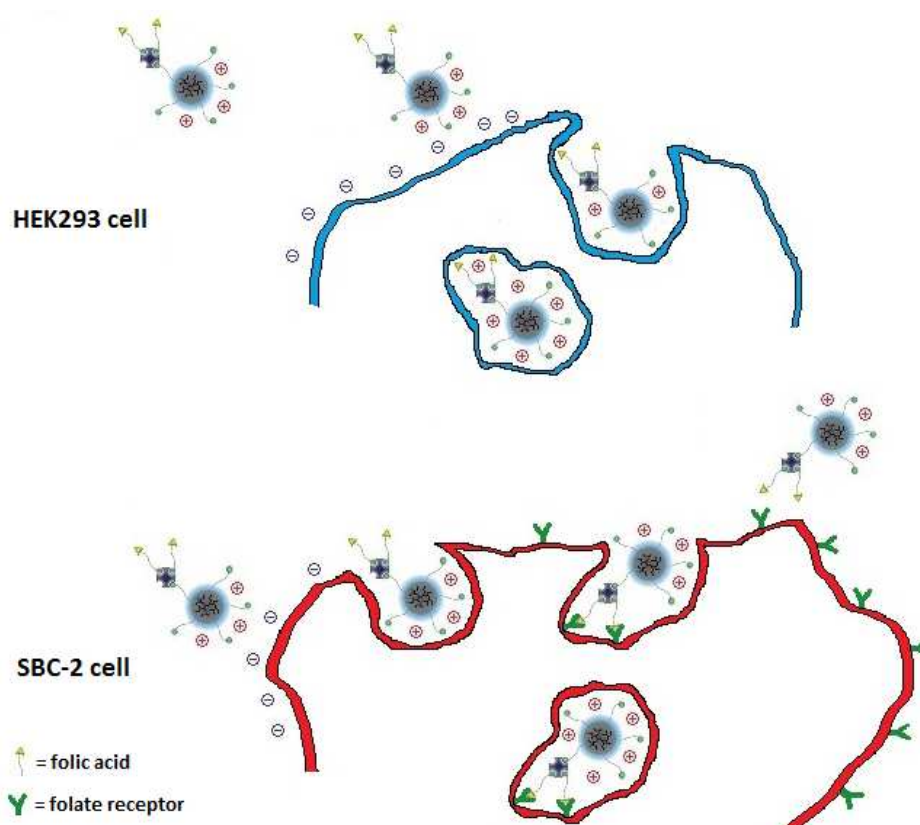
Figure 36: Cell internalization pathways for HEK293 and SBC-2 cells.

Higher uptake in the purified samples suggests that the free folate groups present in the non-purified solution occupy part of the folate receptors and do not allow the BHS to enter the cell. The MFI for SBC-2 cells obtained by the BHS modified with the high ratio of folic acid, namely 1/1/10 and 1/1/8, was much lower compared with the non-modified BHS and BHS modified with Folate2k in the ratio 1/1/6 and 1/1/2. Interestingly, the MFI results obtained for the HEK293 cells were similar. It can mean that too high number of the spacers attached to the BHS causes the steric problems for the folic acid to reach the folate receptors expressed on the cancer cell. Additionally, the high number of spacers surrounding the BHS can contribute to the shielding effect of the positive charge of BHS which will decrease the cellular uptake. The other possibility is that all of the binding pockets of SA were saturated and high number of free folate groups that were not removed during the purification step caused the receptors blocking (Figure 35).
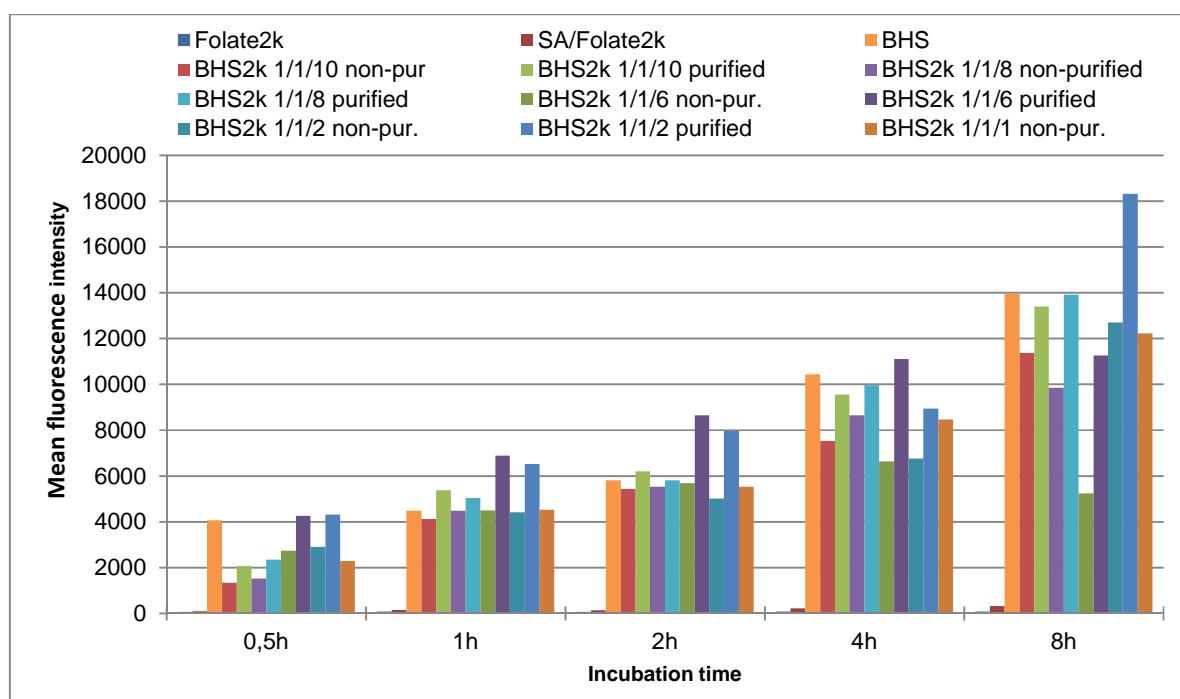
Figure 37: Cellular uptake of HEK293 cells after different incubation times. BHS2k = PEI-biotin/SA/Folate2k, non-pur. = non-purified.

In Figure 37 the time dependency of molecular uptake in HEK293 cells for different structures is presented. The molecular uptake for all the systems increases with the longer incubation

time. The highest MFI values were obtained for the purified BHS modified with different folate ratios (1/1/10, 1/1/8, 1/1/6 and 1/1/2). Values of the purified samples were always higher compared with the non-purified ones. It means that free folate groups present in the solution not only decrease the uptake in the cancer cells but can also contribute to the lower uptake in the normal cells due to generating the stealth properties. In HEK293 cells the cationic charge is a driving force for the molecular uptake of BHS inside the cells or interaction with the membrane.

Figure 38: Cellular uptake of SBC-2 cells after different incubation times. BHS2k = PEI-biotin/SA/Folate2k, non-pur. = non-purified.

Figure 38 presents the cellular uptake of SBC-2 cells incubated with different BHS modified with Folate2k. For all the time points the highest uptake in cancer cells was obtained for non-modified BHS and BHS modified with Folate2k in the ratios 1/1/6 and 1/1/2. For the structures with the other folate ratios, the uptake was lower compared with non-modified BHS. As explained earlier, the molecular uptake in cancer cells incubated with BHS modified with too high amounts of folate is decreased. The highest MFI was obtained for the structures with the ratio 1/1/6 and this system was chosen for the next experiments. In SBC-2 cells the

there is a competition between the charge-driven interaction with the cell membrane surface and folate-mediated uptake inside the cell.

5.3. BHS modified with long folate moieties

In order to investigate the influence of folate chain length, similar experiments were performed with the modification of BHS with the folate ligand of the mass 5000 Da. Structures with different molar ratios of PEI-biotin/SA/Folate5k were prepared, namely 1/1/10, 1/1/8, 1/1/6, 1/1/2 and 1/1/1. Additionally the cellular uptake after incubation with only Folate5k and the conjugation of SA/Folate5k was tested. The importance of the purification step was also investigated. Figure 39 shows the results of molecular uptake after incubation with different BHS modified with long folate ligands.
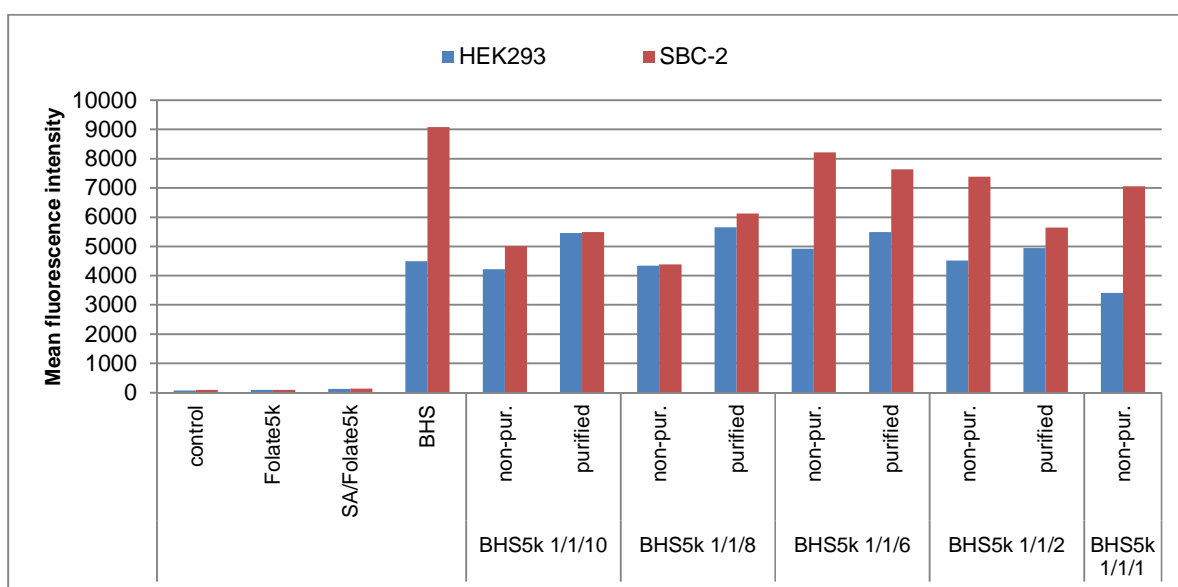
Figure 39: Cellular uptake after incubation with BHS modified with Folate5k or single components for 1 h. BHS5k = PEI-biotin/SA/Folate5k, non-pur. = non-purified

Similarly as for the short chains, the MFI values obtained for Folate5k and SA/Folate5k are very low for both cell lines. The results obtained for the modified BHS are much higher, which again shows the synergetic characteristics of biohybrid materials. The molecular uptake

after incubation with BHS modified with Folate5k was always higher for the cancer cells compared to the normal cells. Among the BHS modified with Folate5k with different folate ratios, the highest molecular uptakes of SBC-2 cells were achieved after incubation with PEI-biotin/SA/Folate5k 1/1/6 and 1/1/2, however the values are lower than for the non-modified BHS. The MFI values for the HEK293 cells are in the similar range for non-modified and all BHS modified with Folate5k. It showed that addition of the long ligands terminated with folic acid did not increase the molecular uptake in cancer cells. The 5000 Da chains are very long and possess backfolding properties. They start to behave like coil-structures where the terminating folic acid is not exposed at the surface of BHS and is not able to reach the folate receptors of the cancer cell.
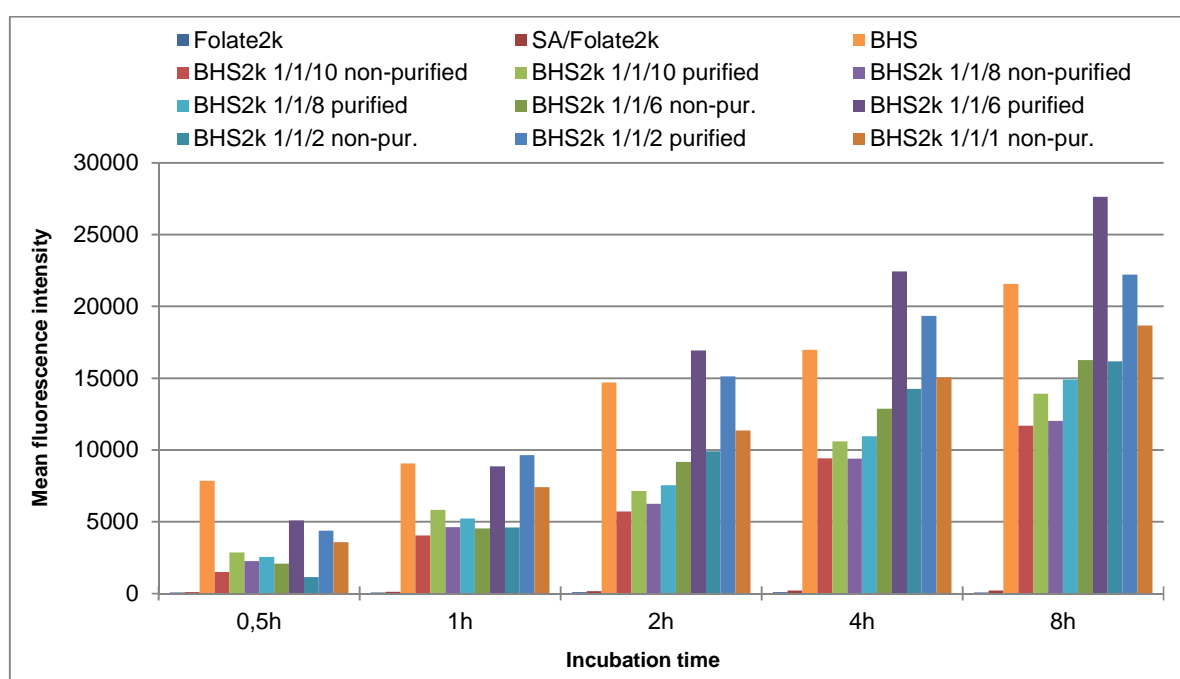

Figure 40: Cellular uptake of HEK293 cells after different incubation times. BHS5k = PEI-biotin/SA/Folate5k, non-pur. = non-purified

Figure 40 presents the time-dependency of the cellular uptake of HEK293 cells after the incubation with different BHS modified with Folate5k. For all the time points the MFI value for all the structures was in the similar range, however always a little bit higher for the non-

modified BHS and BHS modified with Folate5k which were purified. In general for the normal cells there were no significant differences recorded between the non-modified BHS and BHS modified with Folate5k.

In Figure 41 the comparison of cellular uptake of SBC-2 cells incubated with different BHS modified with Folate5k is presented. As can be clearly observed, for all the time points the MFI values obtained for all the BHS modified with Folate5k are much lower compared with the non-modified BHS. The values obtained for SBC-2 cells after the incubation with non-modified BHS are much higher than for HEK293 cells. For the modified structures the differences in the values between the cancer and normal cells are not very radical.
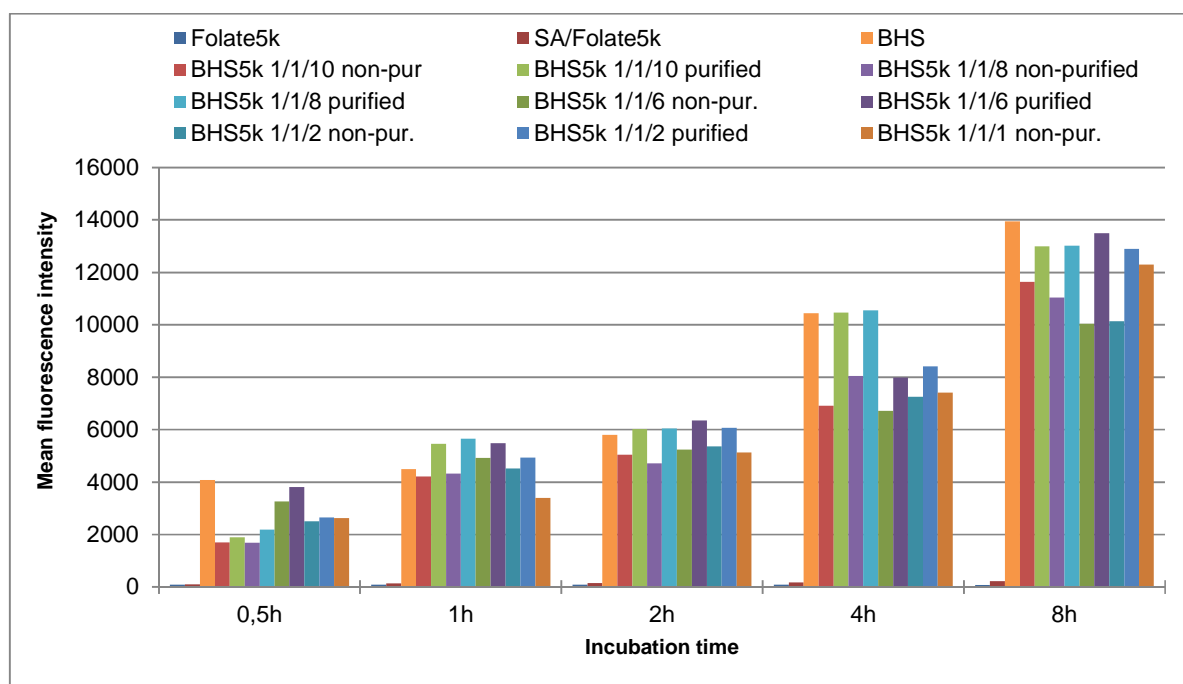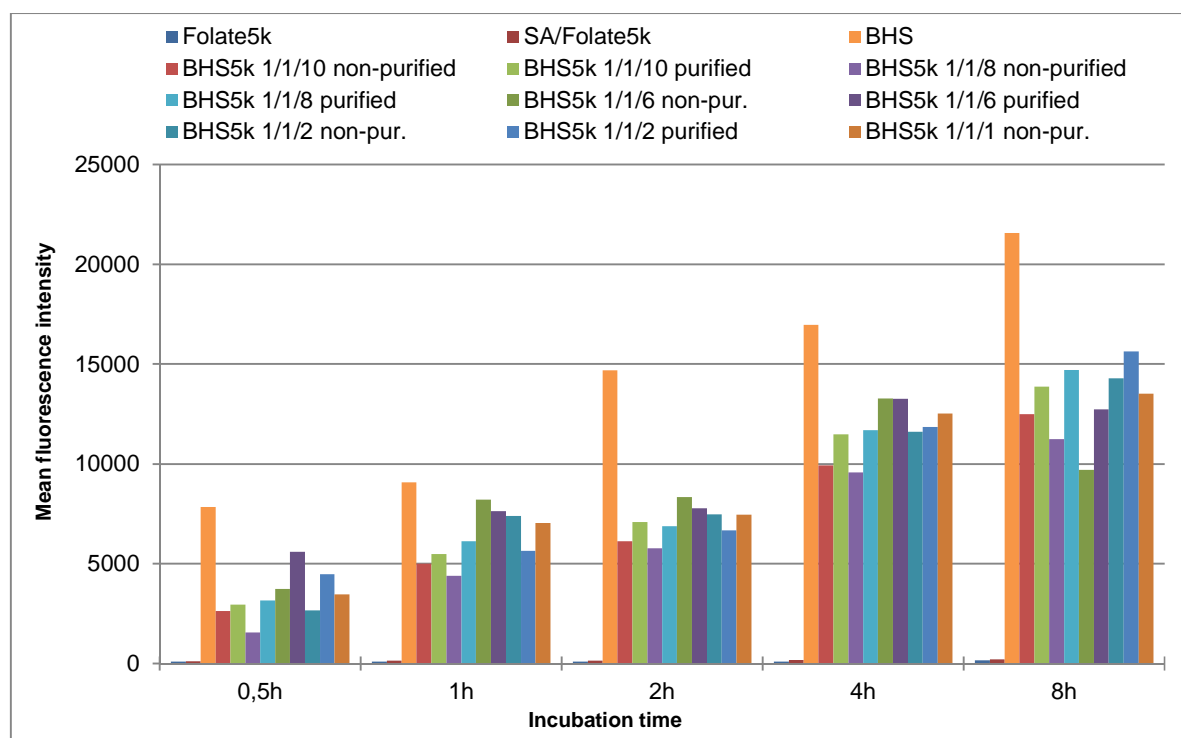

Figure 41: Cellular uptake of SBC-2 cells after different incubation times. BHS5k = PEI-biotin/SA/Folate5k, non-pur. = non-purified

5.4. Comparison between the BHS modified with short and long folate moieties

In order to choose the best system for the future biomedical application, the comparison between the results obtained for the BHS modified with Folate2k and Folate5k was performed. For the structures with lower and medium ratios of folate, namely PEI-biotin/SA/Folate 1/1/6, 1/1/2 and 1/1/1, the results look similar and are illustrated by example of the purified 1/1/6 samples in Figure 42. For HEK293 cells, the MFI values obtained for the BHS modified with Folate2k and with Folate5k are very similar. There are no significant differences in the molecular uptake of normal cells after modification with the chains of different lengths. For SBC-2 cells the differences in the uptake are striking. After the short incubation times, the MFI values obtained for the BHS modified with 2k moieties are similar to the values obtained for the BHS modified with 5k moieties. However, after the longer incubation times, the results measured for BHS-Folate2k are around two times higher compared with the values obtained for BHS-Folate5k.
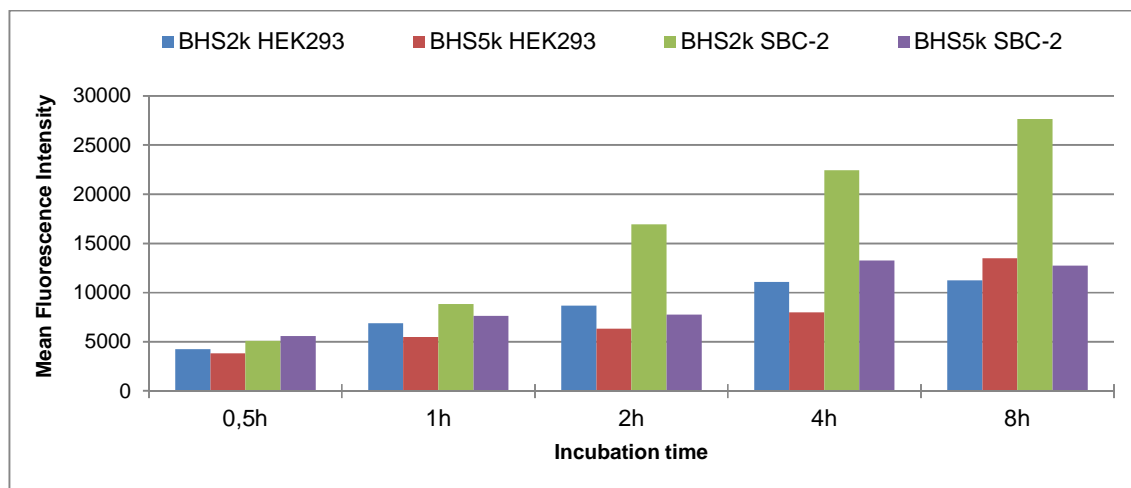
Figure 42: Cellular uptake of HEK293 and SBC cells after incubation with purified PEI-biotin/SA/Folate 1/1/6 with different chain lengths after different incubation times

The situation of the cellular uptake between the BHS modified with folate chains of different lengths looked distinct after incubation with the structures with the higher folate ratios (1/1/8

and 1/1/10) what is presented in Figure 43. In such a case, there are no differences between the BHS modified with Folate2k and with Folate5k. The results obtained for both of the cell lines are in the same range. It means that too high amounts of the added folate moieties cause the steric problems and folic acid is not exposed to reach the folate receptors on the cancer cell. The binding pockets of SA are fully saturated and not available for the further modifications. It suggests that unknown molecular rearrangement takes place. With too many folate moieties shielding effect of BHS also contributes to the decreased molecular uptake.

As the results obtained for the BHS-Folate2k for medium amounts of folate are the most promising, only the samples of BHS modified with Folate2k with the ratio 1/1/6 were chosen for the next studies of the molecular uptake mechanism.
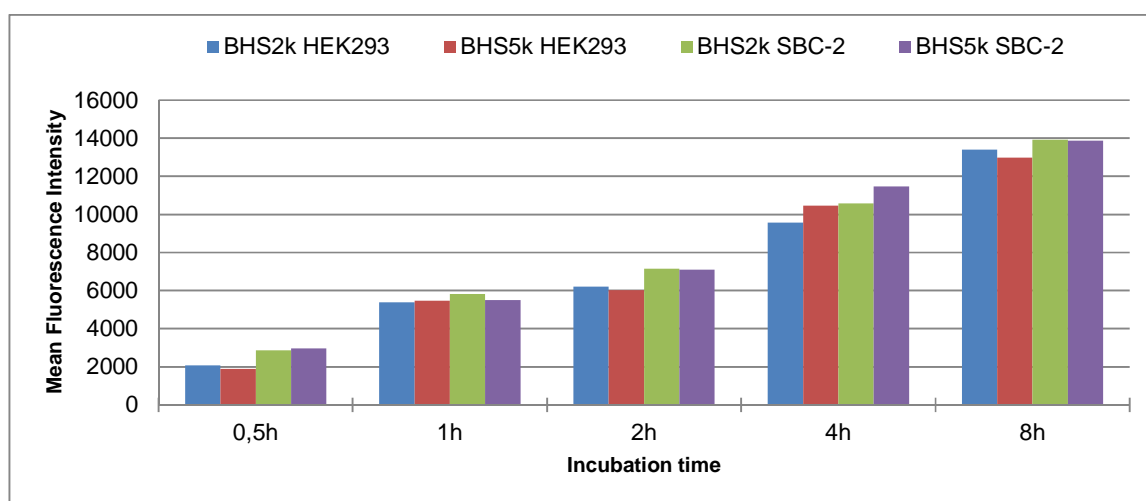
Figure 43: Cellular uptake of HEK293 and SBC cells after incubation with purified PEI-biotin/SA/Folate 1/1/10 with different chain lengths after different incubation times.

5.5. BHS modified with Biotin-PEG and BHS modified with folate

In order to investigate the real influence of addition of folic acid groups, BHS were modified with Biotin-PEG chain of the same lengths as folate groups. The only difference between BHS modified with Biotin-PEG and modified with folate is the presence of the folic acid molecules at the end of the chains. Folic acid should enhance the cellular uptake in cancer cells due to the

successful recognition by the folate receptors overexpressed on the SBC-2 cells. BHS were modified with Biotin-PEG and with folate of the lengths 2 kDa and 5 kDa in the ratio 1/1/6. The overview of the structures is presented in Figure 44. Additionally, the influence of purification step was investigated. In Figure 45, the comparison between non-modified BHS, BHS modified with folate and BHS modified with Biotin-PEG is presented.
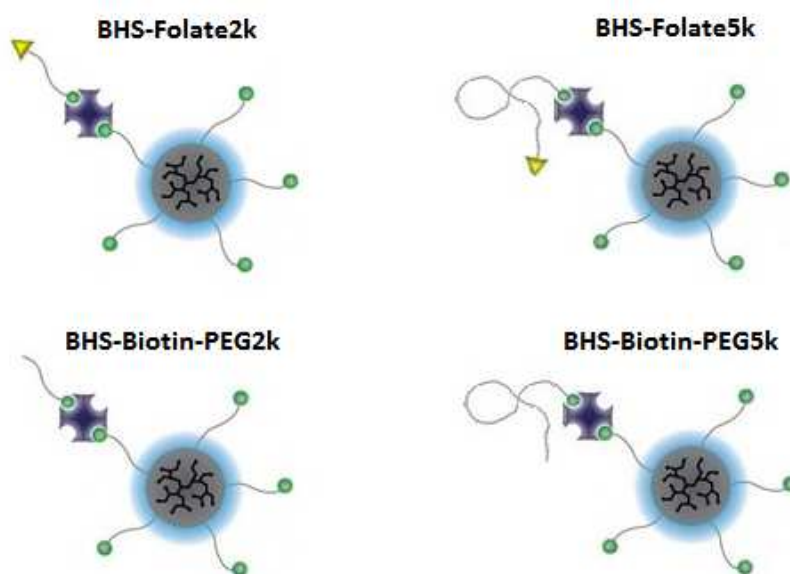
Figure 44: The overview of different modifications of BHS.

The highest MFI for SBC-2 cells was obtained for the purified BHS-Folate2k and the value is much higher compared with the purified BHS-Biotin-PEG. The MFI values obtained for those structures for HEK293 cells are very similar. Increased uptake in the cancer cells and no difference in the normal cells prove that presence of folic acid significantly increases the uptake in cancer cells due to the successful recognition by folate receptors and the possibility to enter inside the cell through the folate receptor mediated endocytosis process in addition to the non-receptor mediated uptake (charge-driven interaction with the cell membrane).
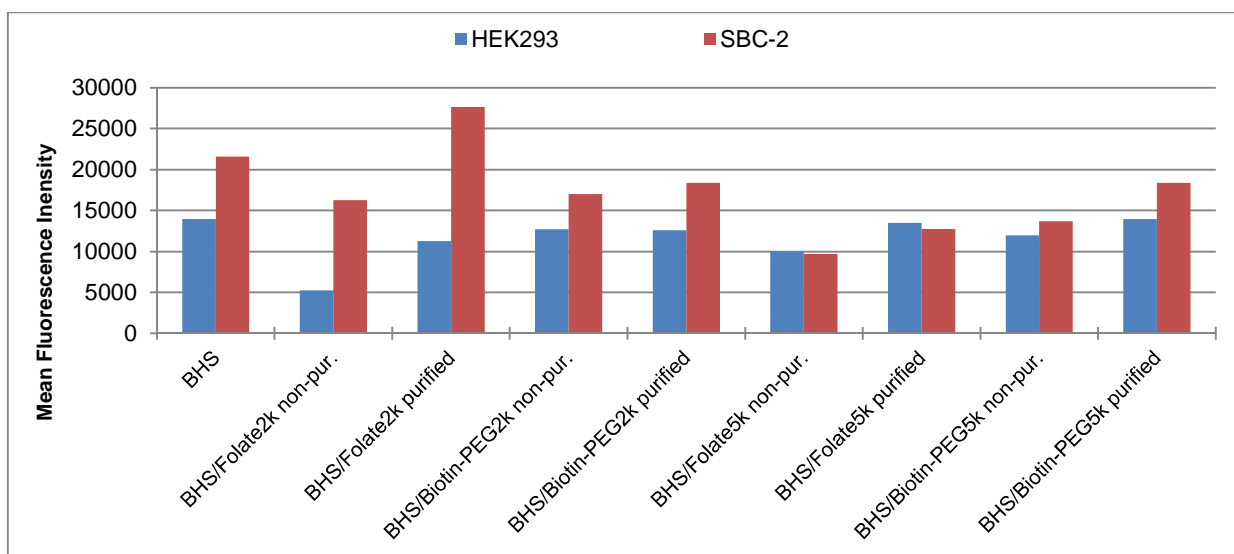
Figure 45: Cellular uptake after incubation with BHS modified with folate and Biotin-PEG for 8h. BHS = PEI-biotin/SA, non-pur. = non-purified.

Comparing the results for the short chain non-purified samples of BHS-Folate and BHS-Biotin-PEG, it can be seen that the molecular uptake in cancer cells was very similar for both of the structures. It means that free folate groups present in the non-purified sample block the folate receptors on the surface of the cancer cell and the uptake will be similar to the structures without the presence of folic acid. For the BHS modified with longer chains, the outcome is different than for the BHS modified with shorter ligands. After incubation with BHS modified with 5k chains, the molecular uptake is similar for the structures with folate and Biotin-PEG. It confirms that 5 kDa chains are too long and the back folding of the ligand appears. The chain behaves like a coil and terminating folate groups are not available for the binding pockets. Folic acid is not able to reach the folate receptors and the molecular uptake is not increased. It means that internalization inside the cell is non-receptor mediated (only charge-driven uptake via interaction with the cell membrane).
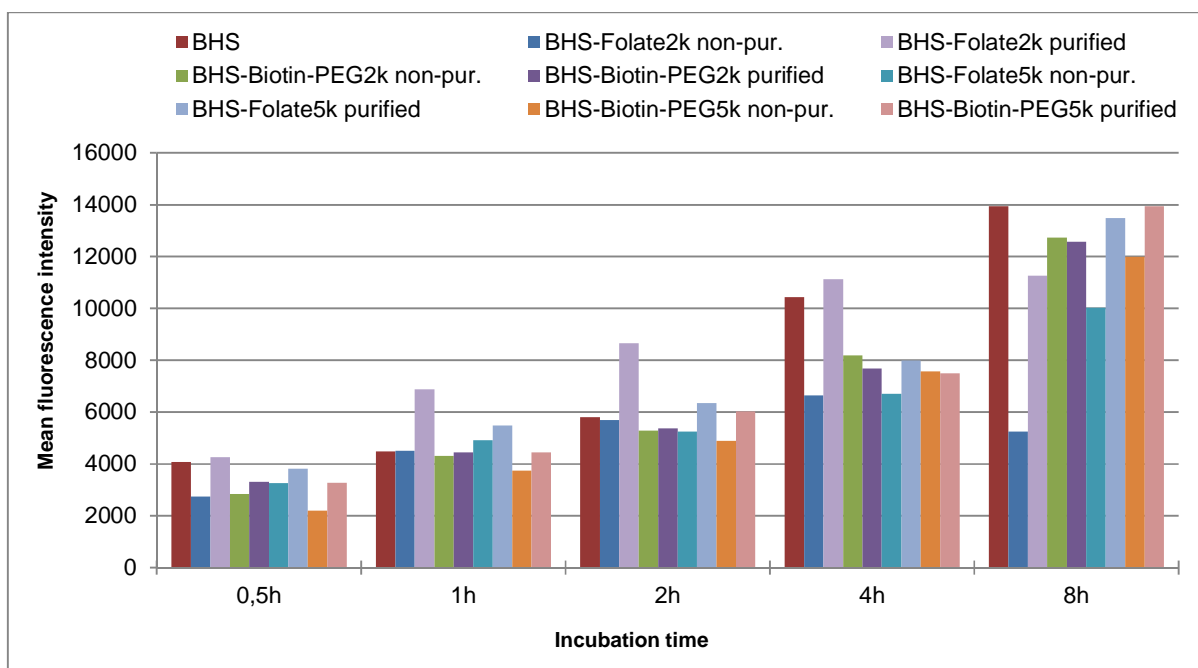
Figure 46: Cellular uptake of HEK293 cells after different incubation times

In Figure 46 the comparison of molecular uptake of HEK293 cells incubated with different BHS is presented. For all the structures the cellular uptake increases with the incubation time. The highest MFI values were obtained for non-modified BHS and purified BHS modified with Folate2k. Values obtained for the other BHS modified with folate and BHS modified with Biotin-PEG were in the similar range after all the time points.

Figure 47 shows the comparison of molecular uptake in SBC-2 cells after incubation with different BHS. The highest cellular uptake was achieved after the incubation with purified BHS modified with Folate2k and was significantly higher compared to the BHS modified with Biotin-PEG2k after every time point. For the BHS modified with longer spacers, it can be seen that MFI values obtained after modification with folate and Biotin-PEG are very similar for all the incubation times. This proves the back folding of the chain and unavailability of the folic acid to reach the folate receptors.
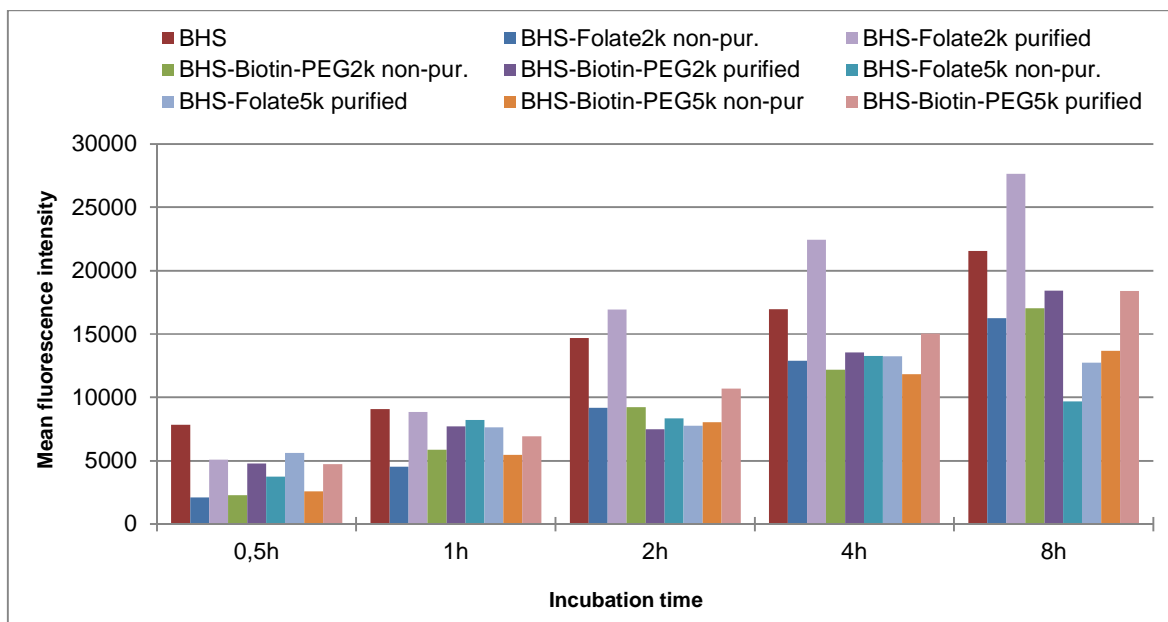
Figure 47: Cellular uptake of SBC-2 cells after different incubation times

5.6. Cellular uptake mechanism

To analyze the cell uptake mechanism of BHS, the flow cytometry experiments in the presence of inhibitor of endocytosis were performed. Mammalian cells use different endocytotic pathways for the internalization of nanoscaled particles, which can be distinguished between clathrin-dependent, caveolin-dependent and clathrin- and caveolin-independent endocytosis as presented in Figure 48. Clathrin-dependent endocytosis acts through the formation of clathrin-coated vesicles from clathrin-coated pits, which then form endosomes and fuse with lysosomes.[70] Chlorpromazine, which interferes with the intracellular clathrin processing, is an inhibitor of this mechanism[22] and was employed here.
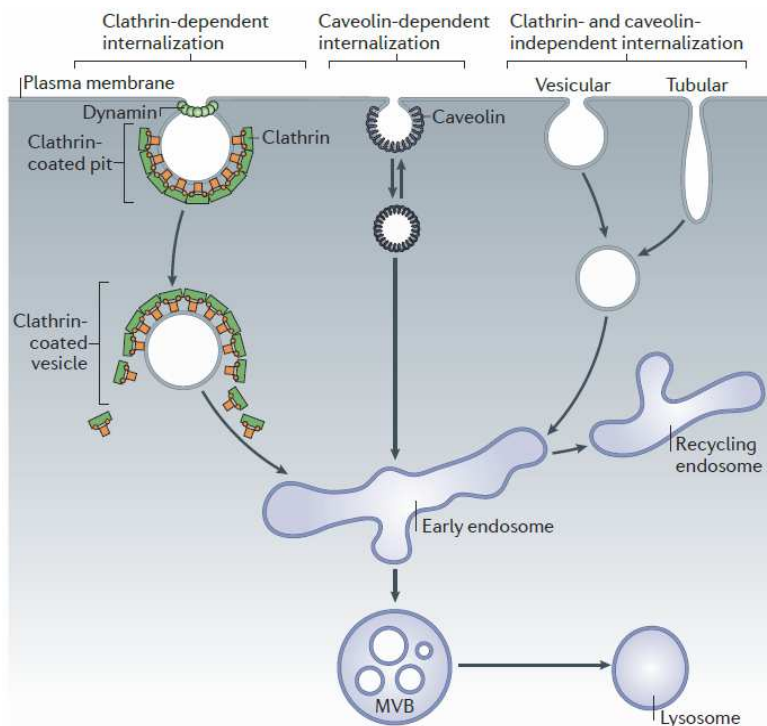
Figure 48: Clathrin-dependent and -independent internalization pathways.[71]

Different concentrations of chlorpromazine were added to the cell culture medium before incubation with BHS. The absence of cytotoxic effects which may otherwise influence subsequent analysis of uptake mechanisms was confirmed (the results shown in appendix on the page 88). The measurements were performed for non-modified BHS and BHS modified with Folate2k. Figure 49 presents the results obtained for non-modified BHS. There are no significant differences between the results obtained for the structures incubated with and without the presence of inhibitor in both cell lines. It means that internalization of BHS inside the cell does not take place through the clathrin-dependent endocytosis. It probably happens through the clathrin-independent process, cellular uptake is non-specific or BHS was bound to the cellular membrane and did not translocate inside the cell.
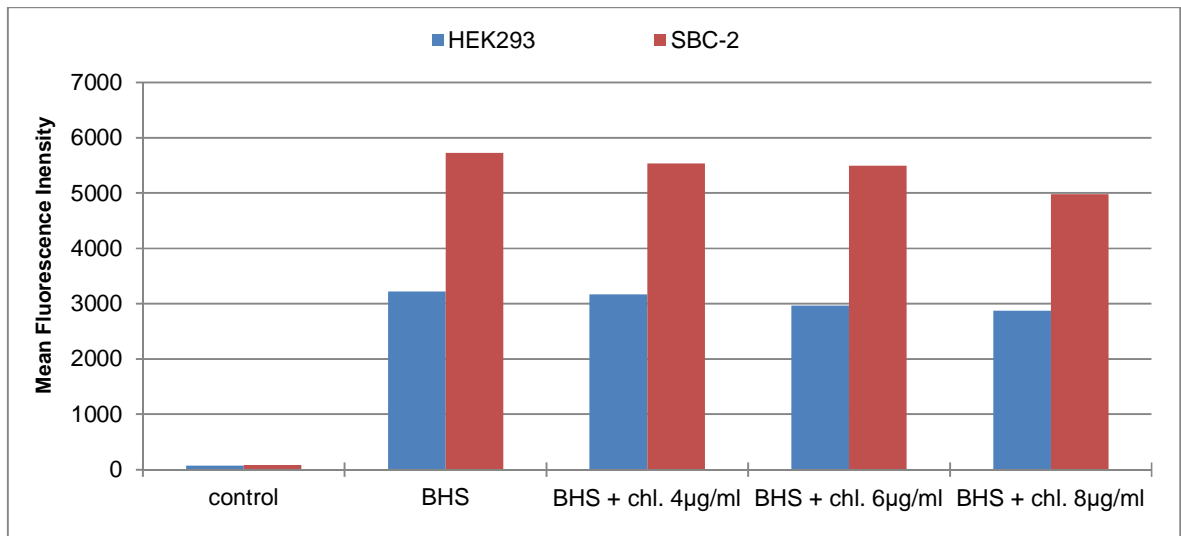
Figure 49: Cellular uptake after incubation with non-modified BHS incubated and different concentrations of inhibitors of endocytosis for 0.5 h. chl. = chlorpromazine

.
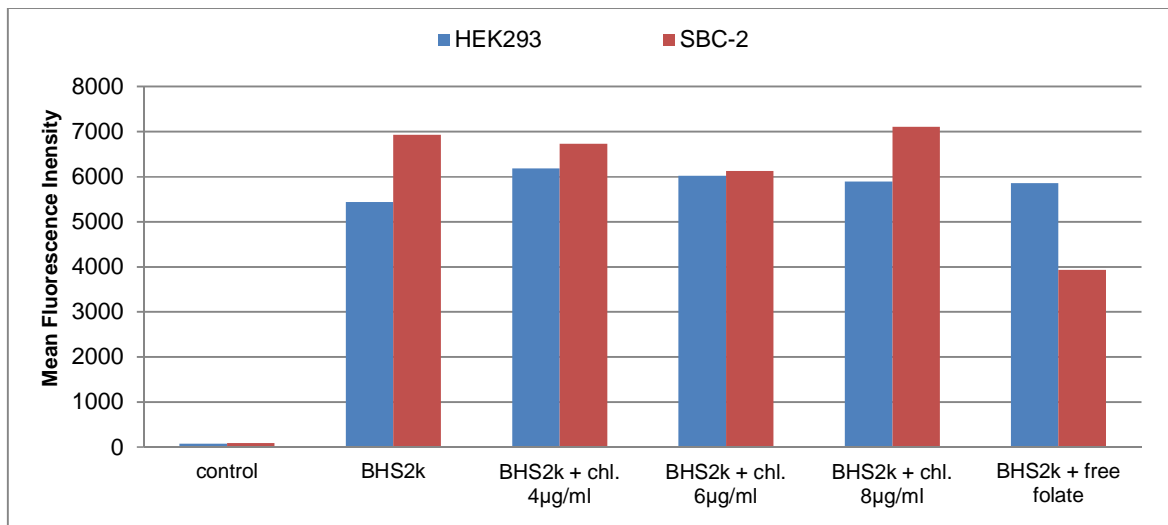
Figure 50: Cellular uptake after incubation with BHS modified with Folate2k and different concentrations of inhibitors of endocytosis for 2 h. BHS2k = PEI-biotin/SA/Folate2k, chl. = chlorpromazine

In the next step similar experiment was performed with BHS modified with Folate2k. Additionally, in order to verify that enhanced uptake of folic acid-containing BHS was mediated by folate receptors on the cancer cells, free folate was added to the cell culture medium before incubation with BHS. As shown in Figure 50, similarly to non-modified BHS, the uptake of both cell lines was not inhibited after incubation with chlorpromazine and the cellular uptake is not mediated through the clathrin-dependent endocytosis. The uptake of SBC-2 cells was significantly reduced when the folate receptors were blocked with free folic acid, whereas the uptake of HEK-293 cells was not decreased. Accordingly, blocking of the folate receptors in SBC-2 cells inhibited the folate-receptor mediated endocytosis process

IV. Conclusion

The aim of the thesis was the fabrication and characterization of biohybrid structures (BHS) with defined size based on streptavidin (SA) and pentavalent biotinylated dendritic glycopolymer through non-covalent SA-biotin conjugation and further functionalization with biotinylated PEGylated folic acid for the selective targeting to tumor cells. It was demonstrated that the use of polyassociation reaction allows the formation of BHS with the control over their sizes. Modification with folic acid via another biotin-streptavidin conjugation does not cause the disaggregation of the structures and the long term stability properties were confirmed. Addition of free biotin molecules or biotin-PEG$_{12}$ eventually caused the rearrangement of the structure due to a slight change in size but no degradation to initial components took place. Zeta potential measurements showed that the surface charge of BHS is slightly cationic.

The cytotoxicity of the BHS was investigated. It was shown that fabricated BHS are biocompatible, with regard to both normal and cancer cells. Modification with folic acid or biotin-PEG did not cause toxicity to the cells.

In the flow cytometry studies it was demonstrated that the molecular uptake of cancer cells incubated with BHS is up to two times higher compared with the normal cells. It showed that BHS are suitable materials as nanocarriers for the selective targeting to tumor cells. After incubation with the single components of the structures the cellular uptake was very low, however, using BHS it was significantly higher. It proved that BHS are extraordinary materials with synergetic functions that combine the features of both natural and synthetic components resulting with outstanding properties. Modification of BHS with folic acid ligand of short length with the ratio 1/1/6 increased the molecular uptake in cancer cells compared with the non-modified BHS. As the cellular uptake in normal cells was similar, it was proved that folic acid is a tumor-targeting agent, because it enhances the cellular uptake in cancer cells due to the successful recognition of folic acid by the folate receptors overexpressed on the cancer cells. It was shown that the cationic charge of BHS is a driving force of

internalization inside the cell or interaction with the negatively charged cellular membrane of normal cells, while internalization inside the cancer cell is a competition between the charge-driven and folate-mediated endocytosis process.

Furthermore, the impact of the purification step was investigated. It was demonstrated that after incubation with purified samples the molecular uptake in cancer cells was higher than without the purification. The presence of free folate groups in the solution leads to the occupation of the folate receptors and prevents the BHS from entering inside the cell.
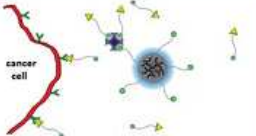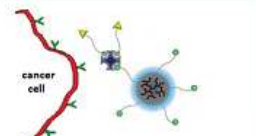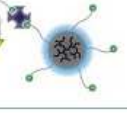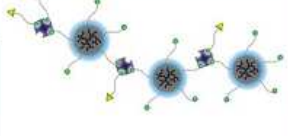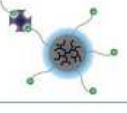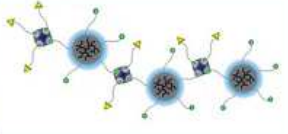
Figure 51: Summary of the influencing key points in the conjugation of biotinylated dendritic glycopolymers and streptavidin

Additionally, the direct influence of folic acid was analyzed by comparison of the cellular uptake after incubation with BHS modified with biotin-PEG-folic acid and BHS modified with biotin-PEG-COOH. It was shown that after modification with chains of short length, the uptake in cancer cells is significantly higher for the structures containing folic acid, whereas in normal cells is similar. After modification with chains of higher molar mass, the uptake in both cell lines was at the same level for both biotin-PEG-folic acid and biotin-PEG-COOH modifications. Modifying with short length biotin-PEG-folic acid moiety, folic acid is exposed at the surface of the structure and is able to directly interact with the folate receptors

expressing tumor cells. Modification with long length moiety results in backfolding of the chain and folic acid is not available to bind to the cell. When high number of folate molecules saturates all the residual binding pockets of SA, the shielding effect of BHS appears and the uptake is decreased. Figure 51 provides a summary of the main points investigated in the flow cytometry experiments. In the last step, the mechanism of cellular uptake was investigated. It was proved that both non-modified and modified with folate BHS are not taken up inside the cell through the clathrin-dependent endocytosis process. Future experiments are necessary to investigate the uptake mechanism of BHS. Additionally, BHS modified with folate were incubated with free folate molecules in order to prove receptor blocking. The uptake was decreased which proved that free folate present in the solution inhibited the folate-receptor mediated endocytosis process.

V. Experimental section

1. Reagents and materials

Modification of hyperbranched poly(ethylene imine) with maltose and biotinylation were performed by the working group as previously described by Appelhans et al.[14] and Ennen et al.[59].

Table 4. List of the used substances and their suppliers

Substance	Supplier
Hyperbranched poly(ethylene imine) with M_w 25000 g·mol^{-1}	BASF SE
Streptavidin	Prozyme
Neutravidin	Thermofisher
Folic acid-PEG-biotin with M_w 2000 g·mol^{-1}	Nanocs
Folic acid-PEG-biotin with M_w 5000 g·mol^{-1}	Nanocs
Biotin-PEG-COOH with M_w 2000 g·mol^{-1}	Creative PEGWorks
Biotin-CONH-PEG-COOH with M_w 5000 g·mol^{-1}	RAPP Polymere
Biotin	Sigma Aldrich
Biotin-PEG$_{12}$-COOH	Iris Biotech GMBH
Biotin-4-Fluorescein	Sigma Aldrich
Phosphate buffered saline (PBS)	Sigma Aldrich
Dulbecco's modified eagle medium (DMEM)	Life Technologies
Dulbecco's Phosphate Buffered Saline (DPBS)	Life Technologies
Trypsin-EDTA (0.05 %)	Life Technologies
AlamarBlue cell viability reagent	Thermofisher
Dialysis tubes from Cellulose Ester (MWCO 20000 Da)	SpectrumLabs
Chlorpromazine hydrochloride	Sigma Aldrich

2. Instruments

2.1. Dynamic light scattering and zeta potential

Characterization of the particle size, size distribution and zeta potential was performed using Nano Zetasizer (Malvern Instruments Ltd), equipped with a He-Ne laser (4 mW) and a digital autocorrelator. The measurements were carried out at 25°C at a fixed angle of 173°.

In the size measurements the disposable plastic cuvettes (PLASTIBRAND, UV) of BRAND GmbH&Co. KG, Wertheim, Germany with 1cm pathlength were used.

For the zeta potential measurement the disposable folded capillary cells of Malvern Instruments were used.

2.2. UV-Vis spectroscopy

UV/Vis spectra were recorded at room temperature (25 °C) on Specord 20 Plus UV/Vis spectrometer (Analytik Jena AG).
All photometric measurements were performed in quartz microcuvettes.

2.3. Cell culture

All the experiments with cell cultures were performed in laminar flow work bench Laminair HB2472 (Heraeus Instruments GmbH). Cells were kept in the BBD 6220 CO_2 incubator (Thermo Scientific Heraeus) under constant conditions at 37 °C in 5% CO_2 atmosphere.

2.4. Cytotoxicity

Fluorescence intensities in the cytotoxicity experiments were recorded on Synergy 2 Multi-Mode Reader (BioTek Instruments) at room temperature (25 °C).

2.5. Flow cytometry

Flow cytometry experiments were performed on MACSQuant® Analyzer 10 (Miltenyi Biotec) which is equipped in three lasers (violet, blue and red with excitation wavelengths 405nm, 488nm and 635nm, respectively) and 10 optical channels.

3. Formation of biohybrid structures

The general protocol for the preparation of BHS consisted of few steps. First step included the preparation of SA and PEI-biotin solutions which were kept overnight before the assembling of BHS. The solvent of the BHS formation was phosphate buffered saline (PBS). The next day, the solutions of SA and PEI-biotin were filtered with 0.1 and 0.25 µm filters, respectively, and mixed for the assembling process of BHS. The solutions were let to equilibrate for 24 hours at 7 °C. After the assembling process of BHS was finished, the modification with folate was done by mixing solutions in the required ratios. After the assembling time of 18 hours, the characterization of modified BHS could be performed. If the purification step was required, samples were purified in a dialysis process. Samples were placed inside the membrane with the cut-off of 20 kDa and dialyzed against PBS solution under constant stirring for 24 hours. Amount of folate that was flashed out during the dialysis was controlled through UV-Vis measurement. Absorption spectra were recorded before and after the dialysis and the comparison of absorbance values at 350 nm and 500 nm enabled the estimation of the sample dilution during the dialysis and the amount of folate that was bound to BHS (data not shown).

The molar concentrations used for preparation of BHS for DLS measurements are presented in Table 5. Volume used for the measurement was 500 µl. For the experiments with the excess of biotin, free biotin or biotin-PEG$_{12}$ in the corresponding concentrations were added to the solution of BHS 24 hours after assembling of the structures. The PEI-biotin/SA/Folate molar ratios used for all the experiments are presented in Table 6. For the zeta potential measurements, the solutions of BHS were prepared with the SA concentration c=2.5 mol·L^{-1}

and corresponding PEI-biotin and folate concentrations in Millipore water and purified in distilled water for 24 h.

Table 5. Molar concentrations used for fabrication of BHS in DLS measurements.

	c_{SA}, mol·L^{-1}	$c_{PEI-biotin}$, mol·L^{-1}	c_{Folate}, mol·L^{-1}	Total mass concentration, mg·ml^{-1}
SA	7.5	0	0	0.655
PEI-biotin	0	10	0	0.743
SA/PEI-biotin 1/0.5	2.5	1.25	0	0.311
SA/PEI-biotin 1/1	2.5	2.5	0	0.404
SA/PEI-biotin 1/2	2.5	5	0	0.590
PEI-biotin/SA/Folate2k 1/1/6	2.5	2.5	15	0.434
PEI-biotin/SA/Folate5k 1/1/6	2.5	2.5	15	0.479

For the cytotoxicity measurements the solution of BHS with the highest concentration (c=2.5 g·L^{-1}) was prepared and the samples with smaller concentrations were obtained by dissolution of the highest concentrated sample in PBS.

For the flow cytometry experiment, the solutions were prepared in a way that the final mass concentration of each sample was 200 μg·mL^{-1}. Staining of the samples with fluorescent dye was desired to conduct the experiment. In the measurements of single components, PEI-biotin and SA labeled with fluorescein isothiocyanate (FITC) were used. PEI-biotin was labeled with SCN-FITC during the formation process and SA was stained by mixing with the biotin-FITC solution in the molar ratio 1/1. Modification of PEI-biotin with FITC was performed by Johannes Fingernagel, member of Dr Appelhans group. The samples of folate were not labeled, because folic acid exhibits fluorescent behavior. BHS samples used in the flow cytometry were fabricated with the use of PEI-biotin stained with FITC and non-labeled SA.

72

Table 6. Molar ratios of the PEI-biotin/SA/Folate and PEI-biotin/SA/biotin-PEG used in different experiments.

BHS	DLS	Zeta potential	Cytotoxicity	Flow cytometry
SA/PEI-biotin	1/0.5, 1/1, 1/2	-	1/1	1/1
PEI-biotin/SA/Biotin	1/1/1, 1/1/2, 1/1/4, 1/1/10, 1/1/50 and 1/1/100	-	--	-
PEI-biotin/SA/Biotin-PEG$_{12}$	1/1/1, 1/1/2, 1/1/4, 1/1/10, and 1/1/100	-	-	-
PEI-biotin/SA/Folate2k	1/1/6	1/1/6	1/1/6	1/1/1, 1/1/2, 1/1/6, 1/1/8 and 1/1/10
PEI-biotin/SA/Folate5k	1/1/6	1/1/6	1/1/6	1/1/1, 1/1/2, 1/1/6, 1/1/8 and 1/1/10
PEI-biotin/SA/biotin-PEG2k	-	-	1/1/6	1/1/6
PEI-biotin/SA/biotin-PEG5k	-	-	1/1/6	1/1/6

4.   Characterization of biohybrid structures

4.1.   Dynamic light scattering

To characterize the particle size and size distribution, DLS measurements were performed in 5 runs, with 12 x 10 seconds. Thus only measurements with a good fit and an exponential graphic representation were considered here. The results were analyzed by merging identical curves from different measurement runs. The particle size distribution was determined using a multimodal peak analysis by volume.

4.2. Zeta potential

Zeta potential measurements conditions were 3 runs with 50 x 1 second at 40V. The solutions used for titration were 0.1M HCl and NaOH.

4.3. Cell culture

Human Embryonic Kidney 293 cells (HEK293) and Human Cervix Carcinoma cells (SBC-2, derivative of HELA) were obtained from Neurosurgery Department, University Hospital Carl Gustav Carus, Germany. Cells were cultured in DMEM growth medium supplemented with 10% (v/v) fetal calf serum, 2 mM L-glutamine, 1 mM sodium pyruvate, 100 units mL^{-1} penicillin and 100 µg mL^{-1} streptomycin. Cell were grown in a humidified incubator at 37 °C in 5% CO_2 atmosphere. The medium was replaced every two days and cells were subcultured by trypsinization.

4.4. Cytotoxicity assay

HEK293 and SBC-2 cells were seeded in a 96-well plate at an initial density of 2×10^4 cells per well in 200 µL of complete DMEM medium. After 24 h incubation cell culture medium was replaced with 200 µL of DMEM containing the corresponding BHS with the desired concentrations for further 24 h. AlamarBlue reagent (10% v/v) was added to each well and cells were further incubated for 4 h at 37 °C. Finally, the fluorescence intensities were recorded by a microplate reader. Each experiment was done in triplicate and the data are shown as the mean value plus standard deviation (SD).

4.5. Flow cytometry

HEK293 and SBC-2 cells were seeded at density of 2×10^5 cells per well in 1,5 ml of complete DMEM medium in a 12-well plate and incubated for 24 h. Cells were then incubated with 1

ml of DMEM containing 200 μg mL^{-1} of the corresponding sample at 37°C in a humidified 5% CO_2 incubator. After desired incubation time, cells were washed with PBS and harvested by trypsinization followed by centrifugation at 1100 rpm for 5 min at 4°C. The resulting pellets were resuspended in 200 μL PBS and analyzed by the flow cytometer. A minimum of 3×10^4 cells have been analyzed for each sample and the data was analyzed by FlowJo software.

For the experiments of cellular uptake mechanism, cells were incubated for 1 hour with the cell culture medium containing the corresponding concentration of chlorpromazine. Afterwards, medium was replaced with DMEM containing chlorpromazine and corresponding BHS. For the experiments of receptors blocking, cells were incubated with cell culture medium containing 200 μg mL^{-1} of folic acid-PEG-biotin. After 30 minutes, BHS were added and the instruction was followed as for the previous experiments.

VI. References

[1]   Abbasi, E.; Aval, S. F.; Akbarzadeh, A.; Milani, M.; Nasrabadi, H. T.; Joo, S. W.; Hanifehpour, Y.; Nejati-Koshki, K.; Pashaei-Asl, R. Dendrimers: synthesis, applications, and properties. *Nanoscale Research Letters* 2014, 9.

[2]   Dykes, G. M. Dendrimers: a review of their appeal and applications. *Journal of Chemical Technology and Biotechnology* 2001, 76, 903-18.

[3]   Carlmark, A.; Hawker, C. J.; Hult, A.; Malkoch, M. New methodologies in the construction of dendritic materials. *Chemical Society Reviews* 2009, 38, 352-62.

[4]   Buhleier, E.; Wehner, W.; Vogtle, F. Cascade-Chain-Like and Nonskid-Chain-Like Syntheses of Molecular Cavity Topologies. *Synthesis-Stuttgart* 1978, 155-58.

[5]   Fischer, M.; Vogtle, F. Dendrimers: From design to application - A progress report. *Angewandte Chemie-International Edition* 1999, 38, 885-905.

[6]   Nanjwade, B. K.; Bechra, H. M.; Derkar, G. K.; Manvi, F. V.; Nanjwade, V. K. Dendrimers: Emerging polymers for drug-delivery systems. *European Journal of Pharmaceutical Sciences* 2009, 38, 185-96.

[7]   Jang, W. D.; Selim, K. M. K.; Lee, C. H.; Kang, I. K. Bioinspired application of dendrimers: From bio-mimicry to biomedical applications. *Progress in Polymer Science* 2009, 34, 1-23.

[8]   Holter, D.; Burgath, A.; Frey, H. Degree of branching in hyperbranched polymers. *Acta Polymerica* 1997, 48, 30-35.

[9]   Gillies, E. R.; Frechet, J. M. J. Dendrimers and dendritic polymers in drug delivery. *Drug Discovery Today* 2005, 10, 35-43.

[10]   Cheng, Y. Y.; Man, N.; Xu, T. W.; Fu, R. Q.; Wang, X. Y.; Wang, X. M.; Wen, L. P. Transdermal delivery of nonsteroidal anti-inflammatory drugs mediated by polyamidoamine (PAMAM) dendrimers. *Journal of Pharmaceutical Sciences* 2007, 96, 595-602.

[11]   Najlah, M.; Freeman, S.; Attwood, D.; D'Emanuele, A. In vitro evaluation of dendrimer prodrugs for oral drug delivery. *International Journal of Pharmaceutics* 2007, 336, 183-90.

[12]   Quintana, A.; Raczka, E.; Piehler, L.; Lee, I.; Myc, A.; Majoros, I.; Patri, A. K.; Thomas, T.; Mule, J.; Baker, J. R. Design and function of a dendrimer-based therapeutic nanodevice targeted to tumor cells through the folate receptor. *Pharmaceutical Research* 2002, 19, 1310-16.

[13]   Yemul, O.; Imae, T. Synthesis and characterization of poly(ethyleneimine) dendrimers. *Colloid and Polymer Science* 2008, 286, 747-52.

[14]   Appelhans, D.; Komber, H.; Quadir, M. A.; Richter, S.; Schwarz, S.; van der Vlist, J.; Aigner, A.; Muller, M.; Loos, K.; Seidel, J.; Arndt, K. F.; Haag, R.; Voit, B. Hyperbranched PEI with Various Oligosaccharide Architectures: Synthesis, Characterization, ATP Complexation, and Cellular Uptake Properties. *Biomacromolecules* 2009, 10, 1114-24.

[15]   Fischer, D.; Bieber, T.; Li, Y. X.; Elsasser, H. P.; Kissel, T. A novel non-viral vector for DNA delivery based on low molecular weight, branched polyethylenimine: Effect of molecular weight on transfection efficiency and cytotoxicity. *Pharmaceutical Research* 1999, 16, 1273-79.

[16]   Liang, B.; He, M. L.; Xiao, Z. P.; Li, Y.; Chan, C. Y.; Kung, H. F.; Shuai, X. T.; Peng, Y. Synthesis and characterization of folate-PEG-grafted-hyperbranched-PEI for tumor-targeted gene delivery. *Biochemical and Biophysical Research Communications* 2008, 367, 874-80.

[17]   Rudd, P. M.; Wormald, M. R.; Dwek, R. A. Sugar-mediated ligand-receptor interactions in the immune system. *Trends in Biotechnology* 2004, 22, 524-30.

[18]   Gorelik, E.; Galili, U.; Raz, A. On the role of cell surface carbohydrates and their binding proteins (lectins) in tumor metastasis. *Cancer and Metastasis Reviews* 2001, 20, 245-77.

[19]   Veronese, F. M.; Pasut, G. PEGylation, successful approach to drug delivery. *Drug Discovery Today* 2005, 10, 1451-58.

[20]   Appelhans, D.; Klajnert-Maculewicz, B.; Janaszewska, A.; Lazniewska, J.; Voit, B. Dendritic glycopolymers based on dendritic polyamine scaffolds: view on their synthetic approaches, characteristics and potential for biomedical applications. *Chemical Society Reviews* 2015, 44, 3968-96.

[21]   Klajnert, B.; Appelhans, D.; Komber, H.; Morgner, N.; Schwarz, S.; Richter, S.; Brutschy, B.; Ionov, M.; Tonkikh, A. K.; Bryszewska, M.; Voit, B. The influence of densely organized maltose shells on the biological properties of poly(propylene imine) dendrimers: New effects dependent on hydrogen bonding. *Chemistry-a European Journal* 2008, 14, 7030-41.

[22]   Hobel, S.; Loos, A.; Appelhans, D.; Schwarz, S.; Seidel, J.; Voit, B.; Aigner, A. Maltose- and maltotriose-modified, hyperbranched poly(ethylene imine)s (OM-PEIs): Physicochemical and biological properties of DNA and siRNA complexes. *Journal of Controlled Release* 2011, 149, 146-58.

[23]   Sakahara, H.; Saga, T. Avidin-biotin system for delivery of diagnostic agents. *Advanced Drug Delivery Reviews* 1999, 37, 89-101.

[24]   Livnah, O.; Bayer, E. A.; Wilchek, M.; Sussman, J. L. 3-Dimensional Structures of Avidin and the Avidin-Biotin Complex. *Proceedings of the National Academy of Sciences of the United States of America* 1993, 90, 5076-80.

[25]   Livnah, O.; Bayer, E. A.; Wilchek, M.; Sussman, J. L. The Structure of the Complex between Avidin and the Dye, 2-(4'-Hydroxyazobenzene) Benzoic-Acid (Haba). *Febs Letters* 1993, 328, 165-68.

[26]   Fingernagel, J. Untersuchung von Biohybridstrukturen auf Basis von Glycopolymeren und Albuminbindungsdomänen unter Nutzung von Nickel (II)– Nitrilotriessigsäure– Histidin und Biotin– Avidin Wechselwirkungen. Master thesis, Technische Universität Dresden, 2013.

[27]   Dundas, C. M.; Demonte, D.; Park, S. Streptavidin-biotin technology: improvements and innovations in chemical and biological applications. *Applied Microbiology and Biotechnology* 2013, 97, 9343-53.

[28]   Bruch, R. C.; White, H. B. Compositional and Structural Heterogeneity of Avidin Glycopeptides. *Biochemistry* 1982, 21, 5334-41.

[29]   Weber, P. C.; Ohlendorf, D. H.; Wendoloski, J. J.; Salemme, F. R. Structural Origins of High-Affinity Biotin Binding to Streptavidin. *Science* 1989, 243, 85-88.

[30]   Vermette, P.; Gengenbach, T.; Divisekera, U.; Kambouris, P. A.; Griesser, H. J.; Meagher, L. Immobilization and surface characterization of NeutrAvidin biotin-binding protein on different hydrogel interlayers. *Journal of Colloid and Interface Science* 2003, 259, 13-26.

[31]   Technical data sheet 779.; The benefits of neutravidin over streptavidin and avidin. *Polysciences, Inc., 2008*.

[32]   Sinha, R.; Kim, G. J.; Nie, S. M.; Shin, D. M. Nanotechnology in cancer therapeutics: bioconjugated nanoparticles for drug delivery. *Molecular Cancer Therapeutics* 2006, 5, 1909-17.

[33]   Hilgenbrink, A. R.; Low, P. S. Folate receptor-mediated drug targeting: From therapeutics to diagnostics. *Journal of Pharmaceutical Sciences* 2005, 94, 2135-46.

[34]   Ross, J. F.; Chaudhuri, P. K.; Ratnam, M. Differential Regulation of Folate Receptor Isoforms in Normal and Malignant-Tissues in-Vivo and in Established Cell-Lines - Physiological and Clinical Implications. *Cancer* 1994, 73, 2432-43.

[35]   Weitman, S. D.; Weinberg, A. G.; Coney, L. R.; Zurawski, V. R.; Jennings, D. S.; Kamen, B. A. Cellular-Localization of the Folate Receptor - Potential Role in Drug Toxicity and Folate Homeostasis. *Cancer Research* 1992, 52, 6708-11.

[36]   Cole, A. J.; Yang, V. C.; David, A. E. Cancer theranostics: the rise of targeted magnetic nanoparticles. *Trends in Biotechnology* 2011, 29, 323-32.

[37]   Bailey, L. B.; Gregory, J. F. Folate metabolism and requirements. *Journal of Nutrition* 1999, 129, 779-82.

[38]   Stanger, O. Physiology of folic acid in health and disease. *Current Drug Metabolism* 2002, 3, 211-23.

[39]   Marchetti, C.; Palaia, I.; Giorgini, M.; De Medici, C.; Iadarola, R.; Vertechy, L.; Domenici, L.; Di Donato, V.; Tomao, F.; Muzii, L.; Panici, P. B. Targeted drug delivery via folate receptors in recurrent ovarian cancer: a review. *Oncotargets and Therapy* 2014, 7, 1223-36.

[40]   Leamon, C. P.; Low, P. S. Delivery of Macromolecules into Living Cells - a Method That Exploits Folate Receptor Endocytosis. *Proceedings of the National Academy of Sciences of the United States of America* 1991, 88, 5572-76.

[41]   Wang, Z. L.; Xu, B.; Zhang, L.; Zhang, J. B.; Ma, T. H.; Zhang, J. B.; Fu, X. Q.; Tian, W. J. Folic acid-functionalized mesoporous silica nanospheres hybridized with AIE luminogens for targeted cancer cell imaging. *Nanoscale* 2013, 5, 2065-72.

[42]   Jung, C. W.; Jalani, G.; Ko, J.; Choo, J.; Lim, D. W. Synthesis, Characterization, and Directional Binding of Anisotropic Biohybrid Microparticles for Multiplexed Biosensing. *Macromolecular Rapid Communications* 2014, 35, 56-65.

[43]   Rao, S. Y.; Guo, Z. B.; Liang, D. W.; Chen, D. L.; Wei, Y.; Xiang, Y. A proteorhodopsin-based biohybrid light-powering pH sensor. *Physical Chemistry Chemical Physics* 2013, 15, 15821-24.

[44]   Sapsford, K. E.; Algar, W. R.; Berti, L.; Gemmill, K. B.; Casey, B. J.; Oh, E.; Stewart, M. H.; Medintz, I. L. Functionalizing Nanoparticles with Biological Molecules: Developing Chemistries that Facilitate Nanotechnology. *Chemical Reviews* 2013, 113, 1904-2074.

[45]   Park, I. K.; Von Recum, H. A.; Jiang, S. Y.; Pun, S. H. Supramolecular assembly of cyclodextrin-based nanoparticles on solid surfaces for gene delivery. *Langmuir* 2006, 22, 8478-84.

[46]   Loftsson, T.; Duchene, D. Cyclodextrins and their pharmaceutical applications. *International Journal of Pharmaceutics* 2007, 329, 1-11.

[47]   Granadero, D.; Bordello, J.; Perez-Alvite, M. J.; Novo, M.; Al-Soufi, W. Host-Guest Complexation Studied by Fluorescence Correlation Spectroscopy: Adamantane-Cyclodextrin Inclusion. *International Journal of Molecular Sciences* 2010, 11, 173-88.

[48]   Paolino, M.; Ennen, F.; Lamponi, S.; Cernescu, M.; Voit, B.; Cappelli, A.; Appelhans, D.; Komber, H. Cyclodextrin-Adamantane Host-Guest Interactions on the Surface of Biocompatible Adamantyl-Modified Glycodendrimers. *Macromolecules* 2013, 46, 3215-27.

[49]   Koopmans, C.; Ritter, H. Formation of Physical Hydrogels via Host-Guest Interactions of beta-Cyclodextrin Polymers and Copolymers Bearing Adamantyl Groups. *Macromolecules* 2008, 41, 7418-22.

[50]   Scott, J. K.; Loganathan, D.; Easley, R. B.; Gong, X. F.; Goldstein, I. J. A Family of Concanavalin a-Binding Peptides from a Hexapeptide Epitope Library. *Proceedings of the National Academy of Sciences of the United States of America* 1992, 89, 5398-402.

[51]   Yin, R. X.; Tong, Z.; Yang, D. Z.; Nie, J. Glucose and pH dual-responsive concanavalin A based microhydrogels for insulin delivery. *International Journal of Biological Macromolecules* 2011, 49, 1137-42.

[52]   Zempleni, J.; Wijeratne, S. S. K.; Hassan, Y. I. Biotin. *Biofactors* 2009, 35, 36-46.

[53]   Ennen, F.; Boye, S.; Lederer, A.; Cernescu, M.; Komber, H.; Brutschy, B.; Voit, B.; Appethans, D. Biohybrid structures consisting of biotinylated glycodendrimers and proteins:

influence of the biotin ligand's number and chemical nature on the biotin-avidin conjugation. *Polymer Chemistry* 2014, 5, 1323-39.

[54]   Wilchek, M.; Bayer, E. A.; Livnah, O. Essentials of biorecognition: The (strept)avidin-biotin system as a model for protein-protein and protein-ligand interaction. *Immunology Letters* 2006, 103, 27-32.

[55]   Hnatowich, D. J.; Virzi, F.; Rusckowski, M. Investigations of Avidin and Biotin for Imaging Applications. *Journal of Nuclear Medicine* 1987, 28, 1294-302.

[56]   Lillich, M.; Chen, X.; Weil, T.; Barth, H.; Fahrer, J. Streptavidin-Conjugated C3 Protein Mediates the Delivery of Mono-Biotinylated RNAse A into Macrophages. *Bioconjugate Chemistry* 2012, 23, 1426-36.

[57]   Qu, W.; Qin, S. Y.; Kuang, Y.; Zhuo, R. X.; Zhang, X. Z. Peptide-based vectors mediated by avidin-biotin interaction for tumor targeted gene delivery. *Journal of Materials Chemistry B* 2013, 1, 2147-54.

[58]   Pulkkinen, M.; Pikkarainen, J.; Wirth, T.; Tarvainen, T.; Haapa-Acho, V.; Korhonen, H.; Seppala, J.; Jarvinen, K. Three-step tumor targeting of paclitaxel using biotinylated PLA-PEG nanoparticles and avidin-biotin technology: Formulation development and in vitro anticancer activity. *European Journal of Pharmaceutics and Biopharmaceutics* 2008, 70, 66-74.

[59]   Ennen, F.; Fenner, P.; Boye, S.; Lederer, A.; Komber, H.; Voit, B.; Appelhans, D. Sphere-Like Protein-Glycopolymer Nanostructures Tailored by Polyassociation. *Biomacromolecules* 2016, 17, 32-45.

[60]   Gun'ko, V. M.; Klyueva, A. V.; Levchuk, Y. N.; Leboda, R. Photon correlation spectroscopy investigations of proteins. *Advances in Colloid and Interface Science* 2003, 105, 201-328.

[61]   Brar, S. K.; Verma, M. Measurement of nanoparticles by light-scattering techniques. *Trac-Trends in Analytical Chemistry* 2011, 30, 4-17.

[62]   Glawdel T.; Ren C. (2008) Zeta Potential measurement. In *Encyclopedia of Microfluidics and Nanofluidics*. (pp 2199-2207); Li D.; Springer

[63]   Rampersad, S. N. Multiple Applications of Alamar Blue as an Indicator of Metabolic Function and Cellular Health in Cell Viability Bioassays. *Sensors* 2012, 12, 12347-60.

[64]   Brown, M.; Wittwer, C. Flow cytometry: Principles and clinical applications in hematology. *Clinical Chemistry* 2000, 46, 1221-29.

[65]   Picot, J.; Guerin, C. L.; Kim, C. L. V.; Boulanger, C. M. Flow cytometry: retrospective, fundamentals and recent instrumentation. *Cytotechnology* 2012, 64, 109-30.

[66]   Torchilin, V. P. Passive and Active Drug Targeting: Drug Delivery to Tumors as an Example. In *Drug Delivery*, Schäfer-Korting, M., Ed. Springer Berlin Heidelberg: Berlin, Heidelberg, 2010; pp 3-53.

[67]   Torchilin, V. P. Targeting of Drugs and Drug Carriers within the Cardiovascular-System. *Advanced Drug Delivery Reviews* 1995, 17, 75-101.

[68]   Capco, D. G.; Chen, Y. S. *Nanomaterial: Impacts on Cell Biology and Medicine*. Springer: 2014.

[69]   Ahn, S.; Seo, E.; Kim, K.; Lee, S. J. Controlled cellular uptake and drug efficacy of nanotherapeutics. *Scientific Reports* 2013, 3.

[70]   Brodsky, F. M.; Chen, C. Y.; Knuehl, C.; Towler, M. C.; Wakeham, D. E. Biological basket weaving: Formation and function of clathrin-coated vesicles. *Annual Review of Cell and Developmental Biology* 2001, 17, 517-68.

[71]   McMahon, H. T.; Boucrot, E. Molecular mechanism and physiological functions of clathrin-mediated endocytosis. *Nature Reviews Molecular Cell Biology* 2011, 12, 517-33.
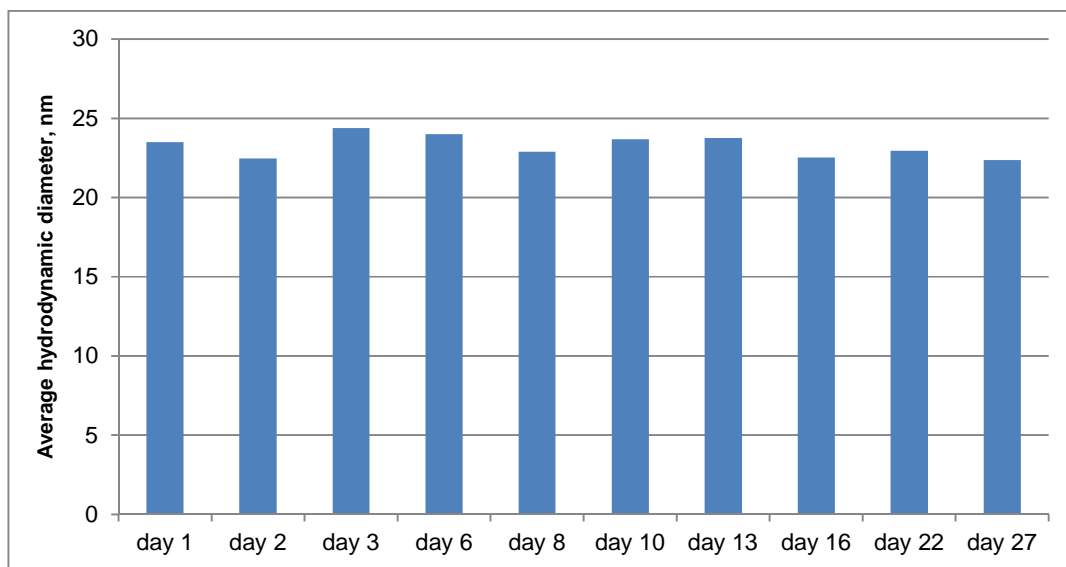
VII. Appendix

Figure 52: Long term stability study of the non-modified BHS consisted of SA/PEI-biotin 1/0.5.
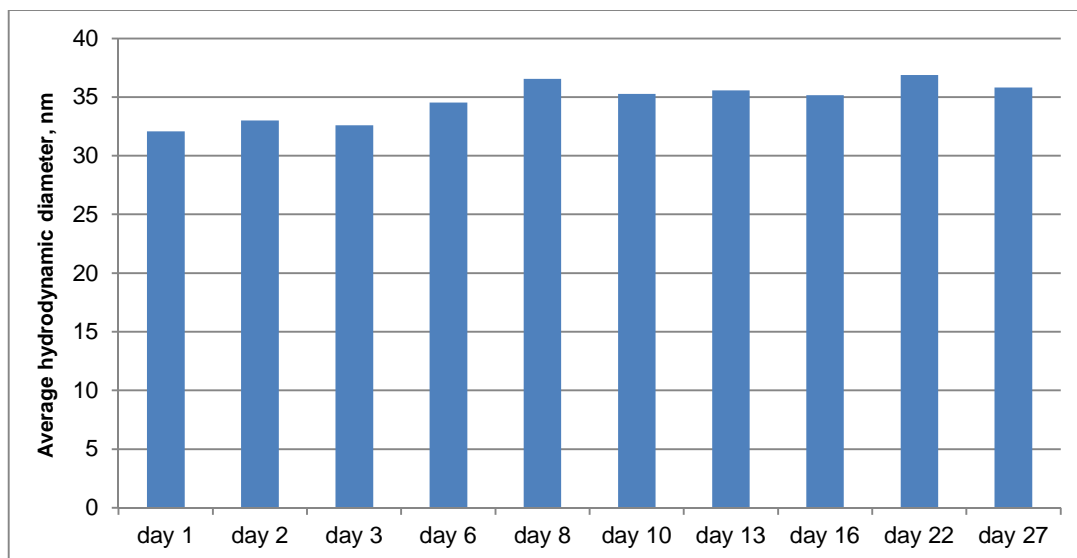

Figure 53: Long term stability study of the non-modified BHS consisted of SA/PEI-biotin 1/2.
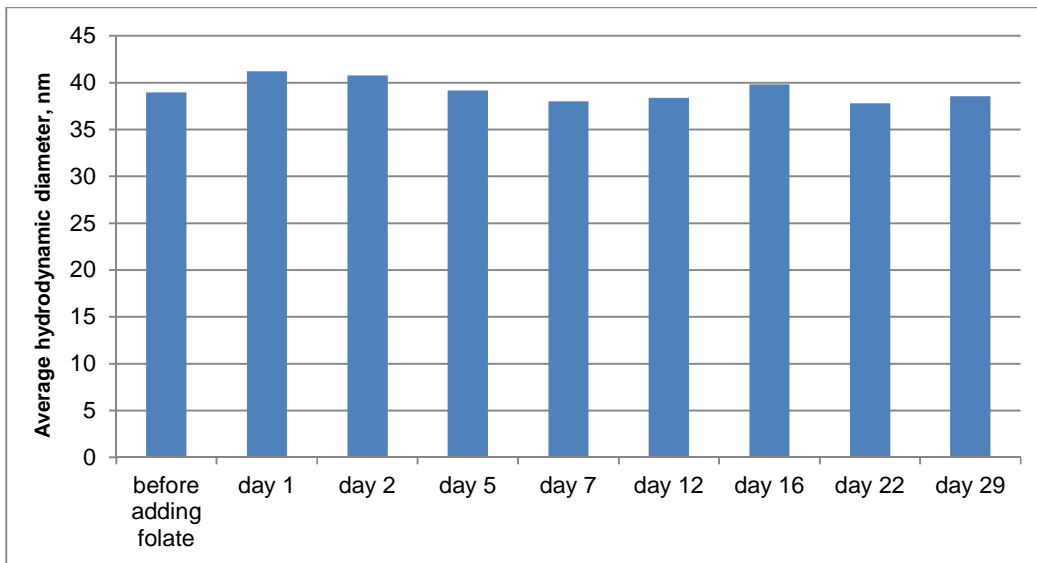
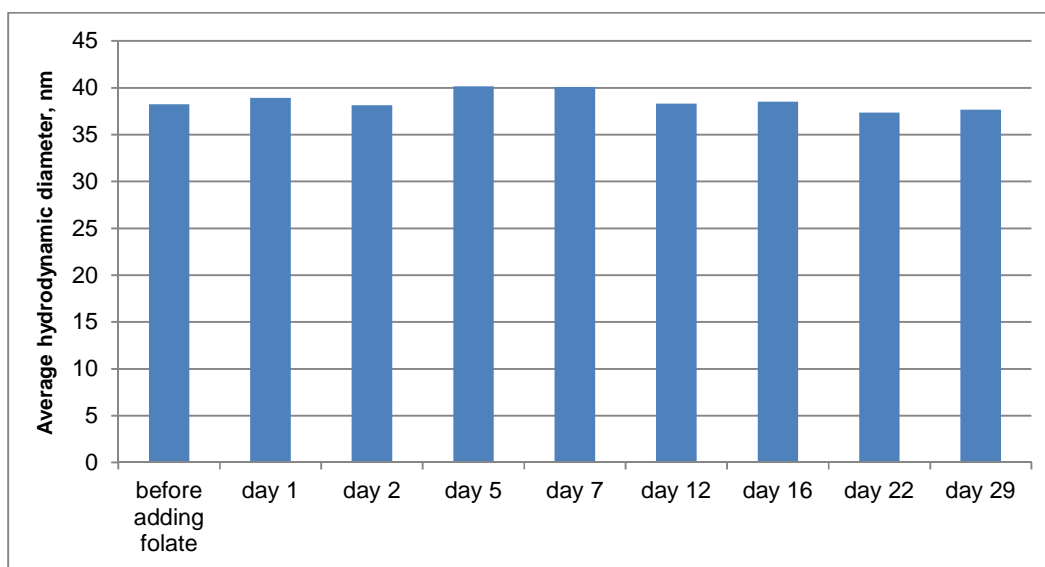**Figure 54:** Long term stability study of the purified BHS modified with Folate2k.

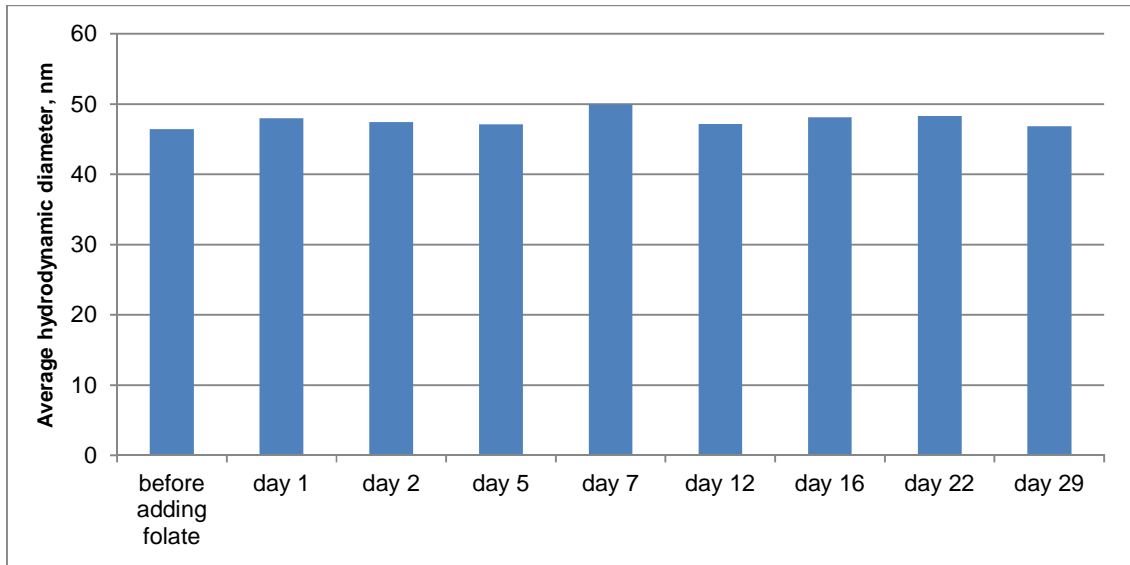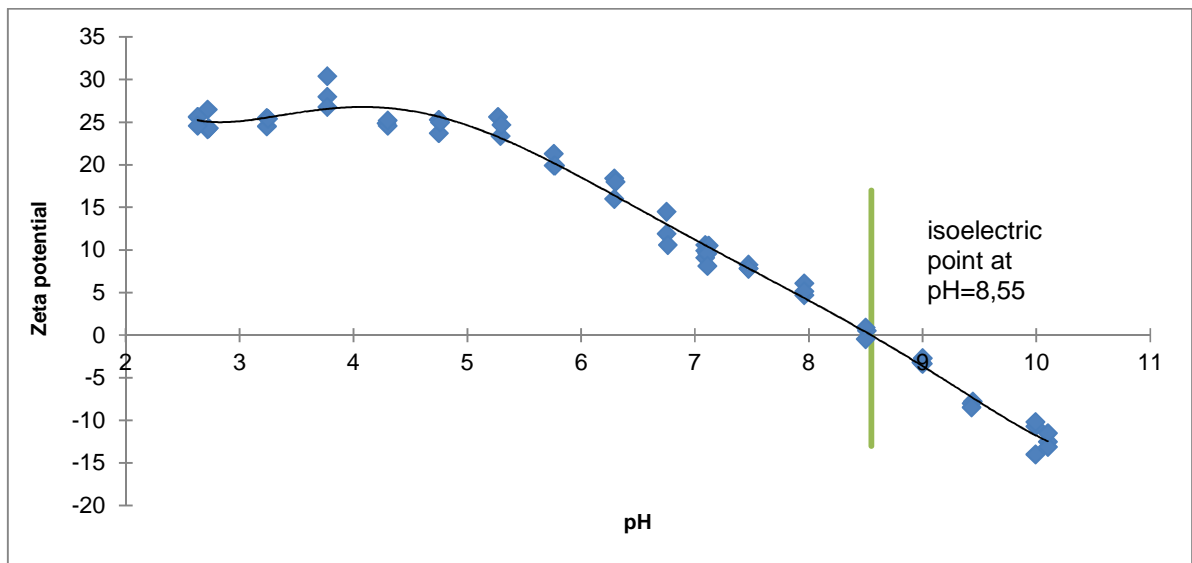**Figure 55:** Long term stability study of the non-purified BHS modified with Folate2k.

Figure 56: Long term stability study of the non-purified BHS modified with Folate5k.

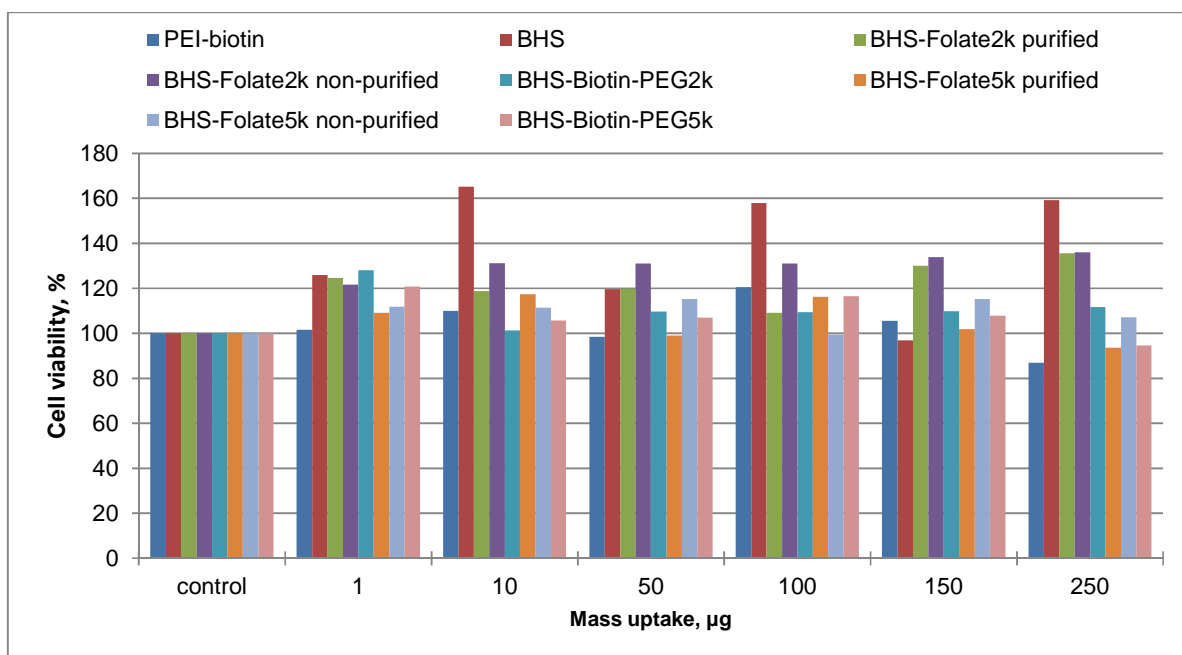**Figure 57:** Zeta potential of BHS modified with Folate5k.

Figure 58: Viability of HEK293 cells after 24 hours incubation with different structures.
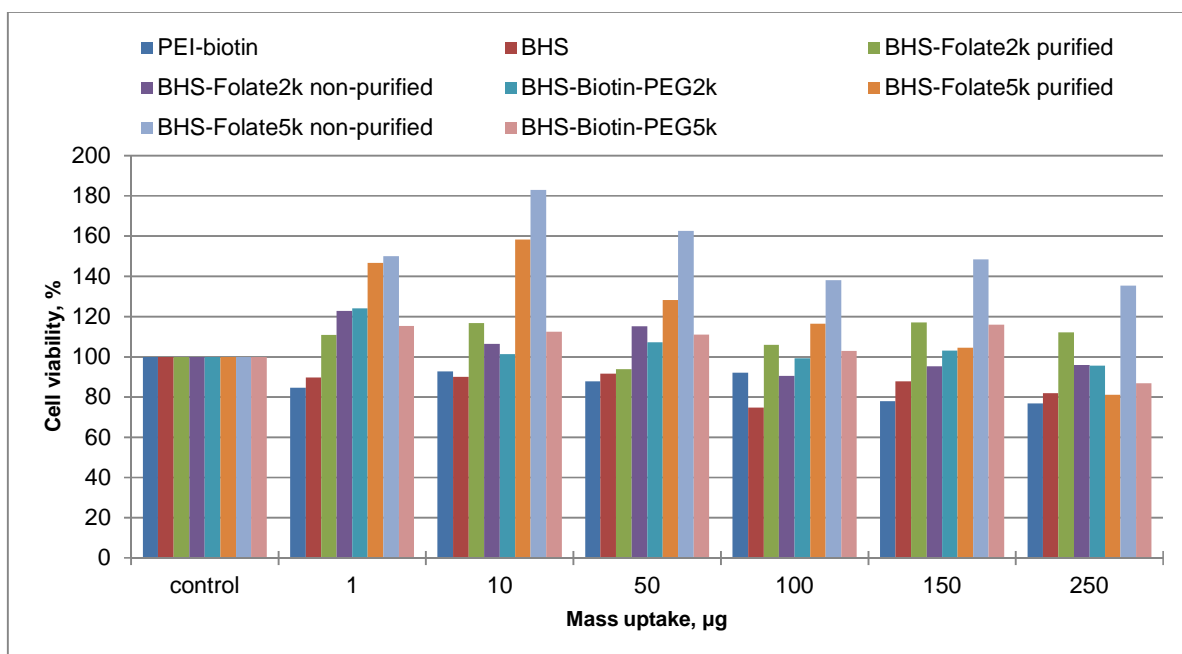

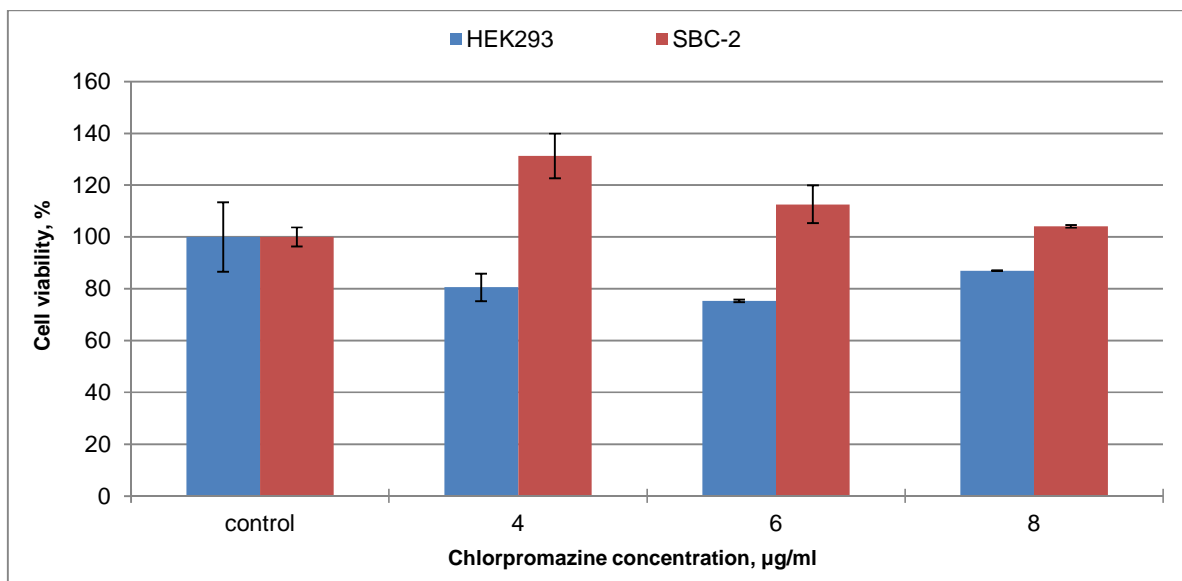**Figure 59:** Viability of SBC-2 cells after 24 hours incubation with different structures.

Figure 60: Viabilities of HEK293 and SBC-2 cells treated for 24h with different concentrations of chlorpromazine.